Mechanistic and kinetic investigations on the role of methanol and dimethyl ether in the Methanol-To-Hydrocarbons reaction

Dissertation for the degree of

Philosophiae Doctor

Juan Salvador Martínez Espín

Department of Chemistry

Faculty of Mathematics and Natural Sciences

UNIVERSITY OF OSLO

June 2017

Series of dissertations submitted to the
Faculty of Mathematics and Natural Sciences, University of Oslo
No. 1887

ISSN 1501-7710

Cover: Hanne Baadsgaard Utigard.
Print production: Reprosentralen, University of Oslo.

Preface

This PhD thesis is written as completion of my work at the Department of Chemistry, University of Oslo (Norway) and Haldor Topsøe A/S (Denmark) during the period March 2014 to April 2017. My employment was framed within the ZeoMorph project, a European Industrial Doctorate project (FP7-ITN-EID) within the Marie Curie actions. Consequently, more than 50 % of my time was spent at the industrial partner, Haldor Topsøe A/S, while I was based at the University of Oslo the rest of time. The research was challenging and stimulating, and the extensive investigations and thorough analysis of the experimental data allowed achieving a novel understanding of the research topic.

To conduct a PhD project, not only perseverance and persistence of the candidate is required, but also strong commitment and support from others. Therefore, I would like to acknowledge an extensive list of people.

Prof. Dr. Unni Olsbye (University of Oslo) acted as main supervisor and I am very grateful to her for giving me the invaluable opportunity to carry out my PhD in her group. Furthermore, I would like to express my sincere thanks for her unbreakable commitment during the entire project. Dr. Pablo Beato, Dr. Ton V.W. Janssens (Haldor Topsøe A/S) and Prof. Dr. Stian Svelle (University of Oslo) were my subsidiary supervisors. Pablo is greatly acknowledged for his guidance, and his continuous and passionate engagement in the project. Ton is acknowledged for his bright insights and fruitful discussions. Stian is acknowledged for his thoughtful considerations of the project and discussions.

I would also like to thank Dr. Kristof De Wispelaere and Prof. Dr. Veronique Van Speybroeck (University of Ghent) for their collaboration to bring together my experimental work with their theoretical work. Furthermore, I am grateful to Dr. Pit Losch, Benoit Louis (University of Strasbourg) and Irina Yarulina, Prof. Dr. Freek Kapteijn and Prof. Dr. Jorge Gascón (Delft University) for their fruitful collaborations and discussions. I am also grateful to the entire Catalysis Section at the University of Oslo for providing an optimally balanced professional and social environment. Special thanks to Irene, Dani, Evgeniy, Magnus, Pablo, Andrea, Malte, Reynald, Marius and Bjørn Tore among others, for sharing with me this unforgettable experience. Furthermore, exceptional thanks are extended to the guys in the "*PhD office*" at Haldor Topsøe A/S: Logi, Peter and Renato.

Finally, my parents, brother and sister deserve a particular note of thanks. Despite the distance and seeing each other less than desired, their unconditional support and affection have been fundamental to reach my goals.

Juan Salvador Martínez Espín

Oslo-Copenhagen, June 2017

List of abbreviations used in this thesis

2M2B	2-methyl-2-butene
AlPO	Aluminophosphate
BAS	Brønsted acid site
CSTR	Continuously stirred tank reactor
DFT	Density functional theory
DME	Dimethyl ether
DOMY	Dimethyloxonium methylide
DPM	Diphenylmethane
FID	Flame ionization detector
FTIR	Fourier transform infrared spectroscopy
GC	Gas chromatography
HMMC	1,2,3,3,4,5-hexamethyl-6-methylene-1,4-cyclohexadiene
IZA	International Zeolite Association
LAS	Lewis acid site
MBs	Methylbenzenes
MeOH	Methanol
MIHT	Methanol-induced hydrogen transfer
MOGD	Mobil's Olefins to Gasoline and Distillate
MP-AES	Microwave plasma atomic emission spectroscopy
MS	Mass spectrometry
MTA	Methanol to aromatics
MTG	Methanol to gasoline
MTH	Methanol to hydrocarbons
MTO	Methanol to olefins
MTP	Methanol to propylene
OIHT	Olefins-induced hydrogen transfer
PFR	Plug flow reactor
PolyMBs	Polymethylbenzenes
SAPO	Silico-aluminophosphate
SEM	Scanning electron microscopy

TCD	Thermal conductivity detector
TIGAS	Topsøe's Improved GAsoline Synthesis
TMO	Trimethyloxonium
WHSV	Weight-hourly space velocity
XRD	X-rays powder diffraction

List of publications

The work in this PhD thesis is based on manuscripts I, II and III listed below. The full manuscripts and supporting information documents are collected in the Appendix. Furthermore, the rest of publications achieved during this work are listed below:

I. *Benzene co-reaction with methanol and dimethyl ether over zeolite and zeotype catalysts: Evidence of parallel reaction paths to toluene and diphenylmethane.* J. S. Martínez-Espín, K. De Wispelaere, M. Westgård Erichsen, S. Svelle, T. V. W. Janssens, V. Van Speybroeck*, P. Beato*, U. Olsbye*. *Journal of Catalysis*, 349, **2017**, 136-148.

II. *New insights in catalyst deactivation and product distribution of zeolites in the Methanol-To-Hydrocarbons (MTH) reaction with methanol and dimethyl ether feeds*. J. S. Martínez-Espín, M. Mortén, T. V. W. Janssens, S. Svelle, P. Beato*, U. Olsbye*. *Catalysis Science & Technology,* **2017** (published).

III. *Hydrogen transfer versus methylation: on the genesis of aromatics formation in the Methanol-To-Hydrocarbons reaction over H-ZSM-5*. J. S. Martínez-Espín, K. De Wispelaere, T. V. W. Janssens, S. Svelle, K. P. Lillerud, V. Van Speybroeck*, P. Beato*, U. Olsbye*. *ACS Catalysis*, **2017** (submitted).

IV. *Syngas to liquids via oxygenates.* M. Westgård Erichsen, J. S. Martínez-Espín, P. del Campo, K. P. Lillerud, S. Svelle, P. Beato*, U. Olsbye*. Book chapter in *"Small-Scale Gas to Liquid Fuel Synthesis"*, CRC Press, **2015**, 431-463.

V. *Fossil Fuels: The Effect of Zeolite Catalyst Particle Morphology on Catalyst Performance in the Conversion of Methanol to Hydrocarbons.* K. A. Lukaszuk, P. del Campo, A. Molino, M. Nielsen, D. Rojo-Gama, J. S. Martínez-Espín, K. P. Lillerud, U. Olsbye, S. Bordiga, P. Beato*, S. Svelle*. Book chapter in *"Nanotechnology for Energy Sustainability"*, Wiley-VCH Verlag GmbH & Co. KGaA, **2017**, 1-40.

VI. *Phosphorous modified ZSM-5 zeolites: impact on methanol conversion into olefins.* P. Losch, G. Laugel, J. S. Martínez-Espín, S. Chavan, U. Olsbye, B. Louis*. *Topics in Catalysis*, 58, **2015**, 826-832.

VII. *On the formation and special role of formaldehyde in the conversion of methanol into hydrocarbons.* K. De Wispelaere, J. S. Martínez-Espín, S. Svelle, P. Beato, U. Olsbye, V. Van Speybroeck (*in preparation*).

The author's contribution

I. The author participated in planning the work and performed all experimental tests. The author was strongly involved in data interpretation, comparison of experimental and theoretical results and preparation of the manuscript.

II. The author designed the experiments and performed the vast majority of experiments. The author carried out data analysis and was strongly involved in the preparation of the manuscript.

III. The author planned and performed all experimental tests. The author actively participated in bringing together experimental and theoretical results and preparing the manuscript.

IV. The author performed the process industrial simulations. The author was strongly involved in planning and writing this publication (Sections 14.1, 14.2 and 14.4).

V. The author participated in writing this publication (Section 5).

VI. The author performed characterization of the samples, data analysis (TPD with *n*-propylamine) and participated in the revision process.

VII. The author provided experimental data and discussed the preparation of the manuscript.

List of conference contributions

I. *Influence of different ZSM-5 morphologies on benzene methylation in the Methanol-To-Hydrocarbons reaction.* J. S. Martínez-Espín, P. Beato, U. Olsbye.
Oral presentation at 1st HTAS PhD/Postdoc Workshop, February 5th, 2015, Copenhagen (Denmark).

II. *The effects of methanol or dimethyl ether as methylating agent during zeolite catalyzed benzene methylation.* J. S. Martínez-Espín, M. Westgård Erichsen, K. De Wispelaere, S. Svelle, P. Beato, V. Van Speybroeck, U. Olsbye.
Oral presentation at XII European Congress on Catalysis, August 30th-September 4th, 2015, Kazan (Russia).

III. *The effects of methanol or dimethyl ether as methylating agent during zeolite catalyzed benzene.* J. S. Martínez-Espín, M. Westgård Erichsen, S. Svelle, P. Beato, U. Olsbye.
Oral presentation at 15th Norwegian Catalysis Symposium, December 3rd-4th, 2015, Bergen (Norway).

IV. *Distinct reactivity of methanol and dimethyl ether toward benzene within MTH context.* J. S. Martínez-Espín, S. Svelle, M. Westgård Erichsen, K. De Wispelaere, V. Van Speybroeck, P. Beato, U. Olsbye.
Oral presentation at 17th Nordic Symposium on Catalysis, June 14th-16th, 2016, Lund (Sweden).

V. *Distinct reactivity of methanol and dimethyl ether toward benzene within MTH context.* J. S. Martínez-Espín, M. Westgård Erichsen, K. De Wispelaere, P. Beato, V. Van Speybroeck, S. Svelle, U. Olsbye.
Oral presentation at 18th International Zeolite Conference, June 19th-24th, 2016, Rio de Janeiro (Brazil).

VI. *Methanol: friend or foe in the Methanol-To-Hydrocarbons (MTH) reaction?* J. S. Martínez-Espín, P. Beato, U. Olsbye.
Oral presentation at 3rd HTAS PhD/Postdoc Workshop, March 8th, 2017, Copenhagen (Denmark).

VII. *Benzene co-reaction with methanol and dimethyl ether over zeolitic catalysts.* J. S. Martínez-Espín, K. De Wispelaere, M. Westgård Erichsen, S. Svelle, T. V. W. Janssens, V. Van Speybroeck, P. Beato, U. Olsbye.
Oral presentation at 25th North American Catalysis Society Meeting, June 4th-9th, 2017, Denver (USA).

VIII. *Syngas to clean-burn fuel via oxygenates: effect of effluent recycling.* J. S. Martínez-Espín, F. Joensen, P. Beato, U. Olsbye.
Poster presentation at Catalysis: Fundamentals and Practice Summer School, July 20th-24th, Liverpool (UK).

IX. *Syngas to liquids via oxygenates within the frame of the OCMOL project.* J. S. Martínez-Espín, M. Westgård Erichsen, F. Joensen, S. Teketel, P. del Campo Huertas, K. P. Lillerud, S. Svelle, P. Beato, U. Olsbye.
Poster presentation at Molecules @ surfaces Winter School, January 31st-February 5th, 2016, Bardonecchia (Italy).

X. *Understanding the role of methanol and DME in the Methanol-To-Hydrocarbons (MTH) reaction over H-ZSM-5.* J. S. Martínez-Espín, P. Beato, S. Svelle, U. Olsbye.
Poster presentation at 2nd HTAS PhD/Postdoc Workshop, February 25th, 2016, Copenhagen (Denmark).

Table of contents

Scope

The main scope of this PhD thesis was to gain knowledge on the mechanistic and kinetic behavior of methanol and DME in the industrially relevant Methanol-To-Hydrocarbons (MTH) reaction with the use of zeolitic materials as catalysts. Industrial MTH processes use methanol, DME or combined methanol/DME feeds over zeolitic catalysts. Methanol and its dehydration product, DME, are conventionally attributed an analogous behavior in MTH; however, a thorough investigation on the theme is still missing, even though the MTH reaction has been studied for 40 years already. Therefore, the first goal of this work consisted on studying methanol and DME as feeds over zeolites and zeotypes because both class of materials are commercially used in MTH. Subsequently, the second goal of this thesis set emphasis on achieving a mechanistic and kinetic insight on the behavior of methanol and DME in single reactions occurring in MTH, aiming to extrapolate the outcome to broader MTH chemistry.

The detailed MTH study over zeolites and zeotypes generated a novel understanding on how methanol and DME are interconverted to a different extent over both class of materials. As a result, remarkable differences in methanol/DME concentrations were observed during MTH operation over zeolites and zeotypes. Furthermore, this study revealed a distinctive behavior of methanol and DME towards catalyst deactivation and effluent product distribution. For these reasons, mechanistic and kinetic studies of carefully selected single reactions, which involved methanol and DME, were launched to further elucidate the role of the two oxygenates in the MTH chemistry. The co-reactions of benzene and isobutene with the two oxygenates were envisioned as ideal reactions to rationalize the findings regarding catalyst deactivation and effluent product distribution. These detailed studies robustly showed faster methylation kinetics for DME compared to methanol. Contrarily, co-reactions with methanol reflected the ability of this oxygenate to carry out hydrogen transfer reactions, which matched well with previous findings on catalyst deactivation and effluent product distribution.

The first two chapters of this PhD thesis present the background of the work. Firstly, a brief introduction to catalysis, zeolitic materials and their characteristics as catalysts are provided. Secondly, it is presented an extensive section on MTH catalysis, comprising its industrial relevance, the state of the art on the understanding of the MTH reaction, and a review with the most relevant single reactions studied in this work. The third chapter gives details on the experimental methods. The fourth chapter summarizes the main findings achieved in this work. Finally, the most relevant articles for this PhD thesis are attached in the Appendix.

Chapter 1

Catalysis and Zeolitic Materials

1 Catalysis and zeolitic materials

1.1. Catalysis

In 1836, the Swedish chemist Jöns Jakob Berzelius first coined the terms *"catalysis"* and *"catalyst"* in a report reviewing previous findings. He wrote: *"It is, then, proved that several simple or compound bodies, soluble and insoluble, have the property of exercising on other bodies an action very different from chemical affinity. By means of this action they produce, in these bodies, decompositions of their elements and different recombinations of these same elements to which they remain indifferent"* [1, 2]. Since the moment Jöns Jakob Berzelius baptized catalysis, more than 1,200,000 research articles that adopted his term, are found today in scientific databases in a broad variety of subjects such as chemistry, chemical engineering, biochemistry, physics, medicine, and pharmacology, among others. This startlingly large number of publications highlights the impact of catalysis and its application.

Nowadays, catalysis is defined as the process of increasing the rate of a reaction, without modifying the overall Gibbs energy, by a substance called catalyst. This means that the overall thermodynamics of the process are unaffected, while the kinetics of the reaction are changed. Basically, the catalyst provides an alternative route for the reaction to occur with lower energy demands, as highlighted in **Figure 1.1**. Nevertheless, this new route is also characterized by its increased complexity due to the larger number of steps compared to the non-catalyzed reaction, involving bonds being formed and broken between the catalyst, reactants and products. As a direct consequence of the lower energetics of catalyzed reactions, they are generally carried out under milder conditions of temperature and pressure than non-catalyzed reactions. Note that the catalyst is not consumed during the process; this fact has been fundamental for the successful implementation of catalysis in industry [3].

Catalysis and its applications are generally divided into three branches: heterogeneous catalysis, homogeneous catalysis and biocatalysis. Heterogeneous catalysis comprises processes where the catalyst and the reactants/products are present in different phases. Typically, the catalyst is a solid, whereas reactants and products are gasses and/or liquids. Homogeneous catalysis refers to processes where the catalyst and the reactants/products are in the same phase, normally as liquids. Biocatalysis engrosses all processes where specific enzymes act as catalysts [3].

The work presented in this PhD thesis focuses on the field of heterogeneous catalysis with the use of solid catalysts, named zeolites, for gas phase reactions involving methanol, DME and hydrocarbons.

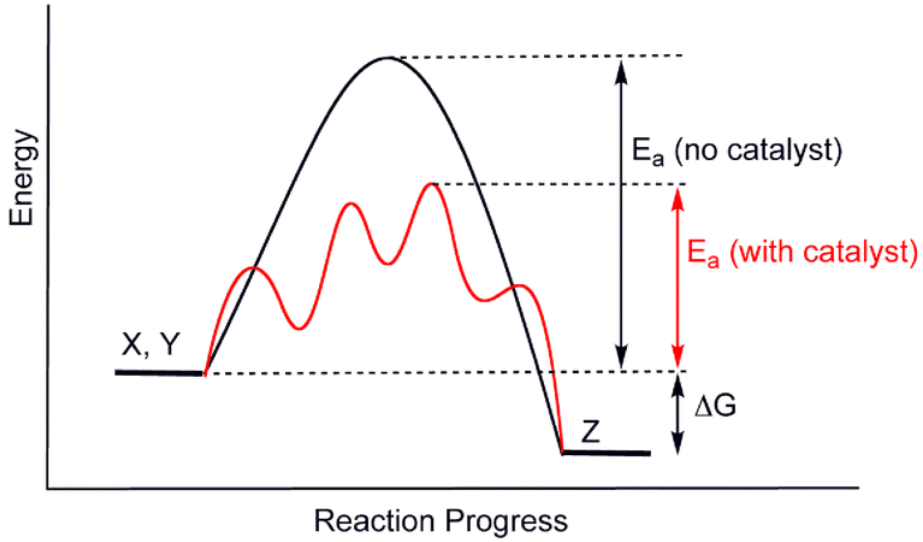

Figure 1.1. Potential energy diagram illustrating the energetic differences in an exothermic chemical reaction in the absence and in the presence of a catalyst.

1.2. Zeolites and zeotypes

Zeolites are a class of materials discovered by the Swedish mineralogist Axel Fredrik Cronstedt in the mid-1700s. He named the materials from the Greek word *"zeolithos"*, meaning "boiling stone", after observing steam escaping from the mineral stilbite upon heating. Zeolites are therefore naturally occurring minerals, but they have also been synthetically prepared [4]. There are around 40 different naturally occurring zeolites, and a total of more than 200 zeolites are already inscribed in the database of the International Zeolite Association (IZA) [5].

Zeolites are aluminosilicates with a well-defined crystalline structure. The structure of the materials is formed by a three-dimensional array of tetrahedral TO_4 building blocks, where T refers to Si or Al, linked to each other via corner oxygen atoms. The fundamental building blocks can arrange in many regular and repeating forms leading to different well-ordered and unique zeolite topologies, as exemplified in **Figure 1.2**. Every topology, with a designated three-letter code, is accordingly characterized by specific microporous/mesoporous interconnected channels, pores and cavities within a molecular scale range 4-20 Å [6].

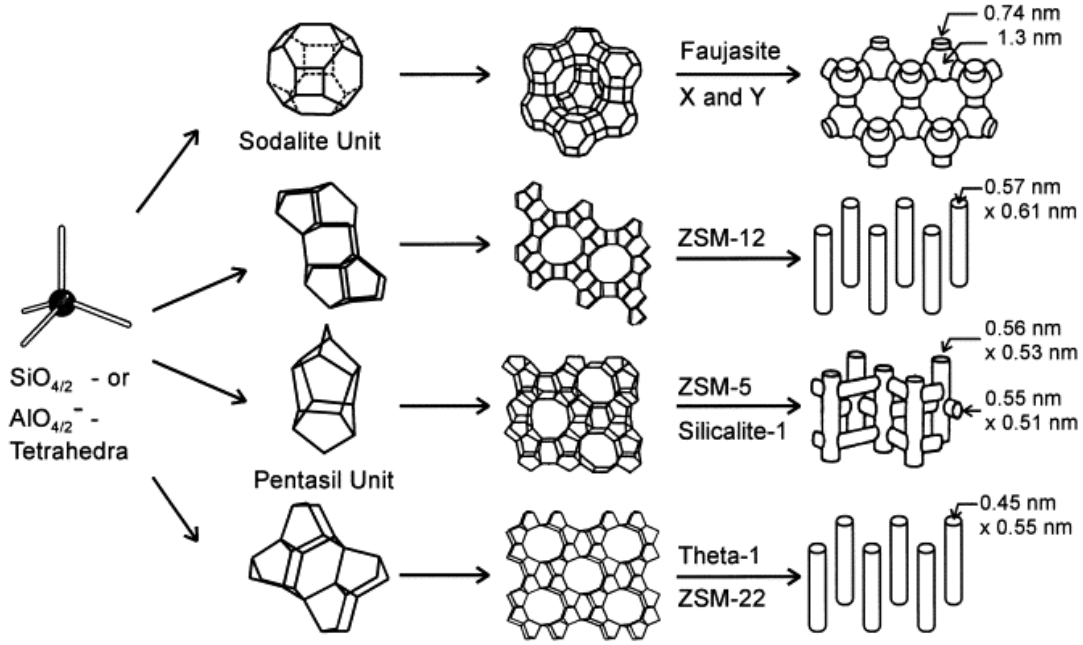

Figure 1.2. Example of zeolites with different microporous dimensions and size provided by the unalike arrangement of TO_4 units. Reproduced from [7] with permission.

Zeolites are categorized considering their pore aperture size, or equivalently, the number of TO_4 units forming the ring openings. The pore apertures of small-, medium-, large- and ultra large-pore zeolites are thus formed by 8, 10, 12 and more than 12 TO_4 units [8]. Furthermore, the connectivity of the pores subdivides zeolites in one-, two- and three-dimensional materials, *i.e.* ZSM-22 and ZSM-5 in **Figure 1.2** as one- and three-dimensional zeolites, respectively. The molecular dimensions of the pore apertures, channels and cavities of zeolites inherently provide them the ability to act as molecular sieves, meaning that small molecules are able to diffuse in and out of the materials, while larger molecules are rejected or diffuse slowly [6, 9, 10].

A direct consequence of the dimensional microporous structure and cavities provides zeolites with large surface areas and large pore volumes able to adsorb great amounts of hydrocarbons and other relevant molecules [6, 11]. Another trait of these materials is found in their acidity. The coordinated TO_4 units present Si^{4+} or Al^{3+} entities connected to four O^{2-}. Each O^{2-} is linked to two T sites, making the tetrahedral block neutral if Si^{4+} is the only T atom. If Al^{3+} is the T atom, a negative charge is created, which needs to be compensated by a cation, typically sodium, ammonium or a proton in the most acidic form (**Figure 1.3** - left). Cations are easily exchangeable and make this family of materials ideal for ion-exchange applications such as active detergents or removal of heavy metals from waste water [12, 13]. The protonic form of a zeolite provides the material a well-defined acidity suitable for catalytic applications [6, 14].

Zeotypes are very similar to zeolites. They share a characteristic crystalline microporous structure and large surface areas with zeolites. They are also built upon tetrahedral TO_4 blocks, but the composition of the TO_4 units is different. The most common family of zeotypes are silico-aluminophosphates, SAPOs. In this case, TO_4 units are connected alternating P^{5+} and Al^{3+} as T sites, leading to neutrally balanced structures. However, Si^{4+} might replace P^{5+} atoms, thereby creating a negative charge, which is balanced by a cation, as is also the case in zeolites (**Figure 1.3** - right). If the cation is a proton, a moderately strong Brønsted acid is generated [15, 16]. The acid strength of the Brønsted sites in zeolites and zeotypes is different, and it affects the chemistry at play during their application in catalysis [6]. The acid strength can be tuned by introducing different metals into the framework instead of silicon. Some examples are boron, gallium, zinc, cobalt, iron, manganese, titanium or magnesium, to name a few [17, 18]. Alternatively, zeotypes can be formed exclusively by phosphorous and aluminum atoms. These materials are aluminophosphates, AlPOs, and do not possess Brønsted acidity [19].

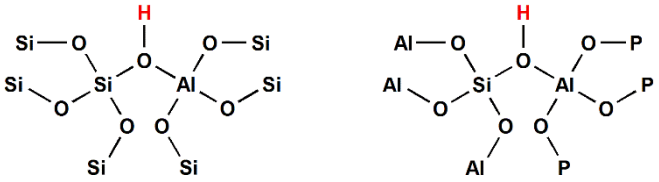

Figure 1.3. Representative Brønsted acid sites in zeolites (left) and Si-based zeotypes (right). In zeolites, an aluminum substitutes a silicon in the hydrophobic silicate framework, whereas in Si-based zeotypes, silicon substitutes a phosphorous in the hydrophilic aluminophosphate framework. Generated charges are compensated by a proton in their Brønsted acidic form.

1.3. Zeolitic materials as acid catalysts

In the early 1960s, Weisz and Frilette pioneered on the application of zeolites as catalysts by reporting shape-selective cracking, alcohol hydration and dehydration reactions over small-pore zeolites [20, 21]. Shortly after, Rabo and co-workers presented the possibility to use zeolites in paraffin hydroisomerization reactions [22], and subsequently, Venuto and associates expanded the catalytic application of zeolites to a broad assortment of reactions such as alkylation, condensation, Beckmann rearrangement, and dehydrogenation [23-27]. These studies each contributed importantly to unlocking the potential catalytic applications of zeolites, and rapidly revolutionized the oil refining industry with the introduction of zeolites as fluid catalytic cracking catalysts by Mobil [28]. Today, zeolites and zeotypes are extensively used throughout industry in a multitude of reactions involving hydrocarbons transformations [6]. However, the vast majority of applications have been limited to "The Big Five" zeolitic materials (FAU, MFI, MOR, BEA, FER), even though more than 200 different structures are now known [29].

The unique properties of zeolites are behind their successful use as catalysts. Their solid form facilitates the separation of gas and liquid reactants and products, hence reducing the costs associated with expensive and time consuming separation [3]. Furthermore, the strong acidity attributed to protonic zeolitic catalysts provides these materials with reaction centers able to carry out a broad assortment of reactions. Importantly, the possibility to modulate and control the acidity of the catalysts, by preparing zeotypes with different acid strength, or also varying the number of acid sites, has led to the design of well-suited zeolitic materials for specific reactions in the oil refining and petrochemical industries [18]. The molecular dimensions of the pores and cavities further complete the properties of these unique catalysts by providing shape selectivity during chemical reactions that discriminates between the behavior of reactants and products [30]. Typically, shape selectivity is divided into three types: reactant, product, and transition-state shape selectivity, as illustrated in **Figure 1.4**.

In reactant shape selectivity, molecules are discriminated according to their size with respect to the size of the pores. Bulky molecules are unable to diffuse inside the zeolitic framework, preventing them from reaching the reaction centers, while molecules smaller in size than the pore apertures diffuse inside the structure and react. In product shape selectivity, molecules are also discriminated in relation to their size and the size of the pores. However, it is most applicable to the products formed within the structure. Bulky molecules formed inside the zeolite cavities are restrictively diffused through smaller pores, and might suffer transformations into other products that diffuse out faster, or alternatively they may be retained inside the catalyst. Transition-state shape selectivity occurs when certain reactions are

prevented due to the available space within the confinement of the pores and/or cavities of the zeolitic framework, but other reactions involving smaller transition-states occur. In this case, the diffusion of reactants and products is unhindered [30].

A: Reactant Shape-Selectivity

B: Product Shape-Selectivity

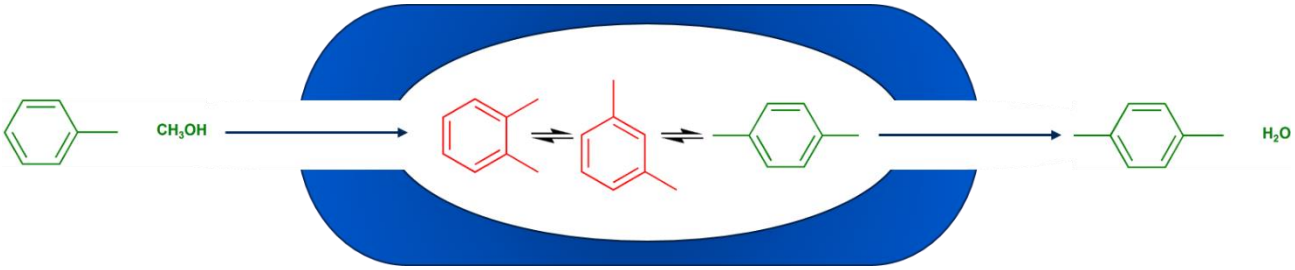

C: Transition-State Shape-Selectivity

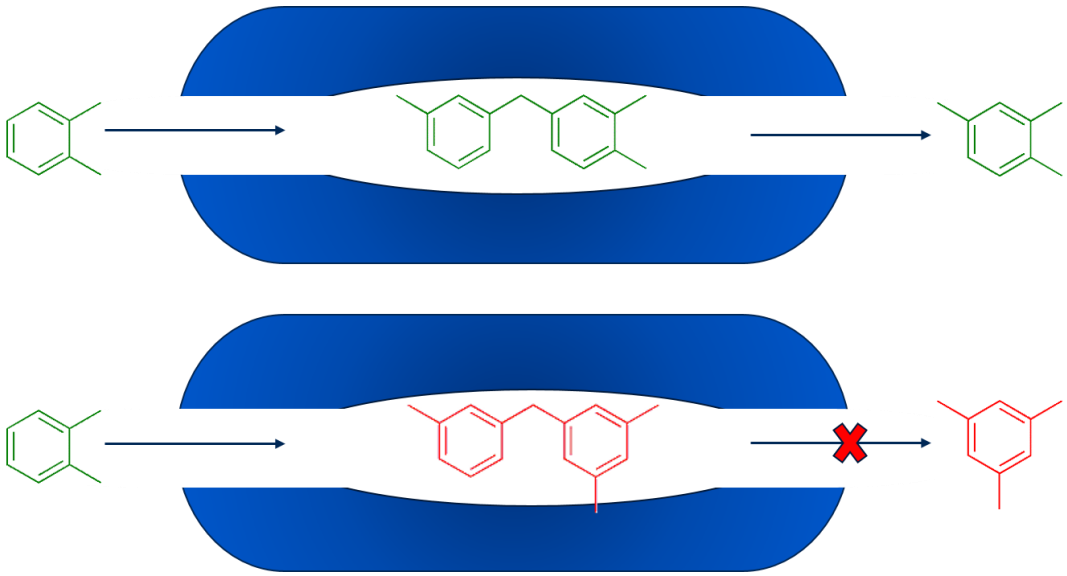

Figure 1.4. A: Reactant shape-selectivity exemplified by cracking of normal- and iso-parafins. **B**: Product shape-selectivity displayed during toluene methylation to xylenes. **C**: Transition-state shape selectivity exemplified by xylene transalkylation reaction to trimethylbenzenes.

1.4. Relevant materials for this work

1.4.1. The MFI framework

The first reports on zeolitic materials with MFI topology date back from the early 1970s, when chemists at Mobil synthesized an aluminosilicate with MFI topology, naming it **Z**eolite **S**ocony **M**obil-5, ZSM-5 [31]. The name H-ZSM-5 identifies the counterbalancing cation as a proton. ZSM-5 is a medium-pore zeolite with 10 T atoms forming the pore apertures of two sets of channels that run perpendicularly to each other. While one of the channels is straight, the other channel zigzags, and their sizes are 5.5 x 5.1 Å and 5.6 x 5.3 Å, respectively. A view of the channels and a three-dimensional representation of the MFI topology are illustrated in **Figure 1.5**. The size of the pores discriminates against molecules larger than 1,2,4,5-tetramethylbenzene to diffuse in and out of the framework. However, the channel intersections are slightly larger and enable larger molecules to be formed.

This well-investigated material has broad applications in catalytic reactions in the chemical industry that exploit its shape selectivity, such as toluene disproportionation, isomerization of *m*- and *o*-xylenes to *p*-xylene and the conversion of Methanol-To-Gasoline (MTG), which belongs to the family of reactions under the umbrella of the reaction studied in this PhD thesis, the Methanol-To-Hydrocarbon (MTH) reaction. The MTH reaction will be described further in **Section 2** [32-35]. According to the targeted application, ZSM-5 catalysts have been prepared in a wide range of acid site densities, crystal sizes and more recently, crystal morphologies and with imbedded mesoporosity [36-40].

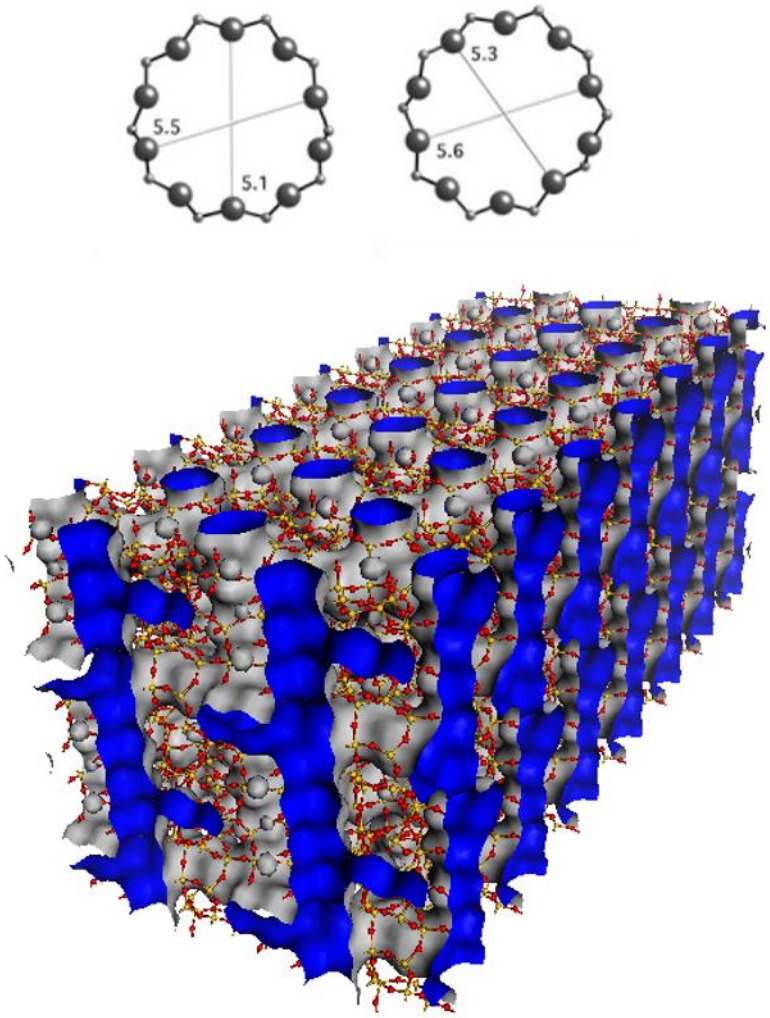

Figure 1.5. Top: view of the MFI topology channels along [100] and [010] planes. Adapted from [5]. Bottom: three-dimensional representation of the MFI topology.

1.4.2. The AFI framework

The first zeolitic material with an AFI framework was synthesized in the aluminophosphate form in 1982 in the same work that first reported zeolitic materials without silicon [19]. The material was then denominated AlPO-5 by scientists at Union Carbide. Just two years later, the same group of scientists reported the first silico-aluminophosphate materials, that included the one with AFI topology, naming it SAPO-5 [16]. Synthesis of the equivalent zeolite was achieved in 1994, and it was denominated SSZ-24 [41]. This is likely one of the few cases in which the aluminophosphate and the silico-aluminophosphate of the same topology were known earlier than their zeolite counterpart. The AFI topology is characterized by its relatively simple structure formed by unidimensional, straight, nearly circular channels with the size of 7.3 x 7.3 Å. Therefore, this framework belongs to the large-pore zeolitic materials family with 12 T atoms forming the pore openings. The view of the channel, together with a

three-dimensional representation of the AFI framework are shown in **Figure 1.6**. In this case, the large pores fit molecules as large as hexamethylbenzene, which are able to diffuse in and out the structure.

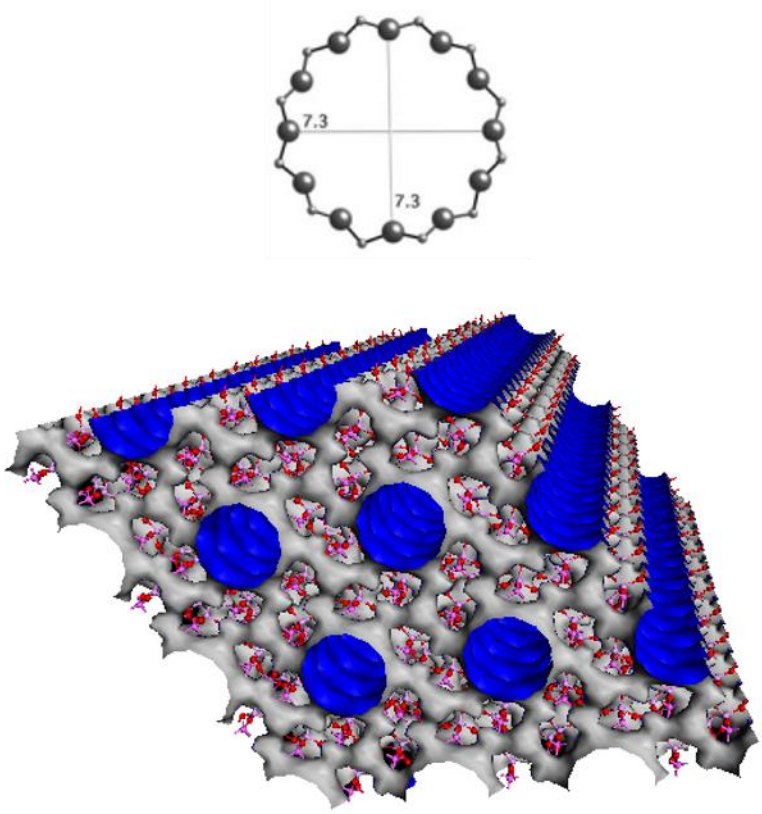

Figure 1.6. Top: view of the AFI topology channels along [100] plane. Adapted from [5]. Bottom: three-dimensional representation of the AFI topology.

Materials with AFI topology lack an industrial application at present. Nevertheless, they have served as model materials for several reasons: (1) The simple framework leads to large channels with a unidimensional structure that facilitates the diffusion of reactants and products, which is particularly useful for studying the kinetics of reactions in zeolites/zeotypes without diffusional constraints; (2) the simplicity of the framework is easier to model as compared to other frameworks in the still-demanding theoretical investigations; (3) the AFI framework is known in the zeolite version and an important number of zeotype versions with different heteroatoms in the framework, facilitating the study of the effect of acid strength in reactions over materials with identical framework [17, 42-44].

Chapter 2

Methanol To Hydrocarbons Catalysis

2 Methanol-To-Hydrocarbons Catalysis

The Methanol-To-Hydrocarbons reaction originated in research laboratories at Mobil in the 1970s, when two independent teams of researchers, working in converting methanol to ethylene oxide and in methylating isobutene with methanol over H-ZSM-5, observed unexpectedly undesired aromatic hydrocarbons [45]. Detailed follow-up investigations determined the "accidental" origin of these hydrocarbons, and enabled Chang and Silvestri to report the transformation of methanol and other oxygenated compounds, *i.e.* DME, *t*-butanol or methylal, into water and a mixture of hydrocarbons such as olefins, paraffins and aromatics. The characteristics of these hydrocarbons resembled those of gasoline [46, 47]. This discovery rapidly attracted important commercial and academic interest due to the ease to produce methanol from syngas with already established technology, opening the door for the potential use of various carbon-based feedstocks such as coal, natural gas or even biomass and waste at present, as source of fuels and valuable chemicals that had traditionally been obtained from oil [48, 49]. The industrial development of MTH-related technology has been strongly connected to the oil market. In spite of the fluctuating interest in MTH commercialization, mainly motivated by changes in the price of oil, major research efforts on the theme have been conducted for over 40 years [35, 49-51] and dozens of industrial MTH plants are operative today [52-54].

The reaction network summarizing the conversion of methanol to hydrocarbons over H-ZSM-5 was described by Chang and Silvestri as a three-stages process [47]. Firstly, methanol is partly dehydrated to DME and water. In a second stage, methanol and DME are converted to light olefins and water, that subsequently react to be converted into aromatics, alkanes and higher olefins, as reflected in **Scheme 2.1** and also in **Figure 2.1**, which shows the reactant and products evolution with space time over H-ZSM-5 at 371 °C. The overall reaction is highly exothermic. Since high temperatures lead to an undesirable hydrocarbon product distribution and fast catalyst deactivation, Chang and Silvestri highlighted the importance of controlling reaction temperatures [46].

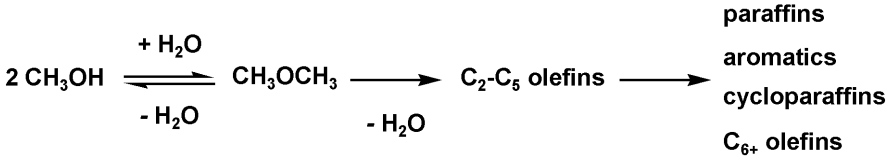

Scheme 2.1. Simplified MTH reaction pathway. Adapted from [47].

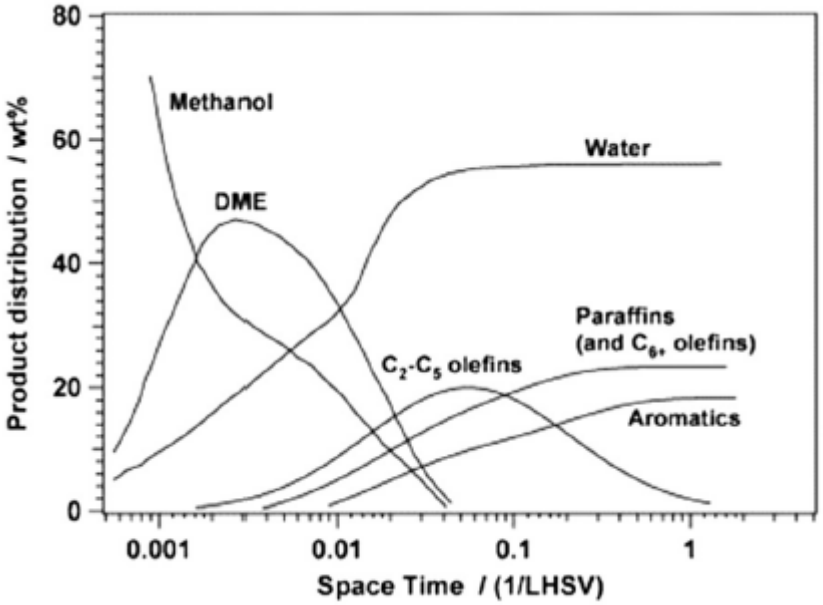

Figure 2.1. Product evolution versus space time for the conversion of methanol to hydrocarbons over H-ZSM-5 at 371 °C. Reproduced with permission from [55].

The term MTH is used to describe the conversion of both methanol and its dehydration product, DME, into hydrocarbons over zeolitic materials. The process conditions and catalyst type are key parameters affecting the complex spectrum of hydrocarbon products, and it will be further discussed in this Section. Therefore, specific MTH processes have been developed according to the targeted products as shown in **Figure 2.2**: Methanol-To-Gasoline (MTG), Methanol-To Olefins (MTO), Methanol-To-Propylene (MTP) and most recently Methanol-To-Aromatics (MTA).

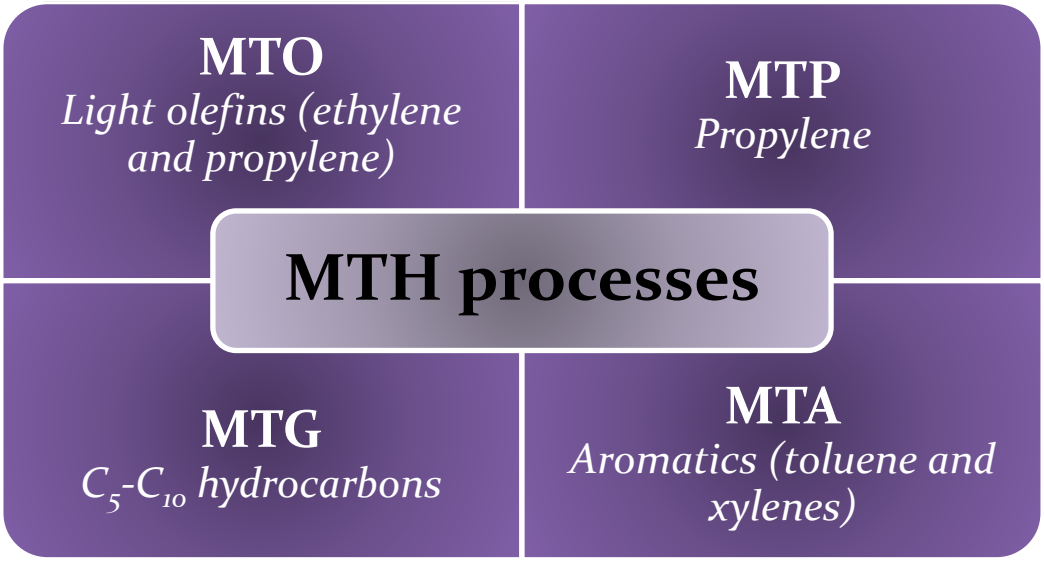

Figure 2.2. Summary of the industrial MTH processes and their targeted products.

2.1. Industrial development of the MTH technology

After the intensive initial research efforts by the pioneers of the MTH technology, the first commercial MTG plant was commissioned by Mobil in New Zealand in 1985, in a joint venture with the government of the country [56, 57]. The plant combined well-established methanol synthesis technology from syngas, with the newly-developed gasoline synthesis technology. As illustrated in **Figure 2.3a**, after methanol synthesis, the Mobil's MTG process presents two sequential reactors: the first one dehydrates methanol to DME and water up to thermodynamic equilibrium, and the second one uses this equilibrated mixture together with undesired recycled olefins as feed over a fixed-bed reactor loaded with H-ZSM-5 based catalyst, which gives high yields of hydrocarbons within the gasoline fraction (C_5-C_{10}). The use of two reactors and the recycling of undesired light hydrocarbons facilitates temperature control during the highly exothermic process [58]. Since oil prices plummeted shortly after the start-up of the plant, the MTG section was shut down in 1995 [45].

Almost in parallel with their MTG efforts, Mobil tried to develop a process to generate mostly lighter olefins based on novel fluidized-bed technology [59-61]. Despite the modifications implemented in their MTG catalyst, ZSM-5, and optimization of the reaction conditions to favor the targeted products, the selectivity to ethylene was still limited [53]. Nevertheless, large amounts of olefins were produced. Using an additional low-temperature reactor loaded with H-ZSM-5 based catalyst, these olefins were oligomerized to gasoline- and diesel-type hydrocarbons. This process was called the Mobil's Olefins to Gasoline and Distillate (MOGD) [62].

In the 1980s, Haldor Topsøe also developed an alternative gasoline synthesis technology from methanol, the Topsøe Integrated Gasoline Synthesis (TIGAS). The singularity of the process is found on the combined synthesis of methanol and DME from syngas, that enhances the process efficiency due to favored thermodynamics compared to the synthesis of only methanol [63, 64]. Consequently, a mixture of methanol, DME, water, CO_2 and recycled unconverted hydrocarbons comprises the feed of the gasoline synthesis reactor loaded with H-ZSM-5 based catalyst (**Figure 2.3b**). The diluted methanol concentrations in the feed contribute accordingly to facilitate the control of the temperature [64]. After successful pilot scale demonstration of TIGAS from natural gas and biomass, the world's largest MTG plant, with an expected production capacity of 15,500 barrels per day, is under construction in Turkmenistan at the present time and will be operative in 2018 [65, 66].

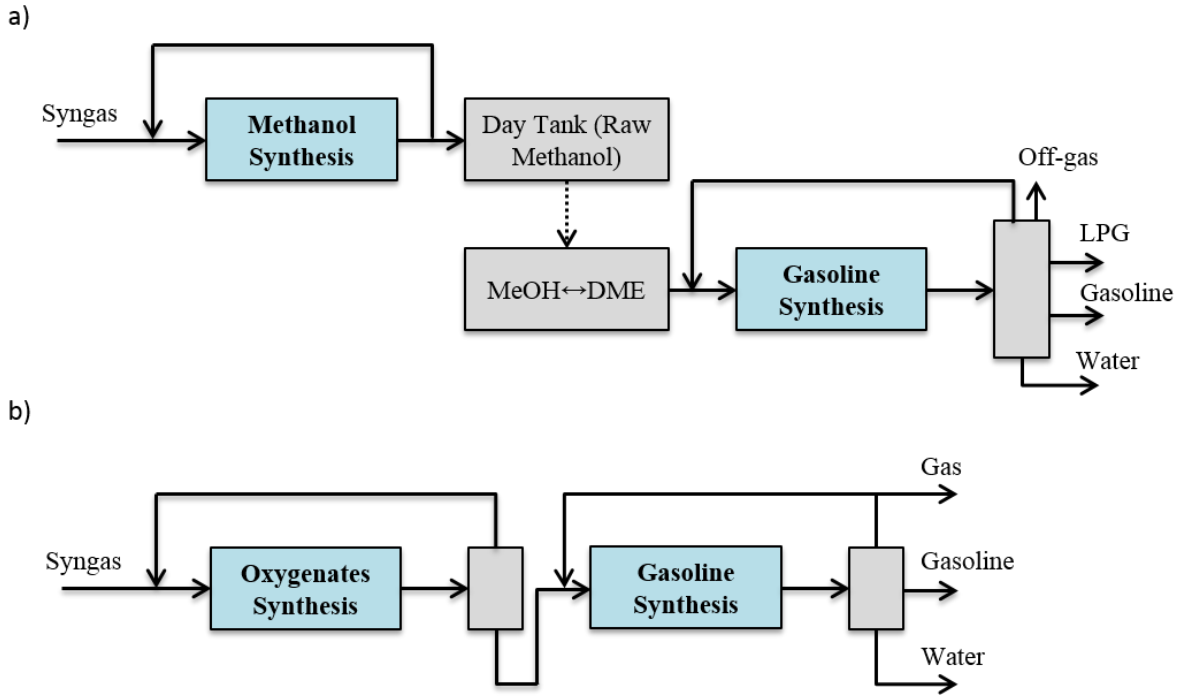

Figure 2.3. a) Mobil's MTG process, b) Topsøe's TIGAS process.

Another important achievement in the development of MTH technology derived from the synthesis of a family of hydrothermally stable silico-aluminophosphates (SAPO) materials by the Molecular Sieve Division of Union Carbide (now UOP) in 1984 [16]. Spurred by the use of zeolites for converting methanol into gasoline and olefins at Mobil, UOP rapidly attempted the reaction over their novel materials [67]. The performance of H-SAPO-34, a zeotype catalyst with small pore openings (8 T atoms) and large cavities, stood out among other SAPO materials in terms of light olefins production with selectivities above 80%, substantially higher than using medium and small pore zeolites, such as H-ZSM-5 and H-ZSM-34 [68, 69]. The outstanding capacity of H-SAPO-34 for olefin production led UOP and Norsk Hydro (now INEOS) to collaborate in the development and commercialization of MTO technology, that culminated with the construction of a 0.9 tons per day demonstration unit in Norway and the availability for licensing in 1995. The process, depicted in **Figure 2.4a**, was developed in a low-pressure fluidized-bed reactor, enabling good temperature control and continuous regeneration of the H-SAPO-34 catalyst [70], that deactivates much faster than H-ZSM-5.

UOP also collaborated with Total Petrochemicals in order to optimize ethylene and propylene production, and combined their MTO process with the Olefin Cracking Process (OCP) developed by Total. These joint efforts led them to successfully demonstrate a semi-commercial MTO-OCP unit in Belgium that was capable of processing 10 tons of methanol per day [71]. Subsequently, Total

Petrochemicals integrated a downstream semi-commercial polyolefins plant for production of polyethylene and polypropylene polymers [72]. In recent years, several MTO plants have started to operate with UOP technology, mostly in China [52, 73]. The same zeolitic catalyst, H-SAPO-34, is used in the commercial DiMethyl ether To Olefins (DMTO) process developed by the Dalian Institute of Chemical Physics. It also operates in a fluidized bed reactor, but it uses DME as feed instead of methanol, and includes recycling of C_{4+} hydrocarbons to maximize the combined productivity of ethylene and propylene. The first MTO plant in the world actually started with DMTO technology in China in 2010 with a production capacity of 600 kt of ethylene and propylene per year [73].

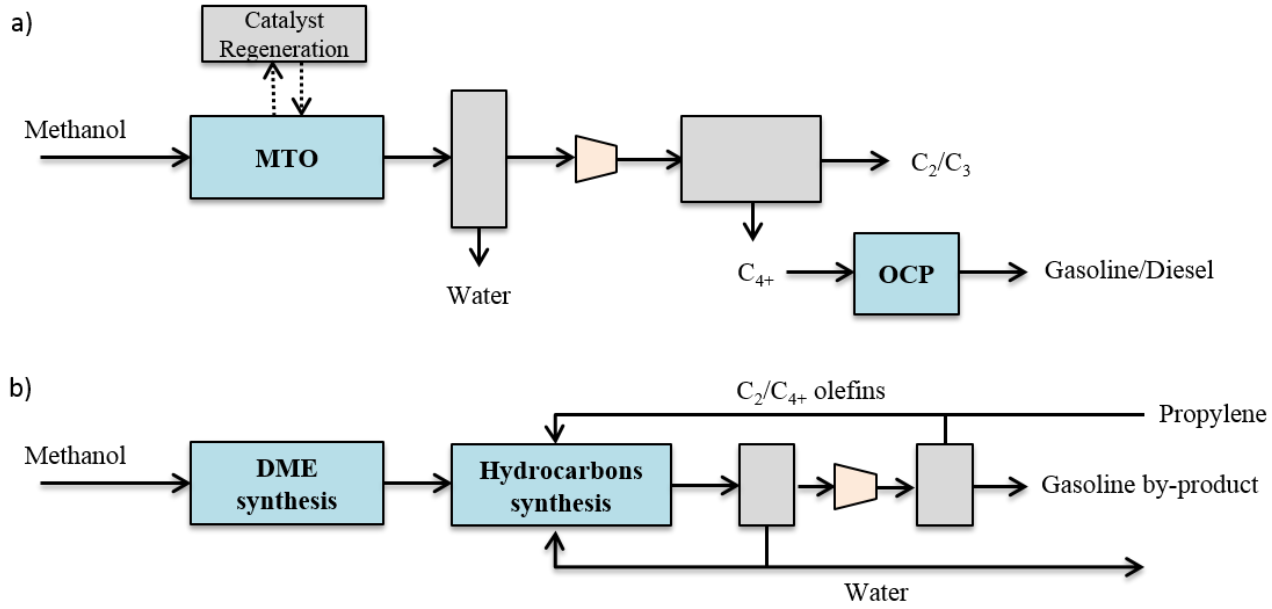

Figure 2.4. a) UOP/Norsk Hydro MTO process combined with UOP/Total OCP, b) Lurgi's MTP process.

Aiming to maximize propylene production over ethylene, Lurgi focused on the development of a MTP technology. In this process, a H-ZSM-5 based catalyst supplied by Süd Chemie is used, enabling the reduction of ethylene yields in favor of propylene [74]. The Lurgi MTP process design comprises a first reactor where methanol dehydrates to an equilibrium mixture of methanol, DME and water steam, which is subsequently directed to an adiabatic fixed-bed reactor operating at 400-500 °C, together with a recycled stream of steam and all olefins, propylene exempted, in order to increase process efficiency and serve as heat sink during the exothermic reaction. The process is schematically illustrated in **Figure 2.4b**. By 2015, three MTP plants were already operative in China, using coal as the feedstock [75]. More recently, JGC Corporation and Mitsubishi Chemicals ventured into MTH technologies by developing an alternative propylene production process. The new process, called the Dominant Technology for the Propylene Production (DTP), is very similar to the Lurgi MTP process. However, the zeolitic ZSM-5

catalyst contains an alkaline earth metal, with calcium suspected to be the preferred one [53]. Using the non-protonic form of the zeolite requires higher temperatures (500 °C) to compensate for the lower activity, compared to protonic zeolites, and near atmospheric pressure is employed.

All the processes earlier outlined show a high degree of flexibility in their MTH chemistry. Catalysts and process conditions play a fundamental role in tailoring the production of a desired product fraction. It has been shown that methanol and/or DME can be used as feeds in the synthesis of hydrocarbons, together with water and recycling of undesired hydrocarbons, typically olefins. This dilution of the feed, achieved with a pre-reactor and/or recycling of products, is beneficial to control reaction temperatures in the highly exothermic process and increases its productivity [64]. Medium-size pore H-ZSM-5 based catalysts are preferred in MTG and MTP processes because of catalyst stability against deactivation and shape selectivity properties to targeted products. The small-size pore H-SAPO-34 is typically preferred in MTO processes due to its very high shape selectivity towards light olefins as well as hydrothermal stability, which is fundamental due to the multiple regeneration cycles needed when using this catalyst. Moderate temperatures around 350-400 °C are employed in MTG process, while higher temperatures 450-500 °C are used in MTO.

The recent demand for light aromatics in China has spurred the academic and industrial research of MTA processes. To selectively form aromatics from methanol, a metal with a dehydrogenation function is combined with a zeolitic material, with ZSM-5 being the most promising option [76, 77]. The rapid emergence of MTA, together with the rest of the processes (MTO, MTP and MTG) proves the versatility of the MTH technology and the adaptability to quickly respond to the dynamic market of fuels and chemicals. The incursion of new hydrocarbon sources, *e.g.* shale gas, biomass, and waste, the continuous oil price fluctuations or even the application of new environmental policies are important parameters to be monitored in order to guarantee the economic viability of MTH technologies. Furthermore, the study of the large number of reactions involved in MTH might also lead to the acquisition of new knowledge that can be extended to other industrial technologies using zeolites and zeotypes materials for hydrocarbon transformations with similar chemistries, such as fluid catalytic cracking (which typically uses H-ZSM-5 as an additional catalyst), xylene isomerization, toluene disproportionation, and aromatics transalkylation, among others [78].

2.2. A journey through the realm of the MTH reaction

Since the first published description of the MTH reaction in 1977 by Chang and Silvestri, hundreds of studies have been devoted to achieving a better understanding of the mechanism and kinetics of the reaction. Incited by the industrial potential to produce a wide variety of relevant hydrocarbons such as olefins, gasoline and aromatics in a less oil-dependent economy, researchers still pursue the arduous task of solving the great puzzle of the MTH reaction forty years later [45, 48, 49, 79-84].

The initial description of the MTH reaction over zeolites, shown in **Scheme 2.1**, was described as a sequential process wherein methanol partially converts to DME, that with methanol forms the first olefins, which subsequently lead to more thermodynamically stable paraffins and aromatics. The following subsections review the important mechanistic concepts that have been reported to rationalize the different stages of the MTH reaction. Firstly, a summary of the most relevant mechanisms that have been proposed to explain the initial hydrocarbons containing C-C bonds is presented in **Section 2.2.1**. Secondly, **Section 2.2.2** describes the evolution and refinement of the mechanisms proposed in the literature to explain the overall MTH reaction. Thirdly, a brief subsection on catalyst deactivation by coking is presented in **Section 2.2.3**.

2.2.1. The unending enigma of the first C-C bonds

The important step in which the first olefins are formed was speculated to occur in a concerted bimolecular manner between carbene species ($:CH_2$) and methanol/DME by Chang and Silvestri in the original MTH contribution [47]. Nevertheless, the authors lacked concluding evidence, and more than 20 mechanisms have been proposed in the literature to rationalize the formation of the first hydrocarbons since then [50, 85].

Chang and Silvestri considered that the generation of carbene species occurred in a cooperative manner between the basic and the acid sites of zeolites. They hypothesized that α-elimination occurred from methanol, leading to water and carbene species, in a mechanistic approach that was earlier proposed by Venuto and Landis on the conversion of methanol over Zeolite X [86]. Subsequently, carbene species could be inserted in the C-O bond of another methanol or DME molecule, that in turn give olefins via protolysis, as shown in **Scheme 2.2** [47]. This mechanism was fairly well debated during the initial studies [80], but later, more sophisticated computational methods led to it being discarded due to unrealistically high activation barriers involved in the formation of the carbene species [87].

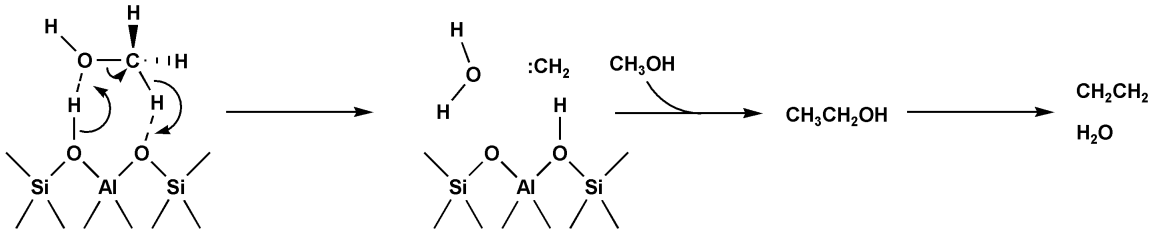

Scheme 2.2. The carbene mechanism. Adapted from [47, 80].

Also in the initial flourishing of the MTH studies, Van der Berg *et al.* and Olah *et al.*, working independently, proposed a mechanism involving a trimethyloxonium (TMO) ion as intermediate in the formation of the first hydrocarbons [88, 89]. The name given to this route is the oxonium ylide mechanism. In this mechanism, illustrated in **Scheme 2.3**, TMO is formed via methylation of DME over a Brønsted site. Subsequently, TMO suffers deprotonation via the conjugate basic site of the zeolite, that gives dimethyloxonium methylide (DOMY). This intermediate either undergoes a Stevens rearrangement to methylethylether that yields ethylene, or either reacts intermolecularly to form an ethyl dimethyloxonium ion, that can lead to ethylene. Even though several indirect pieces of evidence have supported this mechanism, no direct observation of either TMO or DOMY was reported [81]. Similarly to the carbene mechanism, theoretical calculations revealed very high activation energies of this mechanism. Consequently, this route is also unlikely to explain the formation of the first olefins [90].

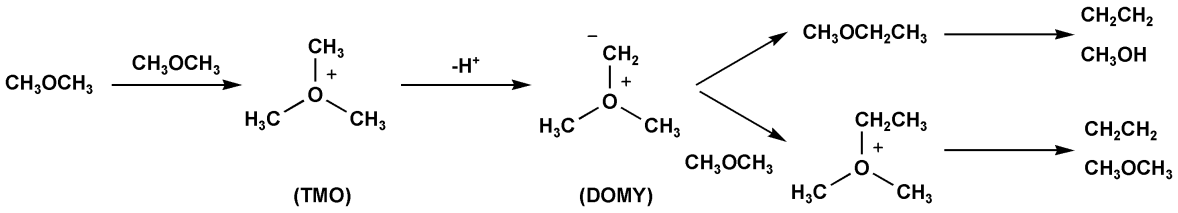

Scheme 2.3. The oxonium ylide mechanism. Adapted from [80].

Another route attempting to explain the first C-C bonds in MTH is the surface methoxy or carbocationic mechanism. According to this pathway, methanol, DME, or even other methylating agents such as methyl halides get adsorbed on Brønsted sites, and form a methoxy or methyloxonium group [91]. These species were detected by infrared spectroscopy prior to the onset of hydrocarbons formation [92, 93]. Once formed, it was proposed that methanol (or DME) abstract a proton leading to an exthoxy carbocation, that desorbs as ethylene, which is shown in the bottom pathway in **Scheme 2.4**. However, Smith and Futrell reacted methylcarbenium ions with methanol, and the hydride abstraction to form methane and CH_2OH^+ was the main reaction observed (85-90 %). Instead, only 7 % of the expected ethylene was detected, rising some doubts about this mechanism [94].

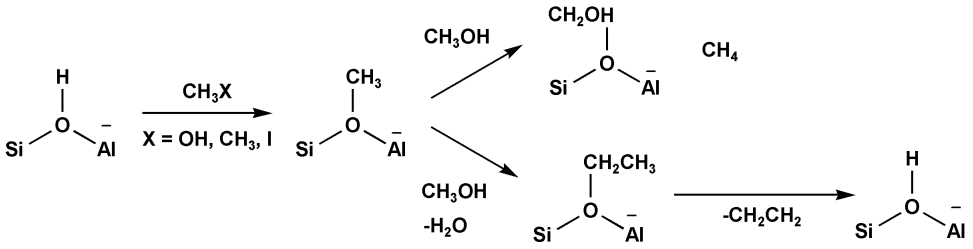

Scheme 2.4. The surface methoxy or carbocationic mechanism. Adapted from [80].

The methane-formaldehyde route is a variant interpretation of the proposed carbocationic route. In this proposal, a hydride abstraction from methanol to methoxy groups occurs with the cooperative effect of the basic oxygen of the zeolite framework, as shown in **Scheme 2.5**, leading to methane and formaldehyde as products. In a second step, methane and formaldehyde couple to form ethanol, that in turn readily dehydrates to ethylene [95]. An indirect piece of evidence supporting this mechanism is that methane is typically observed in the beginning of the MTH reaction, preceding the formation of olefins [91]. However, it should be noted that methane is considered quite an unreactive molecule in the MTH reaction. Indeed, theoretical calculations have shown that the C-C coupling between methane and formaldehyde is very unlikely due to its energetically demanding barrier [87, 90, 96]. However, those theoretical studies also revealed the feasibility of the first step of the mechanism, that yields methane and formaldehyde. Several experimental studies have detected the presence of formaldehyde during the initial stages of the MTH reaction by temperature-programmed reactions [95, 97, 98], transient analysis of products [99], GC-MS analysis [100] and gas phase infrared spectroscopy [101]. Therefore, we might speculate that while the first hydrocarbons might not be formed via this mechanism, methane and formaldehyde are perhaps likely to be formed.

Relevantly within the scope of this work, this mechanism has been suggested for methanol due to the interaction of the alcohol proton and the basic oxygen of the zeolite framework. Nevertheless, DME presents a methyl group instead of the proton, and possibly the extent of the interaction with the basic oxygen is different. Also, DME should not lead to formaldehyde.

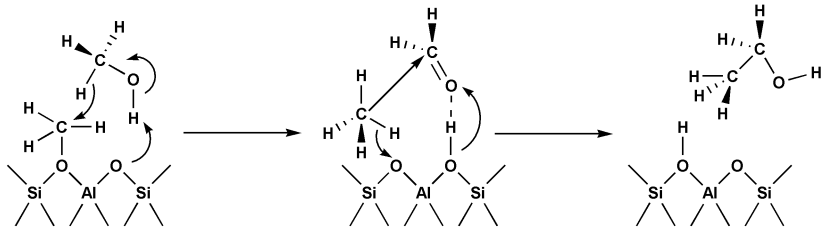

Scheme 2.5. The methane-formaldehyde mechanism. Adapted from [85].

The high activation barriers for all proposed mechanisms up to this point, and the observation that small traces of impurities greatly accelerated the production of hydrocarbons by several orders of magnitude led Haw and co-workers to hypothesize that any direct route to produce hydrocarbons from pure methanol and DME was improbable [100]. Instead, the authors stated that impurities govern the initial formation of olefins in the MTH reaction. They speculated that impurities could be derived from the reactant itself and also from incomplete combustion of organic templates that are typically used in the synthesis of the catalysts. This hypothesis has been assumed by many to be the most plausible until very recently. The groups of Lercher, Weckhuysen and Fan have provided new experimental and theoretical evidence for a direct route in the formation of the first C-C bonds [96, 101, 102]. Lercher and co-workers detected methane, formaldehyde, CO and hydrogen over H-ZSM-5, and suggested that these molecules were formed via methanol dehydrogenation and disproportionation reactions. They also observed acetic acid and methyl acetate intermediates, proposing their formation by carbonylation of methanol or DME with CO, as in **Scheme 2.6**. By means of theoretical calculations, they determined that the carbonylation reaction presents an energy barrier of only 80 kJ/mol, which is much lower than energy barriers computed for the previously presented mechanisms (all above 200 kJ/mol). Almost in parallel, Weckhuysen and co-workers studied the initial C-C bond formation over H-SAPO-34 via solid-state NMR spectroscopy, UV/Vis diffuse reflectance spectroscopy and mass spectrometry, observing surface formate, surface acetate and methyl acetate intermediates. The authors provided spectroscopic evidence supporting the carbene mechanism and the carbonylation route shown in **Scheme 2.6**, and highlighted surface acetates as the first molecule containing C-C bonds.

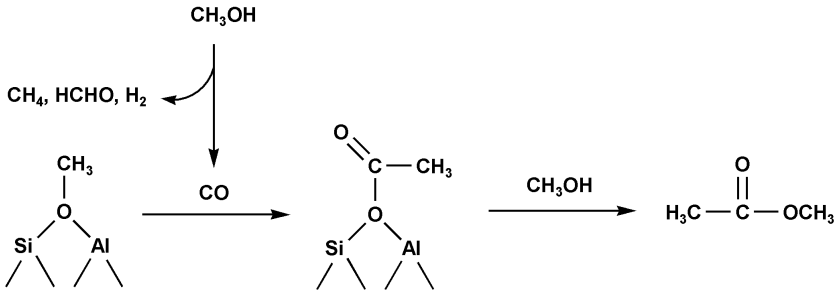

Scheme 2.6. The carbonylation mechanism. Adapted from [101].

Fan and co-workers theoretically studied the reactivity and stability of intermediates in the formation of the first C-C bonds from methanol and DME over H-ZSM-5 [96]. The authors determined that physisorbed formaldehyde (CH_2=O) and chemisorbed methoxymethyl (CH_3OCH_2OZ) were the most stable species formed from methanol and DME upon interaction with methoxy groups, respectively. They also found feasible energy barriers for the reaction between those intermediates and additional methanol or DME molecules to give products containing C-C bonds. Their proposed reaction pathways are summarized in **Scheme 2.7**. It is important to highlight that these studies suggest a different mechanism at play for methanol and DME towards their interaction with methoxy groups.

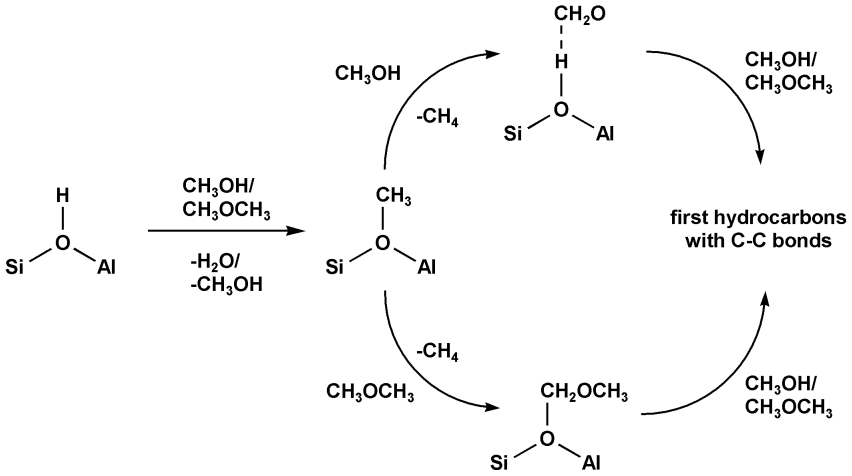

Scheme 2.7. Initial intermediates in the MTH reaction by methanol and DME proposed by Wei *et al.* [96].

In summary, many mechanisms have been reviewed in this section that seek to explain the formation of the first hydrocarbons. Most of the mechanisms proposed in the 1980s seem unlikely to occur according to the prohibitively high energy barriers computed in theoretical calculations. The sophisticated advancement in theoretical methods together with the development of novel experimental methods have started to produce a new wave of proposals for direct mechanisms with plausible energetics. However, it is important to ensure that experimental works are carried out with very pure reactants, since minimal impurities will trigger the formation of hydrocarbons and might mask the targeted goal of the first C-C coupling derived from methanol and/or DME. Importantly, the newly proposed mechanisms resulting from experimental methods have been performed with methanol feeds only. As suggested by Fan and co-workers, it is likely that methanol and DME act differently. Therefore, future experimental studies should tackle the task of investigating the origin of the first hydrocarbons with methanol and DME independently.

2.2.2. Autocatalytic stage of the MTH reaction

The C-C bond formation between C_1 entities in the MTH reaction is kinetically limited. As soon as the concentration of hydrocarbons with C-C bonds arises, methanol and DME conversion is triggered and formation of olefins, paraffins and aromatics is substantially accelerated. Therefore, hydrocarbons act as autocatalytic species. As a consequence, C-C coupling between methanol/DME molecules is largely overshadowed and of little relevance during the steady-state stage of the MTH reaction [49, 103, 104]. The first association between autocatalysis and the MTH reaction was proposed by Chen and Reagan at Mobil in 1979 [105]. They observed a typical autocatalytic S-shaped profile when plotting the conversion of methanol and DME to hydrocarbons versus contact time over H-ZSM-5 catalyst (**Figure 2.5**). The reaction rate is very slow at low conversion levels. When the concentration of products slightly increases, the rate of the reaction rapidly accelerates. Interestingly for this PhD thesis, the authors reported higher conversion levels for DME compared to methanol at similar contact times, but did not comment on this observation.

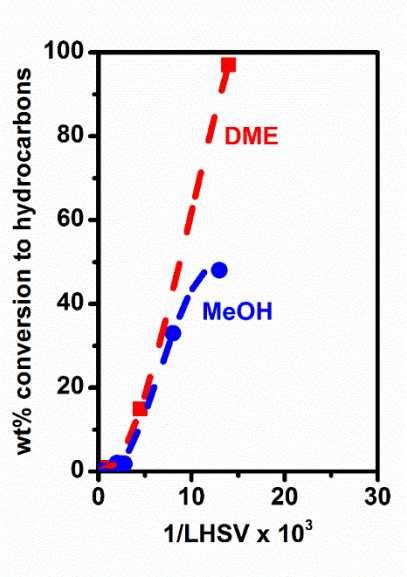

Figure 2.5. Conversion of methanol and DME to hydrocarbons versus contact time (1/LHSV). Adapted from [105].

Ono and Mori also postulated that the conversion of methanol to hydrocarbons proceeds autocatalytically after observing that the addition of ethylene and *cis*-2-butene to a methanol feed greatly enhanced the reaction rate over H-ZSM-5 [92]. A similar conclusion was drafted by Langner *et al*. when co-processing higher alcohols with methanol [106]. The authors then reported a substantial reduction of the initial induction period of the MTH reaction. Dessau and LaPierre described the autocatalysis of the MTH reaction as a sequential methylation of olefins process, followed by either cracking or aromatization to give olefins or aromatics, respectively (**Scheme 2.8**) [107, 108]. In this proposal, the authors envisioned ethylene as a product derived from "re-equilibration" of higher olefins,

while propene and butenes originated from cracking and as initial olefins. Furthermore, aromatics intervened in methylation reactions, generating methylated aromatics, but no other contribution to effluent products was described.

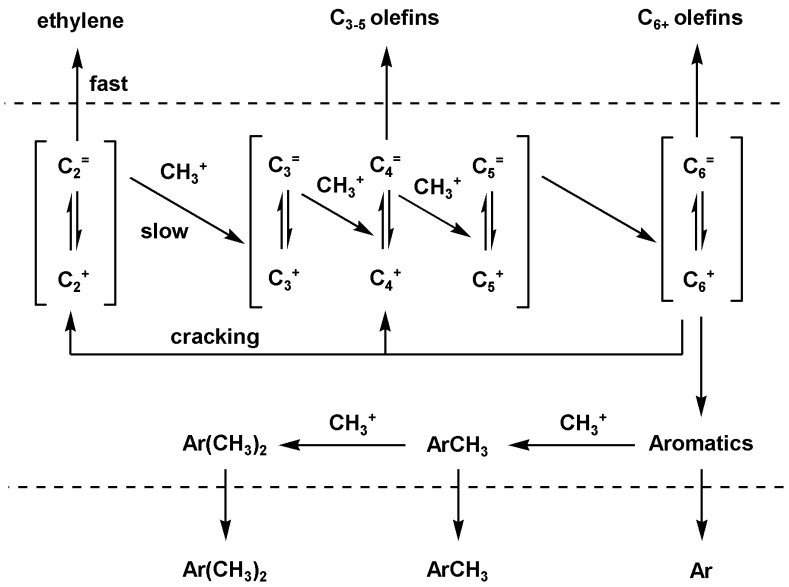

Scheme 2.8. View of the MTH reaction by Dessau and LaPierre: sequential methylation of olefins. Adapted from [107].

Mole and co-workers showed that the autocatalytic effect was also applicable to aromatics, as co-feeding small amounts of toluene, *p*-xylene and cumene with methanol consistently increased the consumption of methanol over H-ZSM-5 [109, 110]. The authors then identified an aromatics-assisted route to ethylene via deprotonated polymethylbenzenes, thereby highlighting the role of aromatics as co-catalysts in MTH via methylation and dealkylation reactions.

In the 1990s, Dahl and Kolboe were responsible for a major breakthrough in the understanding of the MTH mechanism. They performed isotopic labeling studies co-feeding ^{13}C-methanol with ethanol (ethylene precursor) and isopropanol (propylene precursor) over H-SAPO-34, observing that the majority of the fed alkenes were almost unreacted, but the rest of products contained ^{13}C atoms from methanol [111-113]. These results led them to introduce the "hydrocarbon pool" concept simplified in **Scheme 2.9**, since these results were not consistent with the direct olefin methylation mechanisms that had been proposed earlier. Basically, they conceived the pool of trapped hydrocarbons, with overall stoichiometry $(CH_2)_n$, as adsorbate hydrocarbons with "*similar characteristics to ordinary coke*". Methanol is continuously added to the hydrocarbon pool, while olefins are entering and exiting the pool, and paraffins, aromatics and coke were considered as end-products. This vision of the MTH reaction summarized all the indirect synthesis of hydrocarbons earlier proposed in one simple mechanism.

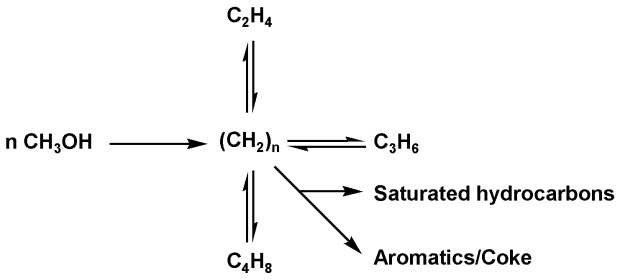

Scheme 2.9. The hydrocarbon pool mechanism proposed by Dahl and Kolboe. Adapted from [113].

The concept of the hydrocarbon pool has prevailed since its proposal to explain the formation of hydrocarbons in the MTH reaction, and subsequent studies have attempted to define the actual chemical composition of the pool, as well as elucidating the mechanisms and kinetics of the reactions preceding and operating the hydrocarbon pool.

The group of Haw commenced the arduous task of identifying active hydrocarbon species within the pool by means of *in-situ* solid-state NMR spectroscopy. Firstly, they observed the presence of a wide range of methyl cyclopentenyl, methyl benzenium cations and neutral cyclic dienes after methanol pulses over H-ZSM-5, and connected these species to the formation of light olefins [114, 115]. The same research group also carried out similar studies over the other preferred MTH catalyst, H-SAPO-34. In marked contrast to H-ZSM-5, the narrow pores of H-SAPO-34 prevent the escape of aromatic hydrocarbons out the structure, facilitating their identification as more persistent species. Importantly, the authors did not observe carbenium ions as in H-ZSM-5, but neutral aromatic species (methylbenzenes and methylnaphthalenes) possibly due to the weaker acidity of H-SAPO-34 compared to H-ZSM-5. Therefore, the authors postulated that well-defined aromatic species, in carbocationic or neutral forms, interact with Brønsted sites to form the active hydrocarbon pool. In the case of H-SAPO-34, ethylene, propylene and linear butenes are observed in the effluent because those molecules are the only ones that can diffuse out through the narrow pores of H-SAPO-34 [116, 117].

With a clearer image of the active pool species, many studies were carried out to elucidate the reactivity of these species to understand the formation of products. With the aid of isotopic labeling experiments, Arstad and Kolboe highlighted the direct role of trapped polymethylbenzenes in the formation of light olefins over H-SAPO-34 [118]. Due to the large size of these molecules, only 12-member ring zeolitic materials allow them to diffuse in and out the framework as observed by Mikkelsen and Kolboe over H-beta [119]. Intelligently, the group of Haw envisioned the possibility to directly feed a wide range of previously identified or potentially active pool hydrocarbons over H-beta, in the presence and absence of methanol. Olefins were produced in all cases, with yields increasing respectively with the number of methyl substitutes in a benzene ring and in the presence of methanol. These findings supported the

formation of light olefins via the side-chain mechanism that had been proposed earlier by Mole and co-workers [109, 110], and led the authors to refine the mechanism as shown in **Scheme 2.10**. The mechanism involves the formation of heptamethylbenzenium cation, followed by deprotonation to 1,2,3,3,4,5-hexamethyl-6-methylene-1,4-cyclohexadiene (HMMC). The exocyclic double bond in HMMC is methylated to form an ethyl side-chain, which is able to be eliminated as ethylene. Deprotonation and methylation might alternatively occur leading to an isopropyl side-chain to be eliminated as propene. An alternative vision of the formation of light olefins via dealkylation reactions was earlier proposed by Sullivan *et al.*[120] in the "paring mechanism", as illustrated also in **Scheme 2.10**. In this case, a heptamethylbenzenium cation is also formed, but a ring contraction to a cyclopentenyl cation with an isopropyl chain is proposed. Propene might be eliminated or reorganized further to eliminate isobutene. Further deprotonation, ring expansion and methylation would lead again to hexamethylbenzene. Recent work by Westgård Erichsen *et al.* strongly supported this route. Heptamethylbenzene with 13C exclusively in the ring positions was fed over the large pore zeolite H-SSZ-24, and the dealkylation products in the effluent reflected an isotopic pattern consistent with the paring mechanism [121]. Experimental and theoretical studies can be found in the literature supporting both mechanisms to explain the formation of light olefins by dealkylation [122-131]. While the leading role of polymethylbenzenes in the hydrocarbon pool mechanism is clearly demonstrated, the exact mechanism through which olefins are formed might vary according to catalyst topology, acidity and even reaction conditions.

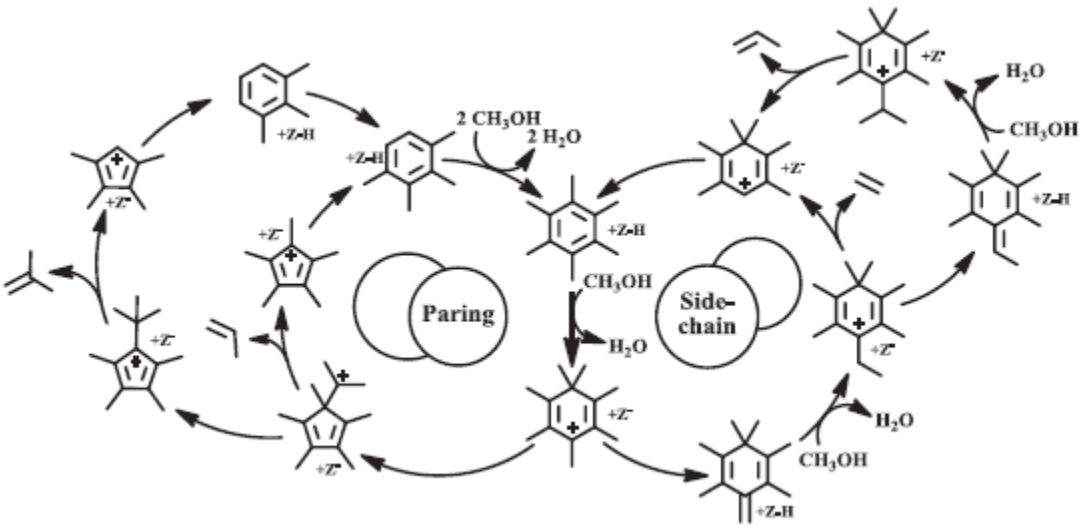

Scheme 2.10. The paring and side-chain mechanisms to explain the role of PolyMBs as active hydrocarbon pool species. Illustration from [132].

The group of Hunger also collected considerable evidence confirming the role of aromatic-type hydrocarbons in the hydrocarbon pool by *in-situ* MAS NMR combined with UV-vis spectroscopy, cementing the hydrocarbon pool concept [133-135]. After years where researchers focused on the important role of aromatic hydrocarbons in the MTH reaction, the group of Olsbye showed that not all olefins are formed via aromatic intermediates. They co-processed isotopically label methanol with higher alcohols over H-ZSM-5, and observed that ethylene presented a different isotopic distribution than the rest of the higher olefins, suggesting a distinct mechanistic origin in the formation of ethylene and the rest of the olefins [136]. In full accordance with this observation, switching ^{12}C-methanol and ^{13}C-methanol as feeds over H-ZSM-5 revealed a faster incorporation of ^{13}C into propene and higher olefins, while the slower incorporation of ^{13}C into ethylene matched well with the isotopic distribution of polymethylbenzenes. These findings led the authors to propose the concept of the dual cycle mechanism, wherein two competing catalytic cycles, governed by alkenes and arenes, comprise the "hydrocarbon pool" and operate simultaneously in the synthesis of hydrocarbon products over H-ZSM-5 [137]. The dual cycle mechanism, represented in **Scheme 2.11**, summarizes many of the findings explained in the previous 30 years of research in one single mechanism.

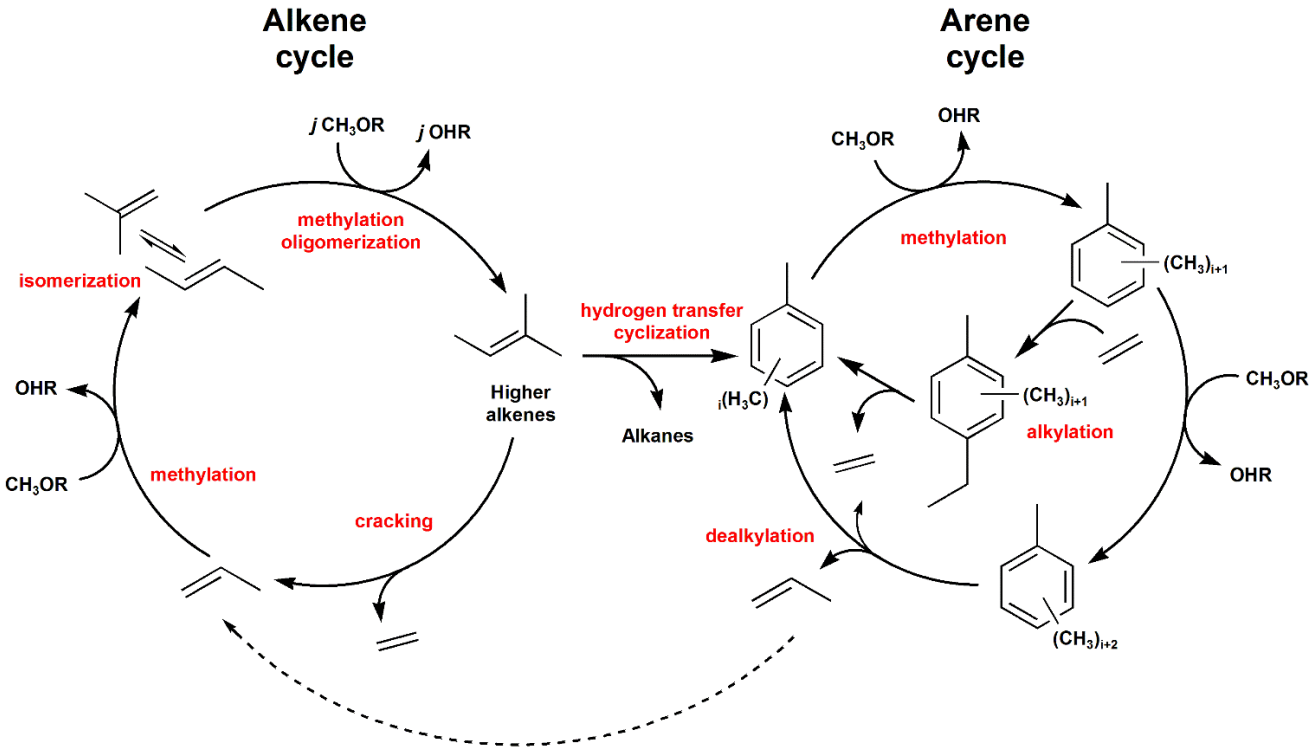

Scheme 2.11. Interpretation of the current understanding of the dual cycle mechanism to explain the autocatalytic- and product-zones of the MTH reaction over zeolitic materials. R = H, CH_3.

On the alkene cycle, methanol and DME are consumed via methylation reactions releasing water and methanol, respectively. Alkene cracking, isomerization, and oligomerization reactions are also conceived in this cycle. On the arene cycle, methanol and DME also intervene as arene methylating agents. Dealkylation and alkylation of arenes are expected in this second catalytic cycle as well. The two cycles are connected via hydrogen transfer and cyclization reactions, wherein higher alkenes form concurrently arenes and alkanes as hydrogen-deficient and hydrogen-rich products, respectively. The dual cycle mechanism rationalizes the autocatalytic stage of the MTH reaction, where methanol and DME react with hydrocarbons, as well as the product reaction zone, where hydrocarbons suffer transformations in the absence of methanol and DME. However, the dual cycle concept does not address the overshadowed initial C-C bond formation and the interconversion reaction between methanol and DME. The different stages of the MTH reaction are reflected in **Figure 2.6**.

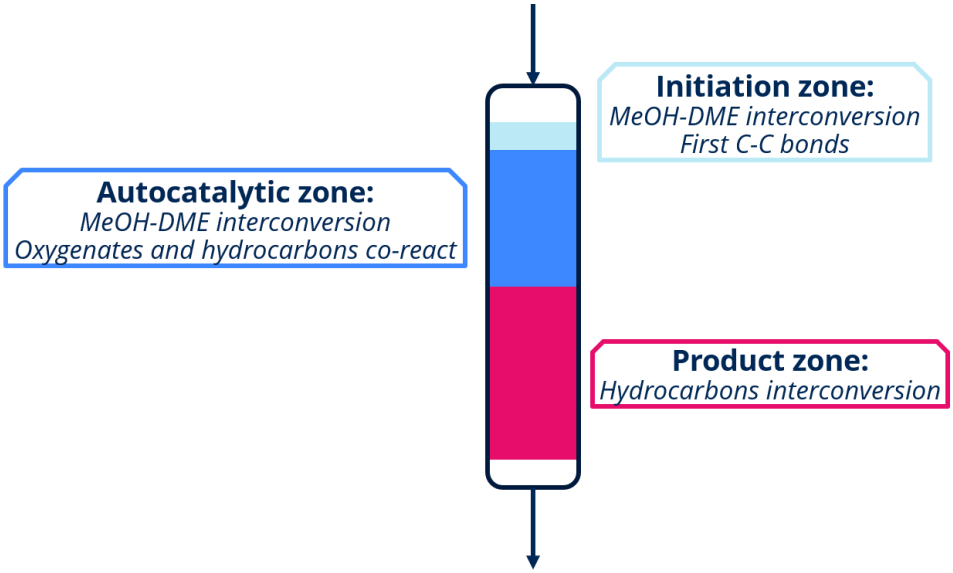

Figure 2.6. Stage of the MTH reaction over zeolitic materals.

The dual cycle concept has been considered the state of the art in the mechanistic understanding of the MTH reaction since 2007. Originally, it was proposed over H-ZSM-5, but the mechanism has been successfully used to explain the operation and product distribution of many other zeolitic structures in the MTH reaction [138-149]. Many studies have attempted to correlate the characteristics of the catalyst (especially topology and acidity) with the relative propagation of the two catalytic cycles, which is fundamental to understand the effluent product selectivities. For instance, catalyst topology has been extensively studied as a key parameter affecting the propagation of either of the two competing cycles. In general, it has been found that zeolites with large pores, such as BEA, MOR, AFI, favor the propagation of the arene cycle compared to medium pores zeolites [119, 150, 151]. The larger pore

apertures of 12-rings zeolites allow the formation and passage of large aromatics like penta- and hexa-methylbenzenes, whose formation and/or diffusion is more suppressed in smaller pores materials. Importantly, the zeolite cavities also play an important role on the relative propagation of the alkene and arene cycles. CHA, a small pore zeolite or zeotype in its industrially relevant SAPO version, presents very large cavities where polymethylbenzenes and naphthalenes are dominating the formation of effluent products [117, 118, 152]. Therefore, the arene cycle prevails in spite of the small pore apertures and only short olefins derived from aromatics dealkylation and linear paraffins diffuse out [117, 153]. In accordance, Bleken *et al*. studied a series of 10-ring zeolites with similar pore apertures and different size of the zeolites cavities, and they reported that polyMBs were more prominent as active hydrocarbon pool species in the materials with larger cavities [139]. The testing of other 10-ring zeolites with an absence of cavities, TON and MTT, which are characterized by straight channels, resulted in almost complete suppression of the arene cycle. The product effluent was dominated by C_{5+} aliphatics in the range of the gasoline fraction, but interestingly aromatics-free [64, 154-157]. Therefore, the specific dimensions of pore channels and cavities, inherent to every zeolitic topology, set spatial constraints that play an important role in directing the dominant catalytic cycle in MTH.

Another characteristic of the catalyst with mechanistic implications is the acidity of the catalyst, *i.e.* using zeotypes instead of zeolites. Westgård Erichsen *et al*. compared two isostructural materials with AFI topology, the strongly acidic zeolite H-SSZ-24 and the moderately acidic zeotype counterpart, H-SAPO-5. Notably, these materials are considered to be model materials to study the effect of acid strength because the large pore apertures and straight channels facilitate the diffusion of large molecules. The authors observed that the stronger acid, H-SSZ-24, showed a product distribution richer in hydrocarbons derived from the arene cycle compared to H-SAPO-5 during MTH operation. Using isotopically labeled methanol reacted with benzene, it was revealed that the incorporation of ^{13}C from methanol in C_2-C_4 olefins was faster over H-SAPO-5. These results were consistent with a higher prevalence of the alkene cycle in the weaker acid, H-SAPO-5, compared to H-SSZ-24 [141]. Bleken *et al*. compared H-SSZ-13 and H-SAPO-34, both with CHA topology. The resulting differences in product selectivities were not large because the aromatic cycle prevails in this topology. Interestingly, however higher ethylene to propylene ratios were observed in the stronger acid material [153]. It should be noted that ethylene is predominantly derived from aromatics dealkylation [49, 137]

Furthermore, acid site density and the location of acid sites have been studied as parameters affecting the propagation of the alkene and the arene cycles. Bhan and co-workers carried out MTH tests over a series of H-ZSM-5 samples with different aluminum content, and observed that ethylene selectivity

monotonically increased with the density of aluminum, and thereby concluded that a high number of actives sites propagates the arene cycle in relation to the alkene cycle [158]. In addition, Liang *et al*. have recently revealed that sites located at the intersections of H-ZSM-5 catalysts also enhance the promotion of the arene cycle compared to sites located in the channels, possibly due the larger space available to form and fit aromatics [159].

Considering that the arene cycle is promoted over the alkene cycle due to hydrogen transfer reactions, one might envision that spatial constraints and acidity are key to understand the propagation of the arene cycle. In general, it has been observed that larger space available in the channels and cavities, strong acid strength, high acid site density and sites located in intersections will propagate the arene cycle and its products.

Apart from the catalyst itself, process conditions also affect the MTH mechanism. For instance, high temperatures are commonly use to favor the formation of light olefins. Indeed, MTO and MTP processes are carried out at higher temperatures than MTG (450-500 °C versus 350-400 °C). Olsbye *et al*. showed that thermodynamics will favor the formation of alkanes and aromatics at high temperatures [81]. Increasing temperatures will increase the kinetics of all reactions and will lead to a less-kinetic dependence on product formation. Therefore, more thermodynamically stable hydrocarbon molecules (aromatics and alkanes) are formed with lower kinetic constraints. This means that a larger proportion of aromatics might be present in the active hydrocarbon pool at high temperatures, thereby promoting light olefins formation via aromatics dealkylation reactions. The process conditions can be also altered by co-feeding hydrocarbons. Ilias *et al.* co-fed propylene and toluene with DME over H-ZSM-5 at 275 °C, reporting that propylene propagated the alkene cycle, while toluene co-feed propagated the arene cycle [142]. Similar conclusions were reached by Sun *et al.* at more relevant industrial conditions, 450 °C, although the effect was reduced [160].

In summary, the level of understanding of the MTH reaction has greatly increased since its discovery in 1977, but we are still far from a complete comprehension of this complex reaction. It is clear that the selection of the catalyst and process conditions strongly influence the reaction mechanism, and consequently the product distribution as well as catalyst deactivation, which will be discussed in the following subsection. As shown in **Scheme 2.12**, a more well defined kinetic and mechanistic description of the reactions taking place in the hydrocarbon pool is needed in order to gain further understanding of the process, and will be useful to optimize industrial MTO, MTP and MTG processes.

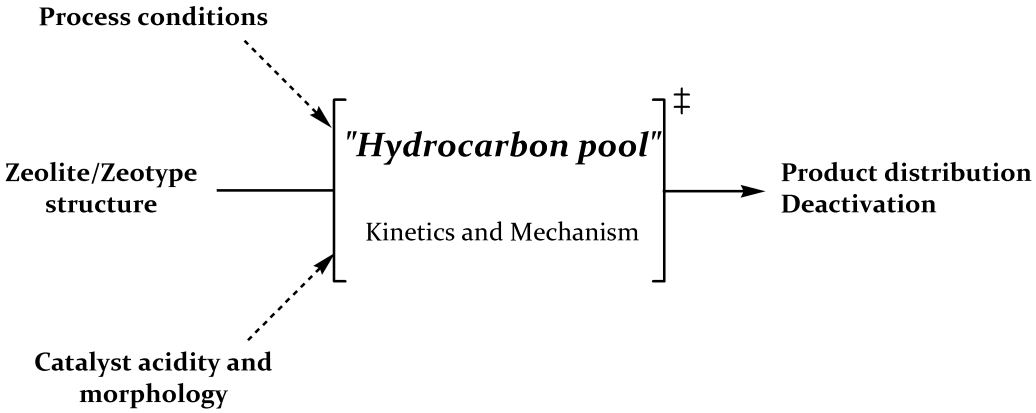

Scheme 2.12. Vision of the parameters influencing the MTH reaction.

2.2.3. Catalyst deactivation

One of the major challenges in the conversion of methanol and DME to hydrocarbons over zeolitic materials is deactivation by coking. Deactivation of MTH catalysts correlates with the formation of (poly-)aromatic coke precursor molecules, which eventually block the pores and active sites and are gradually converted to graphitic type coke [81].

For H-ZSM-5, one of the core catalysts in this PhD thesis, it has been observed that coke formation starts in the first part of the catalyst bed and progresses towards the outlet with time on stream, leading to an inverse S-shaped conversion versus time-on-stream curve [45, 83, 161]. Since the concentration of methanol is high in the first part of the catalyst bed, this suggests that methanol is directly involved in the formation of carbon deposits. A kinetic model based on the assumption that the deactivation rate is proportional to methanol conversion, resulted in a good description of the deactivation and catalyst life time of H-ZSM-5 catalyst [162]. The correlation between methanol conversion and deactivation rate could be ascribed to the formation of coke precursor molecules in a reaction between methanol and the hydrocarbon moieties in the zeolite.

Recent studies suggested that deactivation of MTH catalysts, in which the reactants are the dominant source of coke, might be related to formaldehyde or similar intermediates formed via Reactions (2.1, 2.2, 2.3) [90, 96, 101, 163-165].

$$2\ CH_3OH \rightarrow CH_2O + CH_4 \quad (2.1)$$

$$CH_3OH \rightarrow CH_2O + H_2 \quad (2.2)$$

$$CH_3OH + C_nH_{2n} \rightarrow CH_2O + C_nH_{2n+2} \quad (2.3)$$

Indirect evidence for Reaction (2.1) was revealed by the observation of methane in the reactor effluent at the outset of testing H-ZSM-5 at 250-350 °C [83]. Hutchings *et al*. co-fed formaldehyde with DME to demonstrate that the more hydrogen deficient formaldehyde molecule promoted much faster catalyst deactivation than DME alone [166]. The authors suggested that formaldehyde is formed in the course of the MTH reaction and promotes polymerization of hydrocarbons, thereby enhancing coking rates. Later, the feasibility of Reaction (2.1) via a methoxy intermediate and methanol (not DME) was confirmed by theory, and it was earlier discussed as the first feasible step in the methane-formaldehyde mechanism to explain the formation of the first olefins [90, 96, 167, 168]. Even so, this proposal received little attention by experimental groups during the last two decades, until the Lercher group recently published two papers that emphasize the specific role of methanol as a source of coke formation in MTH. Sun *et al.* co-fed methanol with butanol over H-ZSM-5 at 475 °C and observed a significant increase in carbon conversion capacity with increasing butanol content in the feed [169]. Subsequently, Müller *et al.* compared the time-on-stream behavior of a fixed bed plug flow reactor (PFR) and a continuously stirred tank reactor (CSTR) for methanol conversion over H-ZSM-5 at 450 °C, and observed substantially higher deactivation rate in the PFR [163]. In both studies, the authors ascribed the enhanced deactivation rate to the progress of Reaction (2.1) or similar methanol decomposition reactions in the first layers of the catalyst bed in a plug flow reactor, where methanol-methanol reactions are not out-competed by faster methanol-hydrocarbon reactions [163, 169]. Subsequently, Müller *et al*. suggested that Reaction (2.3) can occur over Lewis acid sites after feeding methanol over H-ZSM-5 samples with increasing Lewis acidity, and observing that the yields of alkanes increased over the samples with larger amounts of Lewis sites [164].

Methanol may also react with mono- and polycyclic aromatic compounds to form additional aromatic rings, as exemplified by Reaction (2.4). Methylation and hydride transfer reactions are important in this type of coking process. However, the mechanism leading to the extra aromatic ring has not been fully revealed. Finally, methanol may react with "coke", either by hydrogen transfer or methylation, as in Reactions (2.5, 2.6) [83, 122, 170, 171]:

$$C_6(CH_3)_6 + CH_3OH \rightarrow C_{10}H_5(CH_3)_3 + H_2O + 6\text{"H"} \quad (2.4)$$

$$\text{Coke (saturated)} + CH_3OH \rightarrow \text{Coke (unsaturated)} + CH_4 + H_2O \quad (2.5)$$

$$\text{Coke} + CH_3OH \rightarrow \text{Coke-}CH_3 + H_2O \quad (2.6)$$

If deactivation is driven by the reactants, the deactivation pattern progresses from the entrance towards the exit of the plug flow reactor as shown in **Figure 2.7** (left) [83, 172, 173], thus creating a reaction front that moves through the reactor with time on stream. However, it may be difficult to differentiate between the case where the reactant alone is driving deactivation (Reactions (2.1, 2.2)) and the case where reactions between the reactant and various products are the main cause of deactivation (Reactions (2.3, 2.4, 2.5, 2.6)), as the deactivation patterns are similar.

An alternative view to deactivation has been reported where products dominate the coking process. Reactions between only hydrocarbon pool species, such as Reaction (2.7), may lead to larger products that get trapped within the pore network [122, 172].

$$C_6H_4(CH_3)_2 + 2\ C_3H_6 \rightarrow C_{10}H_4(CH_3)_4 + 6\ \text{"H"} \qquad (2.7)$$

Typically, large pore-size zeolites, such as H-Beta* and H-MOR, show this type of deactivation. Interestingly, deactivation of these materials does not show a moving reaction front, but is more homogeneous along the catalyst bed, as illustrated in **Figure 2.7** (right) [81, 161].

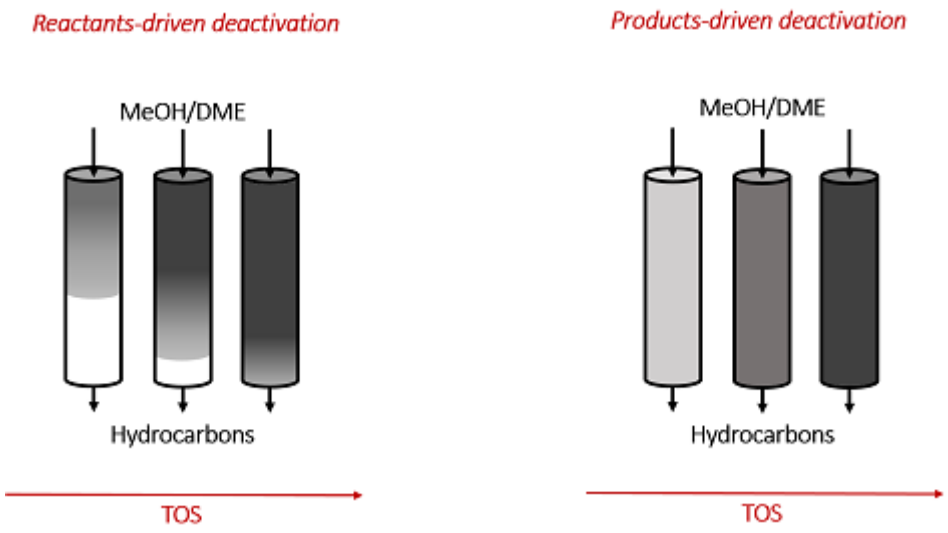

Figure 2.7. Typical MTH deactivation profiles where reactants or reactants/products induce deactivation (left) and mainly products induce deactivation (right).

Importantly, a few studies have attempted to compare methanol and DME as MTH feedstocks and their effect on catalyst deactivation [174-176]. It has been observed that DME is converted to hydrocarbons more slowly over H-SAPO-34 compared to methanol. As a results, it was proposed that a slower build-up of the hydrocarbon pool occurred with DME as feedstock due to the slower diffusion of DME relative to methanol, since the intrinsic rate constants for methanol and DME conversion were similar [174].

Correspondingly, this slower build-up of hydrocarbons in the confinements of the pores and cavities of H-SAPO-34 was suggested to be the cause for the slower deactivation rates observed for DME feed as compared to methanol feed [174-176]. For H-ZSM-5, it has been reported that DME is converted to hydrocarbon more quickly than methanol, but there has not yet been a thorough deactivation study comparing both oxygenates [47, 105]. Remarkably, the group of Bilbao has shown that addition of methanol and water to a DME feed over H-ZSM-5 interestingly leads to lower initial activity of the catalyst, thereby supporting faster MTH kinetics for DME compared to methanol [177, 178]. Furthermore, adding water to methanol or DME feeds has been shown to have a positive effect in catalyst stability over different zeolitic catalysts [177-182], very likely due to the strong competition of water with methanol, DME and hydrocarbons for the acid sites, and therefore helping to avoid the retention of coke molecules [183].

The group of Bilbao studied the effect of binders combined with H-ZSM-5 catalysts on the conversion of DME to hydrocarbons [184]. They used bentonite and boehmite as binders, that upon calcination can be transformed into weakly acidic aluminas. The authors reported that the use of boehmite doubled the acidity obtained with bentonite, and resulted in higher initial activity as well as higher “pseudo-stable” conversion levels.

2.3. Relevant reactions to this work

2.3.1. Methanol and DME interconversion

As the work presented in this PhD thesis focuses on the role of methanol and DME in the MTH reaction, it is highly relevant to discuss the interconversion reaction between methanol and DME as in Reaction (2.8). It is believed that both oxygenates act primarily as methylating agents of alkenes and arenes in MTH, contributing to the growth in size of hydrocarbons as in Reactions (2.9, 2.10), but they are also interconverted simultaneously:

$$2\ CH_3OH \leftrightarrows CH_3OCH_3 + H_2O \quad (2.8)$$

$$CH_3OH + RH \rightarrow RCH_3 + H_2O \quad (2.9)$$

$$CH_3OCH_3 + RH \rightarrow RCH_3 + CH_3OH \quad (2.10)$$

As pointed out by Keil [45], it has been generally accepted that methanol dehydration, and consequently, formation of methanol from DME and water, is considered to be a much faster reaction than other MTH reactions over zeolitic materials. As a consequence, methanol and DME have been assumed to be in thermodynamic equilibrium during MTH, and both species are lumped together as reactants with analogous behavior. In an intense search of the literature, only one article was found in which thermodynamic equilibrium is clearly illustrated [59]. This study was carried out at Mobil over their commercial catalyst, therefore the H-ZSM-5 based catalyst probably contained slightly acidic alumina used as binder. The authors showed that uncompleted methanol conversion in a fluidized bed reactor led to nearly thermodynamic concentrations of DME and methanol in the reactor effluent. No reference is given to the temperatures and pressures used in that particular experiment. Based on the results obtained in this thesis, that will be shown in **Chapter 4**, it is tempting to speculate that industrially-used binders might play a role on methanol-DME interconversion.

Industrially, DME synthesis from methanol or syngas is typically carried out over metal-based catalysts, $Cu/ZnO/Al_2O_3$ [185]. Nevertheless, the use of solid acids as catalysts have been also receiving attention. It is well-known the capacity of γ-alumina, aluminas modified with phosphorous or silicon, zeolites and zeotypes in catalyzing methanol dehydration at lower temperatures than MTH temperatures (200-300 °C) [186-196]. It is therefore worth mentioning that commercial MTH pelletized catalysts are typically formed by the zeolite/zeotype structure together with alumina as binder to enhance the mechanical strength of the industrial catalyst and facilitate its shaping into pellets or extrudates. Kim *et al*. evaluated the catalytic properties of γ-alumina and Na-ZSM-5 catalysts on methanol dehydration, and reported

that methanol readily dehydrates to DME above 200 °C over Na-ZSM-5, while γ-alumina became very active above 320 °C [196]. Considering that industrial MTG, MTO and MTP processes proceed above 350 °C, it is consequential to conclude that the binder used in commercial catalysts will also participate in methanol-DME interconversion, but will be almost inactive to MTH chemistry. Importantly, most reported research studies at laboratory scale use only the zeolitic catalyst, assuming methanol-DME equilibration. This assumption must be further evaluated. Due to the lack of literature concerning the traditional assumption of methanol and DME thermodynamic equilibrium in MTH, and the particular interest of this PhD thesis on assessing the behavior of methanol and DME as reactant molecules in MTH, a thorough study will be reported in the **Section 4.1** using methanol and DME feeds over zeolite and zeotype materials.

The use of H-ZSM-5 as methanol dehydration catalyst has a limited temperature application because hydrocarbons commence formation above 260 °C [197, 198]. Jiang *et al*. reported near thermodynamic concentrations of DME synthesized below that temperature over H-ZSM-5 [198]. Dai *et al*. evaluated the performance of a series of unidimensional SAPO and AlPO materials, including H-SAPO-5 and AlPO-5, which are used in this PhD work. Due to the lower acidity of these materials compared to zeolites, the authors were able to work up to 400 °C with lower amounts of hydrocarbons formed via MTH. The SAPO materials were active in methanol dehydration above 200 °C, however hydrocarbon formation began already at 250 °C and became dominant at higher temperatures. Interestingly, AlPO materials, which lack strong Brønsted acidity, converted methanol to DME with selectivities around 99 % up to 400 °C. The activity of AlPO materials was then attributed to very weak acid sites, likely P-OH groups [193]. No reference to thermodynamics was given in this work.

2.3.2. Methylation reactions

Methylation of alkene and arene hydrocarbons is an important reaction occurring in MTH, where methanol and DME are consumed, and implies the incorporation of a methyl group into the alkene and arene products, resulting in the growth of hydrocarbon molecules.

Two alternative mechanistic pathways have been proposed to explain hydrocarbon methylation over zeolitic materials: the concerted and the stepwise mechanisms [199-202], also called co-adsorbed and surface-methoxide mechanisms. They are illustrated in **Scheme 2.13** for propene, but it should be noted that a similar mechanism is proposed for other alkenes and arenes. In the concerted mechanism, methanol or DME co-adsorb with a hydrocarbon and react in a single step to form a methylated product and H_2O or methanol, respectively. Alternatively, in the stepwise mechanism, methanol or DME first

react unimolecularly on the acid site to form water and a methoxy group. This methoxy group can subsequently act as a methylating agent.

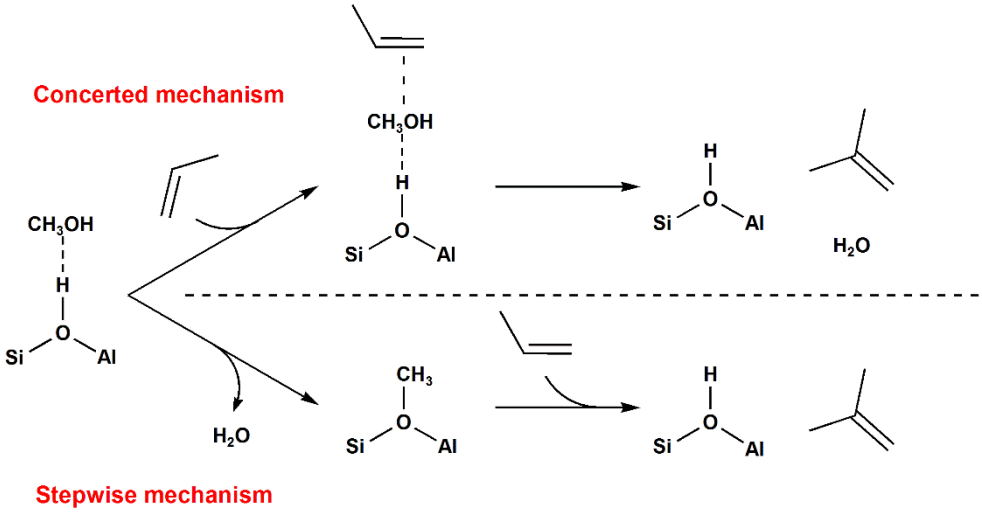

Scheme 2.13. Representation of the concerted and stepwise mechanisms for hydrocarbon methylation illustrated for propene and methanol. Analogous mechanisms are expected for other alkenes or arenes as hydrocarbons and DME as methylating agent.

Numerous studies over the past decades have aimed at elucidating the effects of hydrocarbon size and class, zeolite topology, acid strength, and active site environment on the intrinsic and apparent activation energies as well as pre-exponential factors for the different reaction steps involved. Svelle *et al.* measured the rates of ethene, propene and *n*-butene methylation with methanol over H-ZSM-5 at high space velocities to minimize by-product formation [203, 204]. An increase in alkene size consistently increased the rate and decreased the intrinsic activation energies (135, 110 and 90 kJ/mol for ethene, propene and *n*-butene, respectively). The apparent rate constants follow the trends in theoretical studies carried out by means of a small cluster model consisting of four T-atoms [205], and also with *a posteriori* work by Van Speybroeck *et al.* and Svelle *et al.* with state of the art computational methods [206, 207], reflecting the effect of alkenes size in zeolite-catalyzed methylation reactions. A higher methylation rate with increased size (ethylene, propylene) and branching (1-butene, *cis*-2-butene, *trans*-2-butene, isobutene) of the hydrocarbon molecules has also been found with DME as the methylating agent for H-FER, H-ZSM-5, H-MOR, H-BEA* catalysts [208, 209]. Analogous trends have been reported for arene methylation with apparent activation barriers decreasing with the number of methyl substituents connected to the aromatic ring [199, 202, 210-212]. For instance, the rate of methylation of benzene, toluene and xylenes over microporous and mesoporous H-ZSM-5 crystals becomes faster for larger arenes. However, xylene rates were strongly influenced by the reaction conditions and this phenomenon was ascribed to possible diffusion limitations or a distinct methylation

mechanism at play with respect to benzene and toluene methylation [210]. A diffusion limitation effect has been proposed by Lercher and co-workers who studied toluene, xylene and tri-methylbenzene methylation in large pore-size (H-BEA*, H-MOR) and medium pore-size (H-ZSM-5, H-ZSM-11) zeolites. They suggested that reaction rates can decrease if the size of products is bulky enough to slow down product diffusion as observed in the narrower pores of H-ZSM-5 and H-ZSM-11 [213]. Lesthaege *et al.* pointed out that the deviations in the methylation rate for larger molecules also could be due to a change in the reaction mechanism due to a transition-state shape selectivity [214].

The effect of zeolite topology during benzene methylation by methanol was studied in H-ZSM-5 and H-BEA* by Van der Mynsbrugge and co-workers [200]. Two-fold higher methylation rates were observed in H-ZSM-5 compared to H-BEA* zeolite. Theoretical calculations suggest that the stronger stabilization of the transition state is the cause for the higher activity in H-ZSM-5. Van der Mynsbrugge *et al.* pursued the effects of zeolite topology by studying very distinct zeolites, H-ZSM-58, H-ZSM-22, and H-ZSM-5, as alkene methylation catalysts using DFT methods [215]. They predicted that the methylation rates of ethene, propene and 2-butene were 3 orders of magnitude higher over H-ZSM-5 than over H-ZSM-58 or H-ZSM-22. The high enthalpy barriers in the large cavities of H-ZSM-58 (with weak transition-state stabilization) and the high entropic barriers in the narrow channels of H-ZSM-22 (because of steric hindrance) were reported to be responsible for the pronounced differences. The role of acid strength on zeolite-catalyzed methylation reactions has been recently studied by Westgård Erichsen *et al.* by comparing propene and benzene methylation over highly acidic H-SSZ-24 and weakly acidic H-SAPO-5 [43]. While both hydrocarbons were methylated at similar rates over H-SAPO-5, benzene methylation was significantly faster than propene methylation over H-SSZ-24.

Even though most kinetic studies of methylation reactions are performed at low conversion levels to minimize by-product formation, the microporous structure and high reactivity of zeolitic materials promote the rapid arise of secondary reactions. For instance, typical by-products observed during co-reactions of MeOH/DME with benzene or toluene are polymethyl benzenes (polyMBs) and light olefin products, following the dual-cycle mechanism in **Scheme 2.11** [49, 200, 213, 216].

Only a few studies exist that have compared methylation reactions by methanol and DME. Apart from one theoretical study by Maihom *et al.* [217], these studies report DME as more reactive than methanol over H-ZSM-5 [218, 219]. This difference in reactivity is not fully understood yet, as the chemistries of methanol and DME in zeolite-catalyzed hydrocarbon reactions are closely related. An analogous mechanistic role is generally assumed for methanol and DME during methylation reactions [217, 218, 220].

DFT calculations on alkene methylation reactions in H-ZSM-22 have shown that DME stabilizes the methylation transition states to a larger extent than methanol during a concerted methylation due to an increased entropy effect and additional electrostatic stabilization in comparison to methanol when the gas phase reactants are the reference state, again leading to faster methylation rates [219]. Regarding stepwise methylation, the formation of methoxide is the distinct step between both oxygenates. Van der Mynsbrugge *et al.* reported slightly higher free energy barriers for unassisted methoxide formation for methanol (160 kJ/mol) than for DME (143 kJ/mol) at 397 ºC over H-ZSM-5 [221], and this effect might lead to different coverages of methoxy groups when using DME or methanol. However, the second step of the methylation is identical, as a methoxide reacts with an alkene or arene. Both mechanisms are assumed to occur during zeolite-catalyzed methylation reactions and the occurrence of one or the other mechanism has been shown to depend on the zeolite topology and reaction conditions. Further work regarding the competition of both mechanisms is found in [43, 192, 199, 219, 221].

In summary, the methylation activity for DME is predicted to be higher than that of methanol in most studies in the literature. However, further studies comparing the two oxygenates are needed to better understand the kinetics and mechanisms of methylation reactions. **Sections 4.3** and **4.4**, and Papers I and III thoroughly analyze methanol and DME as methylating agents for benzene and isobutene.

2.3.1. Hydrogen transfer reactions

Hydrogen transfer reactions are also important in MTH because they are considered to occur as part of the connection between the alkene and the arene cycles, and are responsible for the formation of alkanes (**Scheme 2.11**). The hydrogen transfer reactions over solid acid catalysts are described as bimolecular reactions, occurring via carbocationic transitions states. A hydrogen atom is transferred between an adsorbed alkoxide (normally derived from an alkene) and a cyclic/acyclic alkane or an alkene [48, 222]. In the context of the MTH reaction, it has been assumed until recently that alkenes act as hydrogen transfer reactants, leading to alkanes and dienes/trienes, which are precursors of aromatics [48, 223-226]. Therefore, while methylation is viewed as a chain growth reaction, hydrogen transfer is a chain termination reaction, which results in a change of hydrocarbon type (alkene to alkane). The extent of hydrogen transfer in MTH alters the concentrations of alkenes and arenes, and thus, affects the relative propagation of the two cycles. A classical approach to measure the extent of hydrogen transfer reactions in MTH is the hydrogen transfer index (HTI), defined as the ratio of alkanes over alkanes plus alkenes [52, 119, 142, 159, 227-229], which can be a useful descriptor of the dominating catalytic cycle, taking into consideration that deactivation and conversion levels can affect the HTI.

The application of experimental methods to gain mechanistic and kinetic information on hydrogen transfer reactions has been very limited due to the challenges in isolating hydrogen transfer reactions from any other interfering reactions. Indeed, methylation, oligomerization, isomerization and/or cracking reactions can occur simultaneously in a competitive manner with hydrogen transfer in hydrocarbon transformations over zeolitic materials, as shown in **Scheme 2.14** [230-232]. Theoretical methods have proven successful to better understand hydrogen transfer and complement the more challenging experimental results. For instance, DFT methods were applied by Kazansky *et al*. and Boronat *et al*. to show that branched alkanes are better hydrogen donors than their linear counterparts due to more stable carbocationic intermediates [233, 234], although alkanes are generally considered fairly inactive in MTH compared to alkenes and aromatics. Furthermore, theoretical methods have also shown that alkenes can get protonated over Brønsted sites forming carbenium ions at typical MTH conditions [235], and these species can be involved in hydrogen transfer reactions. It has been found that the stability of tertiary carbenium ions is considerably higher than the stability of secondary and primary carbenium ions [235, 236].

The group of Iglesia carried out a series of insightful experimental studies to better understand hydrogen transfer reactions over solid acid catalysts. The authors co-fed label-marked DME with linear and branched C_3-C_8 alkenes over mesoporous solid acids (SiO_2-Al_2O_3, $H_3PW_{12}O_{40}/SiO_2$) and acidic zeolites (BEA, FAU, MFI) at relatively low temperatures, 200 °C. In this way, they examined the effects of acidity and solvation effects of the zeolites on the competitive methylation, hydrogen transfer, isomerization and cracking reactions illustrated in **Scheme 2.14** [230, 232]. It was observed that methylation of C_3-C_7 alkenes occurred selectively, maintaining a four-carbon backbone structure (isopentene, 2,3-dimethylbutene, triptene). Cracking reactions largely increased when C_8 alkene was co-fed, but remained as a minor reaction for C_3-C_7 alkenes. Hydrogen transfer activity became the dominant pathway only when co-feeding isobutene and triptene with DME, which was ascribed to the high stability of the intermediate tertiary carbocations, derived from the most branched alkenes as compared to the rest of alkenes. Similar trends were observed for all zeolitic and non-zeolitic materials, and they hypothesized that despite the fact that the relative rates of hydrogen transfer to the other reactions depend on spatial constraints over the zeolites, methylation (chain growth) and hydrogen transfer (chain termination) are mostly guided by the stability of the carbenium ions rather than solvation effects [230, 237]. In the same series of studies, Iglesia and co-workers observed some differences between the large pore zeolites (BEA and FAU) and the medium pore zeolite (MFI) concerning the competitive pathways presented in **Scheme 2.14**. Hydrogen transfer rates increased more than methylation rates over MFI because of the higher presence of effective hydrocarbon species that are able to promote

hydrogen transfer reactions [230]. The acid strength also affected the probabilities for hydrogen transfer, and the studies clearly reflected that the strongest acid catalyst, $H_3PW_{12}O_{40}/SiO_2$, favored hydrogen transfer compared to the rest of catalysts.

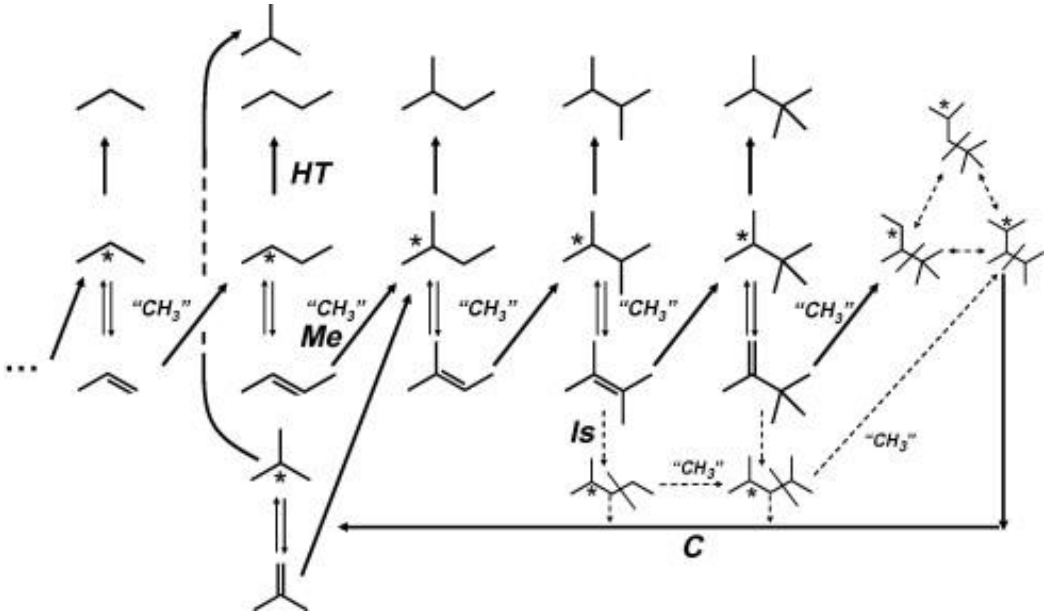

Scheme 2.14. Vision of competitive methylation (Me), isomerization (Is), cracking (C) and hydrogen transfer (HT) reactions over zeolites with alkoxides as common intermediate. The asterisk refers to the position of alkoxide attachment to the zeolite surface. Reproduced from [232] with permission.

Furthermore, Iglesia and co-workers co-fed DME with propene over H-BEA at 200 °C in the presence of adamantane, which has been shown as a hydrogen transfer co-catalyst in homogeneous and heterogeneous catalysis [231, 238]. The authors reported that the sequential methylation of alkenes was reduced in the presence of adamantane because the co-catalyst promoted hydrogen transfer of the alkenes to more inactive alkanes. Basically, adamantane acts as a reversible hydrogen shuttle, donating first a H atom to bound alkoxides derived from alkenes to form alkanes, and subsequently, adamantyl cations can abstract a hydride from an alkane to form a new alkoxide, that might desorb as an alkene. Therefore, adamantane enables the activation of alkanes, but concurrently increase the probability of early chain termination [231].

Very recently, the group of Lercher identified a second hydrogen transfer route in MTH [164, 169]. The authors fed methanol over H-ZSM-5 while varying contact times to reach different methanol conversion levels. The yields of hydrogen transfer products linearly depended on the level of methanol conversion, reaching a maximum in the range of full conversion. Once methanol was depleted, only products were present and a minor increase in hydrogen transfer product yields was measured. This observation led Lercher and co-workers to conclude that the formation of alkanes (and aromatics) in MTH is ascribed

to a reaction where methanol-derived one carbon atom species intervene, naming it as methanol-induced hydrogen transfer (MIHT). Therefore, only a minor contribution of the conventionally assumed hydrogen transfer pathway between olefins, the olefins-induced hydrogen transfer (OIHT), contributes to formation of alkanes and aromatics [169]. In a follow-up study, Müller *et al*. revealed mechanistic details of the two hydrogen transfer pathways [164]. The OIHT pathway was evaluated by feeding 1-hexene over H-ZSM-5 samples with different concentrations of Brønsted and Lewis acid sites. Higher conversion levels were achieved with increasing Brønsted site concentration, and the yield of hydrogen transfer products varied in a similar way. This led the authors to conclude that OIHT is driven by Brønsted sites. The MIHT pathway was evaluated by feeding methanol over a series of H-ZSM-5 samples with similar concentration of Brønsted sites, but different Lewis sites amounts. Under similar conversion levels, larger yields of hydrogen transfer products were observed for samples with higher concentration of Lewis sites, suggesting a specific role of this sites in hydrogen transfer reaction. The detection of formaldehyde formed in MTH in previous studies by the same group [101], led them to propose that MIHT occurs between methanol and alkenes on Lewis sites to give formaldehyde and alkanes as shown in **Scheme 2.15**. In this series of studies, methanol was therefore identified as the main character in the hydrogen transfer reaction. However, no role on hydrogen transfer reactions has been given to DME, which is also present in MTH and has been traditionally assigned an analogous behavior to methanol.

In agreement with the reported hydrogen transfer activity of Lewis sites by the group of Lercher, Sazama *et al*. earlier observed that Lewis acidity by extra-framework aluminum in H-ZSM-5 catalysts promoted the formation of alkanes and aromatics in the MTH reaction [239]. In accordance, Wichterlová et al. studied isomerization of n-butenes over ferriarites, and observed that alkane by-products, formed via hydrogen transfer reactions, were promoted by the presence of LAS. The authors hypothesized that LAS enhanced the strength of BAS to promote hydrogen transfer [240].

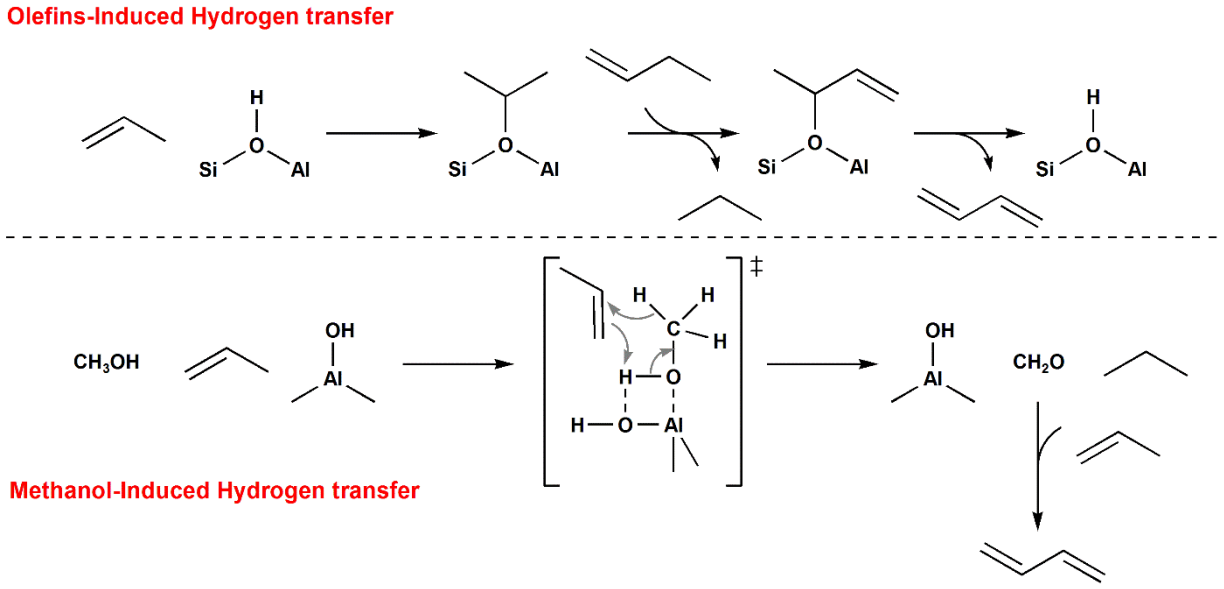

Scheme 2.15. Proposed hydrogen transfer routes via olefins (OIHT) and methanol (MIHT) occurring in MTH in the formation of alkanes. Adapted from [164].

In summary, the latest literature on hydrogen transfer in MTH has revealed a new mechanistic understanding of these reactions; however, the acquisition of precise kinetic data is still an outstanding challenge. It has been demonstrated that the key role of methanol is to directly participate in hydrogen transfer reactions as a hydrogen donor, thereby being oxidized to formaldehyde. MIHT reaction has been proven on samples with both BAS and LAS, and trends suggest their promotion with LAS concentration. However, no evidence has been shown to prove that only LAS are capable of catalyzing hydrogen transfer reactions in MTH.

Section 4.4 and Paper III in this PhD thesis place emphasis on determining the ability of methanol and DME to participate in hydrogen transfer reactions with isobutene from both experimental and theoretical perspectives. **Sections 4.4** and **4.5** briefly discuss possible routes in the formation of aromatics from alkenes in MTH.

Chapter 3

Experimental Methods

3 Experimental methods

3.1. Materials

The materials used in this PhD thesis are commercially available or have been synthesized by other members of the group at University of Oslo. Briefly, two different H-ZSM-5 catalysts have been used: the first sample was obtained from Zeochem (PZ2-100H), whereas the second material was prepared with a nanosheet morphology by reproducing the protocol described by Ryoo and co-workers [37]. Both materials have been extensively characterized in previous contributions from the group [173, 241, 242]. Additionally, three isostructural AFI materials have been utilized throughout this dissertation: H-SSZ-24, H-SAPO-5 and AlPO-5. All of them were synthesized in the group. H-SSZ-24 and H-SAPO-5 have been earlier characterized and tested in different reactions in previous works [132, 141]. A summary of the main properties of the catalysts is found in **Table 3.1**. Dr. Bjørn Tore Lønstad Bleken prepared H-ZSM-5 nanosheets, Dr Marius Westgård Erichsen synthesized H-SSZ-24 and H-SAPO-5, while Magnus Mortén prepared AlPO-5.

Table 3.1. Summary of catalyst properties.

Sample	Structure	Crystal size (μm)	BET surface	Acid site density (mmol/g)[a]	Si/Al or Al+P/Si[b]	ν(OH)[c] shift
H-ZSM-5 (PZ2-100H)	MFI	0.5-3 μm	429 m^2/g	0.28	59	-305 cm^{-1}
H-ZSM-5 (Nanosheets)	MFI	2-4 nm (thickness)	606 m^2/g	0.27	55	-320 cm^{-1}
H-SAPO-5	AFI	1 x 2 μm	340 m^2/g	0.068	80	-265 cm^{-1}
H-SSZ-24	AFI	< 1 μm	360 m^2/g	0.110	74	-317 cm^{-1}
AlPO-5	AFI	1-3 μm	323 m^2/g	-	-	-

[a]Determined via *n*-propylamine TPD. [b]Determined via MP-AES. [c]Shift in OH stretching of Brønsted sites measured by FTIR upon CO adsorption.

3.2. Catalyst characterization

A brief description of the characterization carried out during this PhD work, and the fundamentals to use such techniques is given below.

Powder X-ray diffraction

Powder X-ray diffraction (XRD) was used to identify the phase purity and crystallinity of the materials. A Bruker D8 Discover and a Siemens D-500 instruments with Bragg-Brentano geometry and Cu Kα radiation (1.5406 Å) were used.

Scanning electron microscopy

Scanning electron microscopy (SEM) was used to analyze the crystal size and shape of the samples. A FEI Quanta 200 FEG-ESEM with an Everhart-Thornley secondary electron detector and a detector for backscattered electrons was used. Katarzyna Anna Lukaszuk is acknowledged for acquiring the images for H-ZSM-5 samples.

N_2-sorption measurements

N_2 adsorption was carried out to determine the surface area of the materials using a BEL BELSORP-mini II instrument. The samples were treated in vacuum for 1 hour at 80 °C, followed by 4 hours at 300 °C. Subsequently, N_2 was dosed in a relative pressure range 0-0.99 p/p_0 at -196 °C. Specific surface area was determined by means of the BET equation in p/p_0 range 0.01-0.15.

Elemental analysis

Elemental analysis was employed to quantify Si, Al and P content in the zeolites and zeotypes presented in this work. The measurements were performed on an Agilent Technologies 4100 Microwave Plasma-Atomic Emission Spectrometry (MP-AES) instrument.

Fourier-transformed infrared spectroscopy

Fourier-transformed infrared spectroscopy (FTIR) was employed to investigate the acidic properties of the zeolitic catalysts. Two probe molecules, CO and pyridine, were adsorbed over the samples and their interaction with the acid sites was recorded on a FTIR Bruker vertex 80 with MCT detector. Thin self-supporting wafers of the samples were prepared, pre-treated under vacuum by heating to 150 °C for 1 hour, 300 °C for 1 hour and 450 °C for 1 hour.

For CO adsorption experiments, the probe molecules were dosed into a cell containing the sample wafer at -196 °C. Afterwards, CO was removed by applying vacuum. Spectra of the interaction of CO with acid sites were regularly measured in both the adsorption and desorption processes to determine the strength of Brønsted sites of zeolite and zeotype samples.

For pyridine adsorption experiments, the probe molecules were dosed at room temperature following catalyst activation. After reaching adsorption equilibrium, pyridine was pumped out in vacuum at room temperature and 200 °C, leaving only chemisorbed pyridine on Lewis and Brønsted sites. This technique was only used to qualitatively compare Lewis and Brønsted acidity between samples.

Temperature-programmed desorption of *n*-propylamine and NH_3

Temperature-programmed desorption (TPD) of *n*-propylamine and NH_3 were employed to quantify the acidity of the materials [243, 244]. When *n*-propylamine was used as probe molecule, care was taken to place a small amount of catalyst pellets, typically 15-20 mg (250-420 μm), in a 11 mm wide quartz reactor forming a thin layer of catalyst bed to prevent secondary reactions of products (propene).

The catalysts were pre-treated in a flow of oxygen at 550 °C, cooled to 150 °C under inert flow and subsequently a stream of nitrogen (80 mL/min) saturated with *n*-propylamine at room temperature or a flow of 2 %mol NH_3/N_2 were fed over the catalysts for about 20 minutes. Afterwards, a flow of inert was maintain for 2 h at 150 °C to remove the excess of either *n*-propylamine or NH_3. Then, the temperature was ramped up at 20 °C/min under 80 mL/min flow of nitrogen up to 550 °C while following the evolution of propene (m/z 39 and 41) and NH_3 (m/z 17 and 18) signals using an on-line Pfeiffer Omnistar quadrupole mass spectrometer. Furthermore, a calibration gas mixture containing propene and NH_3 (500 ppm propene and 500 ppm NH_3 in nitrogen) was flowed after finishing desorption to accurately determine the product calibration factors. The total amounts of propene and NH_3 eluted during desorption enabled the quantification of the Brønsted acidity of the catalysts.

3.3. Catalyst testing

3.3.1. Catalytic testing set-up

The schematics of the process flow diagram of the testing unit used in this thesis is shown in **Figure 3.1.** The set-up comprised 12 mass flow controllers for helium, argon, nitrogen, oxygen, light hydrocarbons (C_1-C_4) and DME. Additionally, 3 saturators enabled the feed of liquid reactants (methanol, methanol-3D, ^{13}C-methanol, benzene, toluene and water). The 12 pipe lines from the mass flow controllers were conveniently merged into 5 lines connected to a stream selector that enabled direction of the flow either to the reactor or to a separate waste line. The stream selector contained 5 Swagelok TT2B3 modules operated pneumatically by a solenoid valve. Pipe lines and valves were 316 stainless steel with 1/8" or 1/16" dimensions. The lines before the reactor highlighted in bold were heated to approximately 150 °C to pre-heat the inlet feed and more importantly, prevent condensation of liquid reactants in the lines. The outlet stream from the reactor was split into two streams directed to either waste or to a GC-MS/FID system. All lines in the outlet section were heated above 200 °C to avoid condensation of products. All tests were conducted in a U-shaped fixed bed quartz of either 6 mm or 8 mm inner diameter at atmospheric pressure. The operating temperature was monitored with a thermocouple encased in a quartz sleeve placed on top of the catalytic bed. The system was controlled via LabView interface developed by Terje Grønås from the Department of Chemistry at the University of Oslo.

Due to the wide variety of experiments carried out during this work, the reader is referred to the experimental section in Papers I, II and III for a detailed experimental description of each catalytic test.

Saturators for liquid reactants

Three saturators were connected to the test rig for feeding reactants which are liquid at room temperature based in the design presented in [245]. Basically, glass homemade containers ranging from 10 mL to 1 L were employed. The liquids (methanol, ^{13}C-methanol, methanol-3D, benzene, toluene and water) filled the saturators and were brought to boiling temperatures over a silicone-oil bath. A stream of helium gas was flowed through the boiling reactants and directed to a Vigreux column inside a water jacket, whose temperature was set to precisely select the concentration of reactants in the feed.

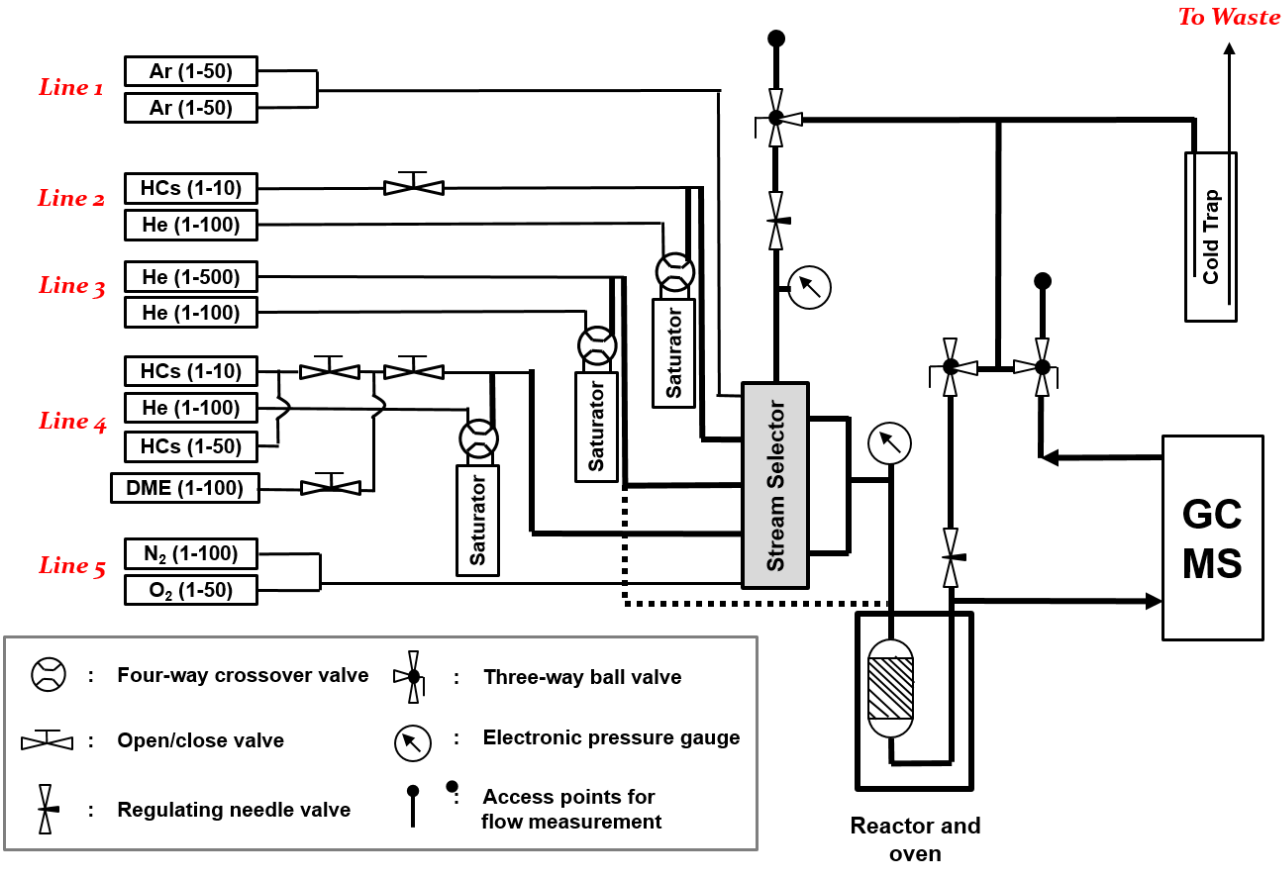

Figure 3.1. Schematic diagram of the experimental testing unit used in all experiments presented in this PhD thesis. HCs refers to hydrocarbons for mass flow controllers being able to operate with C_1-C_4 hydrocarbons. Bold lines refer to lines heated to temperatures about 150 °C before the reactor inlet, and above 200 °C after the reactor outlet. Dash line represents 2 meters long line heated at 530 °C in experiments involving *in-situ* formaldehyde formation as explained below.

In-situ formaldehyde formation

Formaldehyde co-feed experiments are presented in Papers I and II. In order to be able to co-feed formaldehyde into the reactor without polymerizing, a small modification was introduced in the testing unit as shown in **Figure 3.1** inspired by the set-up described in [246] Basically, a stainless steel 1/16" line was connected between a saturator and the inlet of the reactor. In this way, a flow of helium gas saturated with a known methanol concentration was sent through this line heated to 530 °C. As a consequence, 1-2% methanol was converted into methane and formaldehyde as detected by GC-MS/FID.

GC-MS/FID

In all catalytic tests the effluent was analyzed by an online GC-MS/FID (Agilent 7890/5975C GC/MS) using two Restek Rtx-DHA-150 columns. Therefore, the columns were attached to the inlet and two different detectors: a flame ionization detector (FID) to quantify the amounts of products and a mass spectrometer detector to identify the nature of the products. Hydrogen (purity 6.0) was used as carrier gas.

MS and GC

A few experiments presented in Paper I monitored the effluent products by an online Pfeiffer Omnistar quadrupole mass spectrometer and a GC with mol sieve column and TC detector to track hydrogen formation. Therefore, the outlet line of the reactor was split into two streams going to the GC-MS/FID equipment and to either the mass spectrometer or either the GC in separate experiments.

3.3.2. Data analysis

A wide variety of co-feeding experiments were carried out in this thesis and are presented in Papers I-III. However, the methodology to calculate reactants conversion, product selectivities, product yields and net product formation rates has been common throughout each paper.

Paper I addresses co-feed of benzene with methanol and DME, as well as co-addition of toluene or water in some experiments. Paper II involves reactions where methanol or DME were fed independently in most cases. Furthermore, a few experiments involved co-feed of DME/water and methanol/ formaldehyde. Paper III presents co-feeds of isobutene with methanol/DME or isobutene alone.

Total conversion was calculated in all cases assuming that reactants were not formed as a consequence of secondary reactions. To assess in a simplified manner conversion levels, methanol and DME were always considered as reactants regardless of (co-)feeding methanol or DME.

$$\text{Conversion (\%)} = \frac{\text{C in products - C in reactants}}{\text{C in all compounds}} \cdot 100 \qquad (3.1)$$

As this work has focused on studying methanol and DME during MTH-related reactions, the unconverted amounts of methanol and DME were carefully determined. In order to compare this to the thermodynamics in Paper II, the molar relationships between methanol and DME in the effluent were computed.

$$\text{Effluent MeOH in oxygenates fraction (\% mol)} = \frac{\text{C in MeOH}}{\text{C in MeOH} + \frac{\text{C in DME}}{2}} \cdot 100 \quad (3.2)$$

$$\text{Effluent DME in oxygenates fraction (\% mol)} = \frac{\frac{\text{C in DME}}{2}}{\text{C in MeOH} + \frac{\text{C in DME}}{2}} \cdot 100 \quad (3.3)$$

The effluent products were analyzed in terms of yields, selectivities or formation rates as follows:

$$\text{Yield}_{i}\ (\%\ \text{C}) = \frac{\text{C in product i}}{\text{C in all compounds}} \cdot 100 \quad (3.4)$$

$$\text{Selectivity}_{i}\ (\%\ \text{C}) = \frac{\text{C in product i}}{\text{C in all products}} \cdot 100 \quad (3.5)$$

In Papers I and III, the rate formation of products normalized per acid site was calculated when methanol/DME were co-fed with benzene and isobutene, respectively. In benzene co-feed experiments:

$$\text{Product rate formation}\left(\frac{\text{mol product}}{\text{mol H}^{+} \cdot \text{h}}\right) = \frac{\text{mol product}}{\text{mol rings in products}} \cdot \frac{\text{mol rings fed}}{\text{h}} \cdot \frac{1}{g_{cat}} \cdot \frac{g_{cat}}{\text{mol H}^{+}} \quad (3.6)$$

where rings refer to arene ring units.

In isobutene co-feed experiments:

$$\text{Product rate formation}\left(\frac{\text{mol product}}{\text{mol H}^{+} \cdot \text{h}}\right) = \frac{\text{mol product}}{\text{total C products}} \cdot \frac{\text{total C fed}}{\text{h}} \cdot \frac{1}{g_{cat}} \cdot \frac{g_{cat}}{\text{mol H}^{+}} \quad (3.7)$$

3.3.3. Isotopic labeling analysis

Isotopic labeling co-feed studies were carried out to elucidate the mechanisms of some reactions in Papers I and III. In this PhD thesis, benzene was co-reacted with $^{13}CH_3OH$ and CD_3OH, while isobutene was co-reacted with $^{13}CH_3OH$. The analysis was carried out following the methodology described by Rønning in [247]. Single ion chromatograms of the products to be analyzed were extracted and the isotopic compositions were calculated. The analysis was only applied on molecular ions and fragments that maintained intact the carbon skeleton. Furthermore, it was assumed that kinetic isotope effects on MS fragmentations were negligible.

In all cases, the natural abundance of ^{13}C (1.11 %) and D (0.0002 %) was considered for the analysis. In reactions involving isobutene, the expected natural abundance of the products was directly compared to the isotopic distribution of the products. In reactions involving benzene co-feed, special care was

taken due to the large number of C atoms in the products, and it was necessary to correct for the natural presence of ^{13}C in order to assess the insertion of ^{13}C into the products. Therefore, for any ion with N carbon atoms, the probability of containing n ^{13}C atoms is:

$$P_n = \left[\frac{N!}{n!\cdot(N-n)!}\right] \cdot 0.0111^n \cdot 0.9889^{N-n} \quad (3.8)$$

Based on this probability, the area of a single ion peak can be corrected for ^{13}C natural abundance as:

$$A_{corr}(i) = A_{obs}(i) - \frac{\sum_{n=1}^{N} A_{corr}(i-n)\cdot P_n}{0.9889^N} \quad (3.9)$$

In the above equation, A_{obs} (i) refers to the observed area for an ion peak with ion mass i, A_{corr} (i) is the corrected ion peak area and A_{corr} (i - n) is the corrected peak area for ions with mass i-n.

Extracting the integrated signals of single ion peaks from MS data enabled determination of the isotopic composition of the compounds that were analyzed. Based on their natural abundance and the use of labeled reactants, each ion peak will contain contributions from ions of the same mass number, and a different number of hydrogen atoms and/or $^{12}C/^{13}C$ atoms. Hence, the general formula relating the observed area for ion peaks can be expressed as a linear combination of the fractions of $^{12}C/^{13}C$ atoms in the ions:

$$A_{obs}(i) = A_{sum}\cdot D_{12C}(i)\cdot X_{12C} + \sum_{n=1}^{N} A_{sum}\cdot D_{12C}(i-n)\cdot X_n \quad (3.10)$$

A_{sum} is the sum of selected ion peak areas, D_{12C} (i) is the fraction of ions with mass number i in a ^{12}C spectrum of the compound, X_{12C} and X_n refer to the fraction of ions containing ^{12}C and ^{13}C atoms, respectively. Every mass number is represented by a linear equation, and a set of 5-15 mass numbers were typically used to solve the system of equations via regression analysis the fraction of ions containing n ^{13}C atoms.

3.4. Thermodynamic calculations

Pertinent thermodynamic calculations concerning the interconversion of methanol and DME as in Reaction (3.1) were performed to compare the extension of such reactions over different zeolitic materials, and the results are shown in Sections 4.1, 4.2, and partly in Paper II.

In order to facilitate comparison to experimental data and comprehension of the results, we elected to show the extent of Reaction (3.1) by reflecting expected DME/MeOH concentrations in the effluent as a molar ratio. In the absence of competing reactions, DME/MeOH molar ratios are constants. However, when methanol and DME are consumed in other reactions as in MTH via methylation reactions, as reflected by Reactions (3.2a) and (3.2b), water content changes and DME/MeOH molar ratios are affected. To calculate thermodynamic DME/MeOH distributions at different conversion levels, it is assumed that Reaction (3.1) proceeds much faster than Reaction (3.2a) and (3.2b). Adding Reactions (3.2a) and (3.2b), the net MTH reaction is given. Since the two sides of Reaction (3.1) are equimolar, the equilibrium is independent of pressure; and hydrocarbon production only influences it by altering the water concentration. Furthermore, due to the equimolarity of Reaction (3.1), we can ignore the volume change incurred by hydrocarbon formation.

$$2\ CH_3OH \leftrightarrows CH_3OCH_3 + H_2O \quad (3.1)$$

$$CH_3OH + RH \rightarrow RCH_3 + H_2O \quad (3.2a)$$

$$CH_3OCH_3 + RH \rightarrow RCH_3 + CH_3OH \quad (3.2b)$$

$$CH_3OCH_3 + 2\ RH \rightarrow 2\ RCH_3 + H_2O \quad (3.2c)$$

In the following,

M = The sum of C atoms in the methanol molecules present

D = The sum of C atoms in the DME molecules present

X = The sum of C atoms in the hydrocarbon molecules present

Starting from methanol and setting the initial methanol concentration to 100, it follows that X also represents the percentage conversion of oxygenates to hydrocarbons. By combining Reaction (3.1) and Reaction (3.2a) we obtain:

$$M = 100 - D - X \quad (3.11)$$

and:

$$[MeOH] = 100 - D - X \quad (3.12)$$

$$[DME] = D/2 \quad (3.13)$$

$$[H_2O] = D/2 + X \quad (3.14)$$

$$K_{eq,f} = [DME] \times [H_2O] / [MeOH]^2 = (D/2) \times (D/2 + X) / (100 - D - X)^2 \quad (3.15)$$

For each level of conversion, X, D was determined by regression analysis, leading to the corresponding concentrations of methanol, DME and water, and thereby, the [DME]/[MeOH] ratio.

Starting from DME, the initial DME concentration was set to 50. Hence, the initial number of C atoms in DME molecules was set to 100, in order to ensure that X also in this case would represent the oxygenate conversion level. Combining the reverse Reaction (3.1) and Reaction (3.2c), it follows that:

$$D = 100 - M - X \quad (3.16)$$

and:

$$[DME] = (100 - M - X)/2 \quad (3.17)$$

$$[MeOH] = M \quad (3.18)$$

$$[H_2O] = (X - M)/2 \quad (3.19)$$

$$K_{eq,b} = M^2 /[(X - M)/2]*[(100 - M - X)/2] \quad (3.20)$$

Again, for each level of conversion, X, M was determined by regression analysis, leading to the corresponding concentrations of methanol, DME and water, and thereby, the [DME]/[MeOH] ratio.

3.5. Deactivation modeling

A semi-empirical deactivation model was developed in Paper II based on the description of catalyst deactivation as reduction of the effective amount of catalyst in the reactor with time, as earlier proposed by Janssens *et al*. [162]. Furthermore, deactivation was assumed to occur via reactants (A) and/or products (B) as successfully applied by Olsbye and co-workers using a slightly simpler model [81, 248]. Therefore, the deactivation model comprises the three reactions below: reactants to products, reactants to coke and products to coke.

$A \xrightarrow{k_1} B$

$A \xrightarrow{k_2} C$

$B \xrightarrow{k_3} C$

Conversion is calculated as:

$$X = \frac{A_0 - A}{A_0} \tag{3.21}$$

The concentration of reactants and conversion change with deactivation according to the reaction scheme:

$$\frac{dA}{d\tau} = -k_1 A - k_2 A \cong -k_1 A, \text{ because } k_1 \gg k_2 \tag{3.22}$$

$$\frac{dX}{d\tau} = \frac{dX}{dA}\frac{dA}{d\tau} = -\frac{1}{A_0}(-k_1 A) = (1-X)\,k_1 \tag{3.23}$$

In the beginning of the experiment, it is assumed that there has not occurred any deactivation yet, and therefore, $\tau = \tau_0$ and $X = X_0$, which is calculated by:

$$X_0 = 1 - \frac{1}{\exp(k_1 \tau_0)} \tag{3.24}$$

The deactivation rate is then defined as a function of a deactivation "constant", that varies according to the concentration of reactants and products, and conversion.

$$\frac{d\tau}{dt} = k_d * X = -(k_2 A + k_3 B)\,X \tag{3.25}$$

where k_1, k_2 and k_3 are the model rate constants for the sum of methanol and DME to products, for the sum of methanol and DME to coke and for the products to coke, respectively. Then, the conversion evolution with time-on-stream is:

$$\frac{dX}{dt} = \frac{dX}{d\tau}\,\frac{d\tau}{dt} = (1-X)\, k_1 \left(k_2^*[A] + k_3^*[B]\right) X \qquad (3.26)$$

At t = 0, X = X_0. Analytically solving equation (3.26), conversion is calculated for any given time:

$$X = \frac{X_o \exp(-k_1 \left(k_2 A + k_3 B\right) t)}{1 - X_o + X_o \exp(-k_1 \left(k_2 A + k_3 B\right) t)} \qquad (3.27)$$

Chapter 4

Synopsis of Results

4 Synopsis of results

Despite the vast number of publications related to the conversion of methanol and DME to hydrocarbons, only a handful have aimed at investigating the chemistry of the two oxygenates separately. This work originates from the relatively scarce knowledge of the behavior of methanol and DME as independent reactants in the MTH reaction over acid zeolitic materials. Traditionally, similar reactivity has been attributed to both methanol and DME during MTH due to the considered rapid interconversion reaction between the two oxygenates and their ability to carry out similar reactions in MTH. The main objective of this PhD thesis is to gain further kinetic and mechanistic insight into the chemistry of methanol and DME in the course of the MTH reaction over zeolitic catalysts.

Firstly, the extent of the methanol-DME interconversion reaction is analyzed based on the type of catalyst used. Several catalysts comprising zeolites (aluminosilicates) and zeotypes (silico-aluminophosphates and aluminophosphates) were studied to assess whether the interconversion reaction between the two oxygenates is substantially faster than the MTH reaction, thereby determining whether methanol dehydration and the correspondent backward reaction compete with MTH. This study is also important to ensure that conclusions from follow-up kinetic studies, performed with methanol and DME separately, can be strictly related to the oxygenate used.

Secondly, selected zeolites (H-ZSM-5, H-SSZ-24) and a zeotype (H-SAPO-5) were subjected to an in-depth study to evaluate how methanol and DME feeds affect catalyst activity, effluent product distribution and catalyst deactivation during MTH, forming the basis of Paper II (see **Appendix**). Furthermore, a deactivation model was proposed to elucidate the driving forces leading to catalyst deactivation.

Thirdly, the study of the interaction of methanol and DME with selected hydrocarbons, which possess a distinct MTH reactivity, was fundamental to obtain kinetic and mechanistic insights of the observed reactions. Based on the dual cycle concept dominating the autocatalytic stage of the MTH chemistry, wherein alkene and arene cycles are competing during the hydrocarbon transformations, we decided to select isobutene (Paper III in **Appendix**) and benzene (Paper I in **Appendix**) as representative molecules of each cycle to study their reactivity towards methanol and DME. Kinetic analysis of the data was challenging due to the rapid arising of sequential and competitive reactions. Nevertheless, a careful analysis of all products formed revealed important differences in the reactivity of methanol and DME.

These differences were mechanistically rationalized by employing isotopically marked reactants and a wide variety of co-feed experiments. Theoretical calculations performed by our collaborators at the University of Ghent complemented our study and will be briefly discussed.

Fourthly, the disparity observed in the interaction of methanol and DME with hydrocarbons during the MTH reaction is assessed by the selective formation of formaldehyde from methanol. Plausible formaldehyde formation routes are evaluated. Additionally, the formaldehyde chemistry in the MTH reaction is rationalized based on co-feed studies.

This chapter provides the reader a summary of the main findings acquired along this PhD thesis split in five subsections. The main conclusions of this work and suggestions for further work are also found at the end of this chapter.

4.1. Impact of catalyst on methanol-DME interconversion

As a preamble into a detailed behavior of methanol and DME in the MTH reaction, it is highly relevant to describe how the methanol-DME interconversion reaction is affected by the selection of the catalyst. Traditionally, it has been assumed that methanol dehydrates rapidly to DME over zeolitic materials under MTH conditions [34, 47], and therefore the two oxygenates are lumped together and treated as one reactant. In this section, the generally accepted methanol-DME thermodynamic equilibrium is evaluated over different zeolite and zeotype materials at relevant MTH temperatures (≥ 350 °C). Basically, methanol or DME were fed over the catalysts and the extent of Reaction (4.1) was compared to expected thermodynamic effluent concentrations of methanol and DME, calculated as explained in **Section 3.4**. Above 350 °C, in addition to Reaction (4.1), methanol and DME are transformed into hydrocarbon products and water, as in net Reaction (4.2c). The level of methanol/DME conversion to hydrocarbons is proportional to the water concentration, and therefore different conversion levels alter the equilibrium methanol-DME. RH in the reactions below refers to an alkene or an arene hydrocarbon, while RCH_3 is the corresponding methylated hydrocarbon.

$$2\ CH_3OH \leftrightarrows CH_3OCH_3 + H_2O \quad (4.1)$$

$$CH_3OH + RH \rightarrow RCH_3 + H_2O \quad (4.2a)$$

$$CH_3OCH_3 + RH \rightarrow RCH_3 + CH_3OH \quad (4.2b)$$

$$CH_3OCH_3 + 2\ RH \rightarrow 2\ RCH_3 + H_2O \quad (4.2c)$$

We evaluated the equilibrium of methanol-DME over the zeolites H-ZSM-5 and H-SSZ-24, and the zeotype H-SAPO-5 at 350 and 450 °C by using both methanol and DME feeds. The MTH reaction under these conditions generates hydrocarbons and water, and the unconverted quantities of methanol and DME in the effluent were carefully evaluated in **Figure 4.1**. The results are presented as a molar ratio of DME/MeOH versus the conversion to hydrocarbons to facilitate comparisons. Clearly, the thermodynamic equilibrium of DME/MeOH is not established with any of the feeds over the zeolite catalysts, implying that the rates of Reactions (4.1) and (4.2c) are within the same order of magnitude. In contrast, the H-SAPO-5 zeotype catalyst, sharing topology with H-SSZ-24, displayed precise thermodynamic effluent concentrations of methanol and DME with the two feeds at different temperatures. It is therefore important to highlight the different nature of the acid sites in zeotypes compared to zeolites. Catalytic properties for dehydrating methanol to DME and water have been attributed to the weakly acidic P-OH groups in zeotype materials [43, 193], while no references to the

activity of Si-OH groups in zeolites towards the mentioned reaction have been described in the literature. Indeed, the acid strength of P-OH is intermediate between that of strong Brønsted sites in zeolites and zeotypes, and that of weak silanols, Si-OH [249].

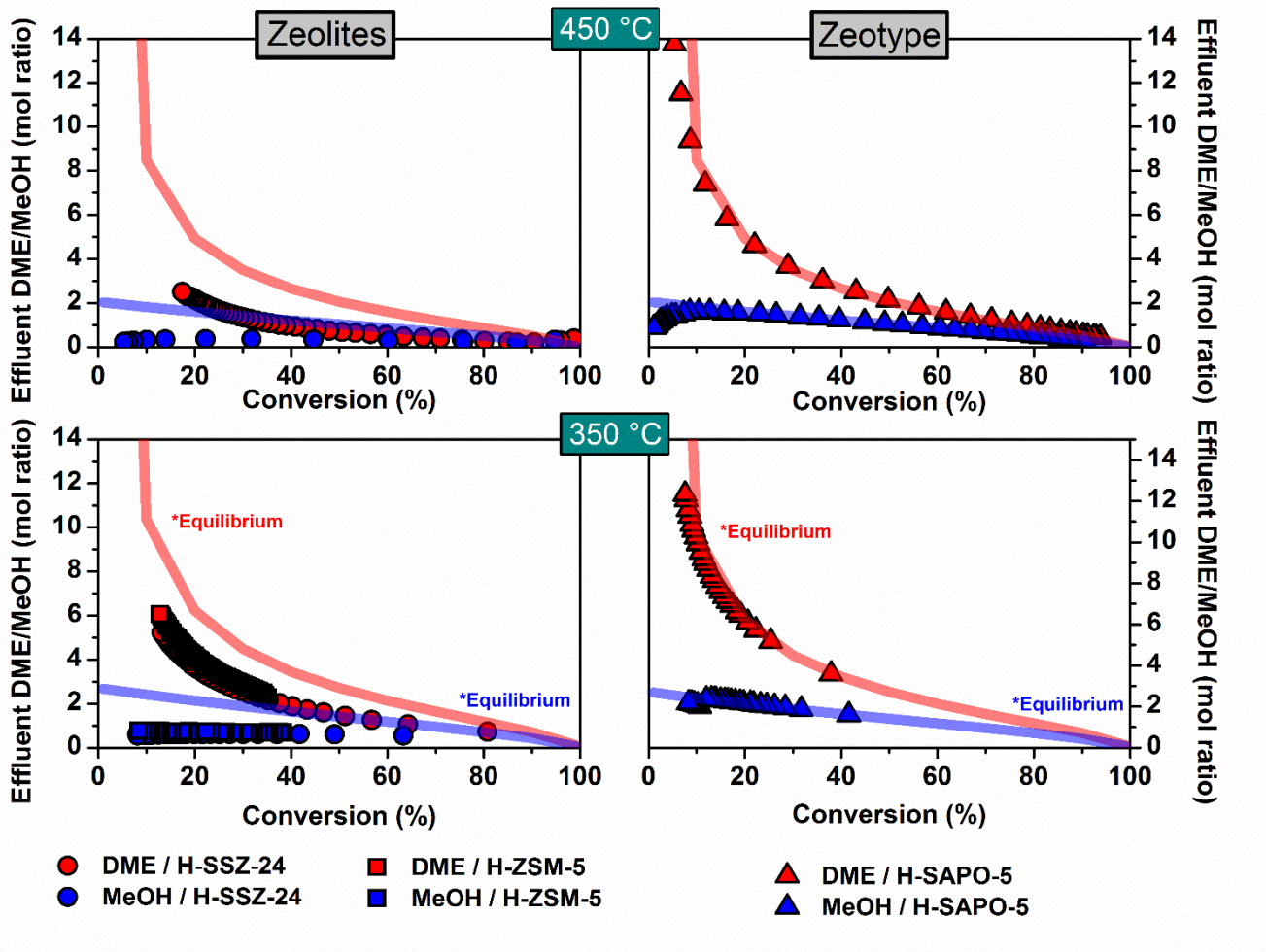

Figure 4.1. Effluent molar DME/MeOH ratios evolution with conversion when feeding methanol or DME over H-ZSM-5, H-SSZ-24 and H-SAPO-5. T = 350-450 °C. $p_{oxygenates}$ = 40-60 mbar. WHSV = 14 g_{MeOH}/g_{cat}*h, 44.4 g_{DME}/g_{cat}*h (H-ZSM-5), 2.8 g_{MeOH}/g_{cat}*h, 3.1 g_{DME}/g_{cat}*h (H-SSZ-24) WHSV = 0.6 g_{MeOH}/g_{cat}*h, 0.9 g_{DME}/g_{cat}*h (H-SAPO-5)

To corroborate the hypothesis that P-OH groups in H-SAPO-5 are behind the faster DME/MeOH interconversion, methanol was fed over AlPO-5. AlPO-5 exhibits the same AFI topology as H-SAPO-5 and H-SSZ-24, but does not possess strong Brønsted acidity. As shown in **Figure 4.2**, AlPO-5 efficiently converts methanol to thermodynamic concentrations of DME at 350 and 450 °C under a wide range of WHSV with negligible observed activity towards hydrocarbons formation. Therefore, the higher extent of Reaction (4.1) over zeotypes compared to zeolites is attributed to additional weakly acidic P-OH groups which are not present in zeolites. For this reason, we hypothesize that zeotypes, such as SAPOs and possibly other metal-aluminophosphates, possess two active sites that play a role during the course

of the MTH reaction. P-OH groups are acidic enough to convert methanol to DME and water, but are presumably inactive to MTH chemistry involving C-C bond formation. However, the stronger Brønsted sites, introduced by the presence of Si atoms in the framework, undergo both methanol-DME interconversion and MTH chemistry. The synergism between the activity of the two sites is therefore responsible for achieving thermodynamic concentrations of methanol and DME throughout the reactor in the experiments conducted over H-SAPO-5. Contrarily, zeolites possess strong Brønsted sites, and possibly Lewis Al-OH sites, that may be acidic enough to catalyze the MTH chemistry and methanol-DME interconversion at relatively similar rates. Consequently, higher methanol concentrations are expected to be found through the reactor under MTH operation with both methanol and DME feeds over zeolitic materials.

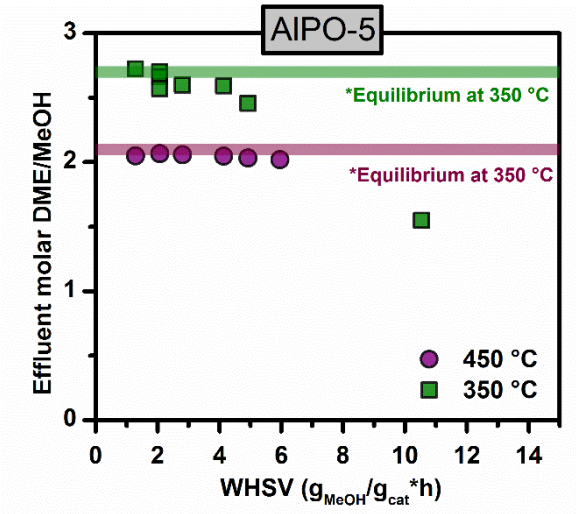

Figure 4.2. Effluent molar DME/MeOH ratios evolution with WHSV when feeding methanol over AlPO-5 at 350 and 450 °C. p_{MeOH} = 40 mbar.

To further validate our hypothesis, we analyzed the behavior of methanol and DME in previous MTH tests carried out in our group over a wide range of zeotype and zeolite catalysts at 400 °C. In this case, all tests were performed using methanol as feed. The effluent molar DME/MeOH ratios for all tests are shown in **Figure 4.3**. In agreement with the results presented previously, the three additional zeotypes tested exhibit fast methanol-DME interconversion while catalyst deactivation proceeds, as thermodynamic concentrations of the two oxygenates are achieved. Nevertheless, none of the extra 7 zeolites tested produced thermodynamic concentration of methanol and DME in the effluent. Intriguingly, the smaller pore zeolites (H-ZSM-22 and H-ZSM-23) and the largest pore zeolites (H-MOR and H-BETA) show the highest and lowest extent of Reaction (4.1) respectively, but it is beyond the scope of the present study to elucidate the differences observed between zeolites topologies. In summary, the results presented in this section show that the commonly accepted concept of oxygenate

equilibration prior to formation of hydrocarbon products is not always applicable, and clear differences in methanol and DME concentrations throughout the reactor during MTH operation are observed depending on the selected catalyst.

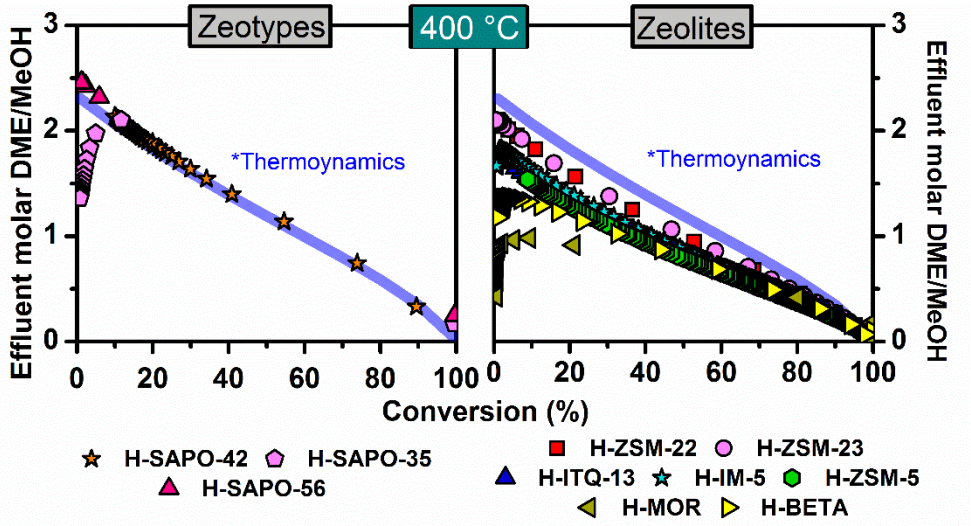

Figure 4.3. Effluent molar DME/MeOH ratios evolution with conversion when feeding methanol over zeotypes and zeolites. T = 400 °C. p_{MeOH} = 130 mbar. WHSV = 10 g_{MeOH}/g_{cat}*h (H-ZSM-5), 2 g_{MeOH}/g_{cat}*h (rest of catalysts).

4.2. Impact of methanol and DME as feed on the MTH reaction

Since we have identified the non-equilibrium conditions of methanol and DME over zeolites during MTH and since both oxygenates act as reactants, it becomes highly relevant to study how they act as MTH reactant molecules as independently as possible. Therefore, this section thoroughly evaluates the activity, deactivation and product distribution associated with methanol and DME feeds over zeolites and zeotypes. We opted in this study for the catalysts: H-ZSM-5, which is the industrial MTG catalyst, and the isostructural H-SSZ-24 and H-SAPO-5 catalysts.

4.2.1. Activity

The inherent activity of methanol and DME as feeds in the MTH reaction is first briefly discussed. The conversion of methanol and DME to hydrocarbons was evaluated over H-ZSM-5 at 350 °C, which is the temperature conventionally used in industrial MTG operations. **Figure 4.4** (top panel) shows the level of conversion versus the applied contact time. Clearly, the conversion of DME is substantially higher than the conversion of methanol at low contact times. Considering the dual cycle concept (**Scheme 2.11**), in which methanol and DME are only consumed via methylation reactions, these results are in agreement with faster methylation rates or formation of active surface methoxides for DME relative to methanol [218, 219, 221], and also with results to be presented in **Sections 4.3** and **4.4** regarding the methylation of benzene and isobutene. Importantly, fairly similar conversion levels (70-80 %) were observed for the two feeds at high contact times. The reason for this behavior might be found in **Figure 4.4** (bottom), which shows that the composition of unconverted oxygenates (methanol and DME) in the effluent changes with conversion as a molar ratio DME/MeOH. At low contact times, the DME/MeOH ratio in the effluent (and inherently, throughout the reactor) is significantly different for DME and methanol feeds, and higher conversion is observed for DME. However, at long contact times, similar conversion levels are achieved with both oxygenates feeds and the DME/MeOH ratio in the effluent tends to equalize because the oxygen content of the oxygenate feed is mainly liberated as water. Therefore, the actual DME/MeOH ratio in the effluent becomes less dependent on the exact composition of the feed. It should also be noted that DME/MeOH equilibrium is not established in the experiments, in full agreement with the results presented in **Section 4.1**.

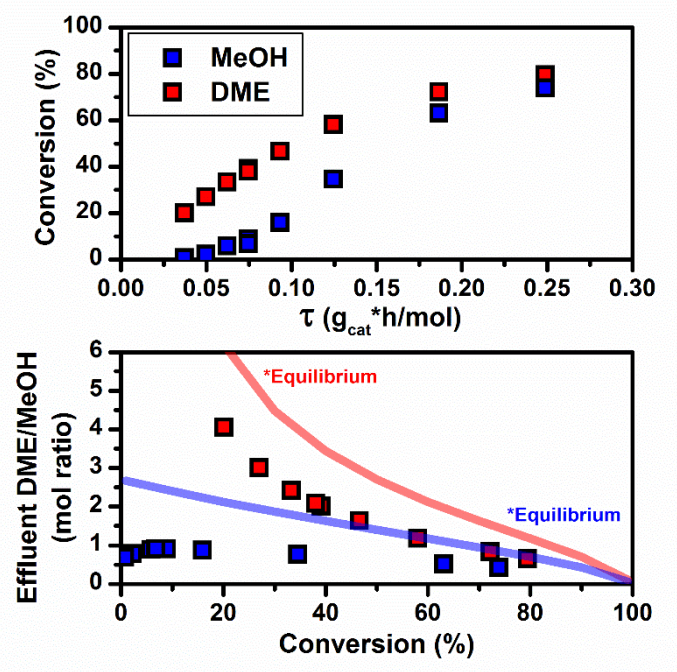

Figure 4.4. Oxygenate (DME or MeOH) conversion as a function of contact time (top) and effluent molar ratios DME/MeOH (bottom) during the MTH reaction over H-ZSM-5 at 350 °C.

4.2.2. Catalyst stability and deactivation modeling

Once a distinct overall MTH activity for methanol and DME over H-ZSM-5 was determined, we selected a contact time leading to similar initial conversion levels (~40 %) to evaluate the stability of the catalyst as a function of methanol and DME feeds over H-ZSM-5. Stability tests were additionally performed over isostructural H-SSZ-24 and H-SAPO-5 because these materials presented an ostensibly different methanol dehydration capacity. Furthermore, additional tests were carried out with the intention of modifying MeOH/DME concentrations throughout the course of the MTH reaction by altering water concentrations. The complete study over H-ZSM-5, H-SSZ-24 and H-SAPO-5 catalysts is described in Paper II, and the reader is referred to that work for extensive further details.

Focusing first on the stability of the H-ZSM-5 catalyst, stability-deactivation tests were carried with methanol, DME and DME/water feeds at 350 °C under relatively high contact time conditions that facilitated a "rapid" deactivation of this extremely stable catalyst and led to similar initial conversion levels (30-40 %), yet significantly different DME/MeOH ratios in the effluent. The comparison of the different contact times used in the tests is validated based on the similar product distribution and conversion capacities of H-ZSM-5 catalysts with contact time variations with methanol feeds [161, 250]. The top panel in **Figure 4.5** shows the deactivation profiles in terms of cumulative carbon conversion normalized per carbon units to account for the different amount of carbon fed with methanol and DME.

Importantly, catalyst conversion capacity has been tagged as a good deactivation descriptor because it is directly related to the deactivation rate and independent of catalyst activity and contact times applied [55, 250]. The absolute numbers for carbon conversion capacity over H-ZSM-5 with the three oxygenate feeds are shown in **Table 4.1**. These values were calculated by extrapolating the cumulative carbon conversion curves to zero conversion levels, following the methodology described by Bleken *et al.* [250]. The carbon conversion capacities are 16.1 and 8.3 times higher when DME and DME/water are used as feeds compared to the methanol feed. Even though DME and methanol are often considered as similar reactants, these results suggest that there are important differences between the two compounds with respect to the deactivation of MTH catalysts.

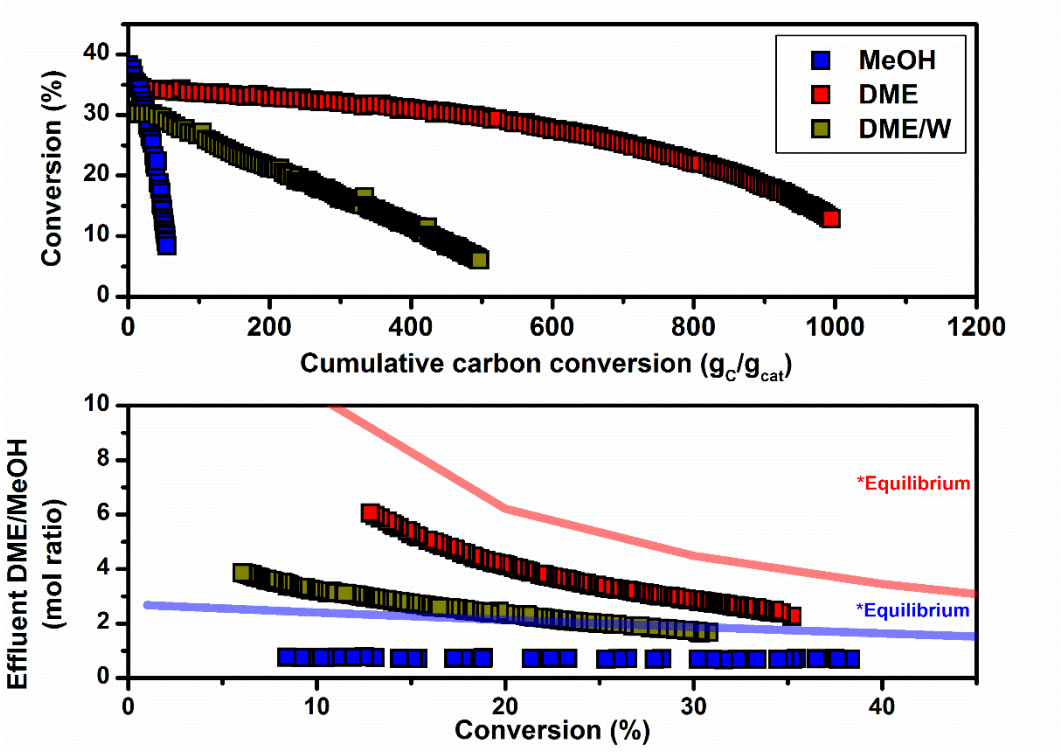

Figure 4.5. Cumulative carbon conversion (top) and effluent molar DME/MeOH ratio as a function of conversion (bottom) during the MTH reaction over H-ZSM-5 at 350 °C with DME, MeOH, DME/Water (DME/W) feeds. WHSV = 44.4, 37.0 and 14.0 $g_{oxygenate}g_{cat}^{-1}h^{-1}$ for DME, DME/W and MeOH feeds. Lines reflect thermodynamic equilibrium values for molar DME/MeOH ratios expected in the effluent if methanol-DME interconversion proceeds much faster than the MTH reaction. The reader is referred to **Section 3.4** for details on the procedure followed to calculate thermodynamic equilibrium values.

The bottom panel in **Figure 4.5** illustrates the evolution of the molar DME/MeOH ratio in the effluent with the conversion for each test, confirming the three distinctive proportions of oxygenates throughout the reactor. Together, the two graphs establish a solid link between high DME/MeOH ratios in the reactor and high conversion capacity of the catalyst. As expected from **Section 4.1**, the DME/MeOH equilibrium was not established with any of the feeds over this zeolite, and adding water to a DME feed

shifted the interconversion of methanol and DME towards intermediate DME/MeOH ratios compared to pure methanol and DME feeds. Since the deactivation rate seems to be sensitive to the proportions of DME and methanol during the MTH reaction, the kinetics of methanol-DME interconversion can play an important role on catalyst deactivation.

Table 4.1. Summary of carbon conversion capacities of the MTH reaction over H-ZSM-5, H-SSZ-24 and H-SAPO-5 with MeOH, DME and DME-MeOH feeds.

Catalyst	Temperature (°C)	Carbon conversion capacity (g_C/g_{cat})			
		MeOH feed	DME feed	DME-MeOH feed[a]	
H-ZSM-5	350	75	1215	625	
H-SSZ-24 (/AlPO-5)	350	8.0	28.0	11.5[b]	not tested
	450	5.3	47.5	16.5[b]	18.0[c]
H-SAPO-5	350	1.3	2.5	not tested	
	450	4.3	8.7	not tested	

[a]DME-MeOH feed refers to DME/water feed over H-ZSM-5 and MeOH feed over H-SSZ-24 combined with MeOH dehydration catalyst AlPO-5. [b]Tests where AlPO-5 catalyst was placed over H-SSZ-24. [c]Tests where AlPO-5 catalyst was placed over and physically mixed with H-SSZ-24.

Furthermore, **Table 4.1** also collects a summary of the carbon conversion capacities achieved over H-SSZ-24 and H-SAPO-5 with methanol and DME feeds at 350 and 450 °C, being the last one the conventional MTO operating temperature. The cumulative conversion curves at 450 °C are shown in **Figure 4.6** (See Paper II for curves at 350 °C). First, the same trends observed previously over H-ZSM-5 are also noticed over H-SSZ-24. The carbon conversion capacity was enhanced with DME feed by a factor of 3.5 and 9.0 at 350 and 450 °C, respectively, compared to methanol feed. These numbers confirm the strong link between high methanol concentrations and rapid catalyst deactivation. To further assess the relationship between high methanol concentrations and deactivation, a methanol dehydration catalyst was combined with H-SSZ-24, in an arrangement that is schematically illustrated in **Figure 4.7**. AlPO-5 was used as a methanol dehydration catalyst due to its capacity to drive MeOH-DME to concentrations of thermodynamic equilibrium under similar WHSVs to those used in the MTH test (2.8 $g_{MeOH}g_{cat}^{-1}h^{-1}$), as it was previously shown in **Figure 4.2**. Placing the AlPO-5 catalyst on top of H-SSZ-24 and combining it with H-SSZ-24 enabled the generation of a distinct DME/MeOH ratio throughout the reactor compared to the experiments over only H-SSZ-24. The combined use of AlPO-5/H-SSZ-24 led to 3-3.5-fold enhanced carbon conversion capacity when methanol was fed compared to the use of only H-SSZ-24. Therefore, these results hold the key to the signicantly different role played by methanol and DME in catalyst deactivation. Even though DME-MeOH thermodynamic equilibrium was achieved in

the presence of AlPO-5 and an important increase in catalyst stability was obtained, pure DME feed still yielded higher carbon conversion capacities. These results not only proved that the reactivity of methanol and DME towards deactivation is substantially different, but also suggest a deactivation route derived from methanol itself.

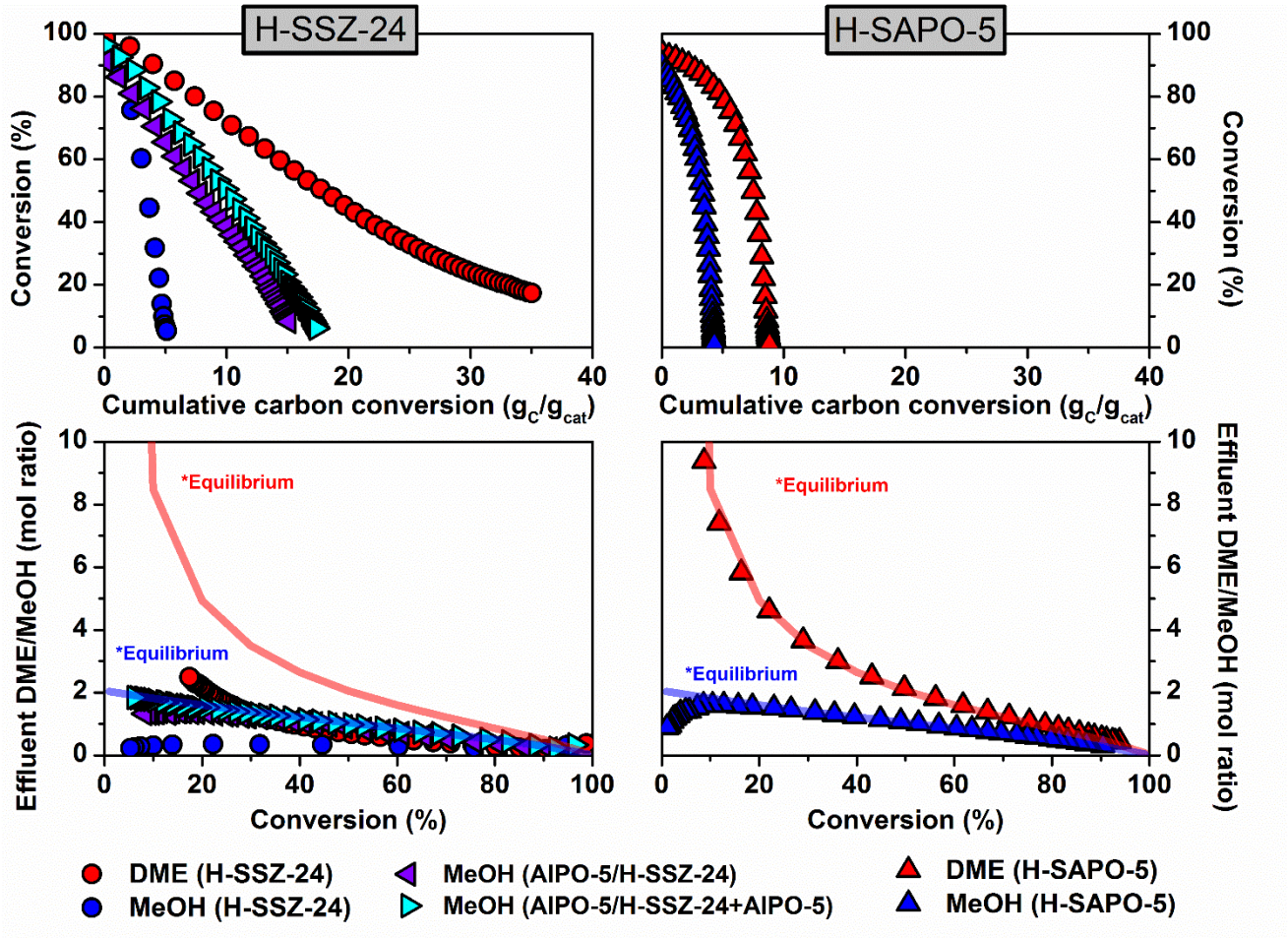

Figure 4.6. Cumulative carbon conversion (top) and effluent molar ratios DME/MeOH as a function of conversion (bottom) during the MTH reaction over H-SSZ-24 (/AlPO-5) and H-SAPO-5 at 450 °C with DME and MeOH feeds WHSV (H-SSZ-24) = 3.1 and 2.8 $g_{oxygenate}g_{cat}^{-1}h^{-1}$ for DME and MeOH. WHSV (H-SAPO-5) = 0.9 and 0.6 $g_{oxygenate}g_{cat}^{-1}h^{-1}$ for DME and MeOH. Lines reflect thermodynamic equilibrium values for molar DME/MeOH ratios expected in the effluent if methanol-DME interconversion proceeds much faster than the MTH reaction. The reader is referred to **Section 3.4** for details on the procedure followed to calculate thermodynamic equilibrium values.

Concerning the stability against deactivation of H-SAPO-5 with respect to methanol and DME feeds, the carbon conversion capacity was only 2.3 and 2.0 times higher with DME at 350 and 450 °C. This moderate increase in catalyst stability is tentatively attributed to the fast kinetics of methanol-DME interconversion reaction, as thermodynamic equilibrium concentrations were achieved with both methanol and DME feeds. As a consequence, higher concentrations of DME are obtained, thereby reducing the local methanol concentrations inside the zeolite structure, and consequently, mitigating

the negative impact of methanol towards deactivation. This may be the reason behind the small differences observed in the literature when comparing methanol and DME feeds over H-SAPO-34 catalysts in the MTO process [174-176, 251], even though some reports provide evidence for slightly higher stability provided by DME feeds, which is in agreement with our findings on H-SAPO-5.

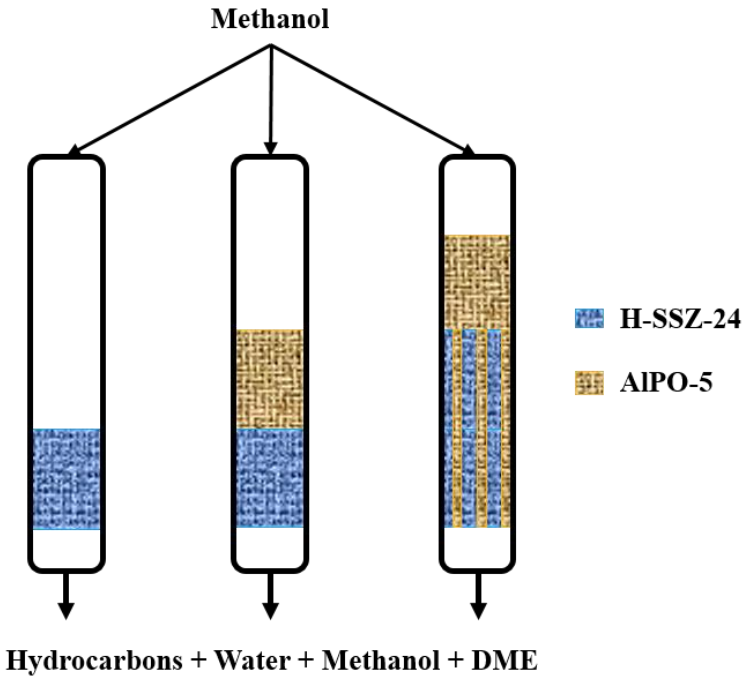

Figure 4.7. Schematic arrangement of the catalysts during the MTH reaction over H-SSZ-24, AlPO-5/H-SSZ-24 and AlPO-5/AlPO-5+H-SSZ-24 (physically miexed) with methanol feed at 450 °C. WHSV = 2.8 $g_{MeOH}g_{cat}^{-1}h^{-1}$.

In order to further assess the contribution of the feed to catalyst deactivation, we employed a simple deactivation model, combining previous models described in [81, 162]. The model, presented in **Section 3.5**, considers that deactivation can be induced by coke formation from reactants (A) and/or from products (B). Coke formation from reactants would correspond to the "burning cigar model" by Haw [172], and to the segmented deactivation of H-ZSM-5 catalysts reported by Schulz [83]. If deactivation is mostly driven by the products, which has been reported to occur over large-pore zeolites (*i.e.* H-Beta* and H-mordenite), deactivation is expected to be rather homogeneous along the catalyst bed [161]. The deactivation model accounts for the following reactions:

$$A \xrightarrow{k1} B$$

$$A \xrightarrow{k2} C$$

$$B \xrightarrow{k3} C$$

where k_1, k_2 and k_3 are rate constants for the sum of methanol and DME to products, for the sum of methanol and DME to coke and for the products to coke, respectively.

This model was successfully applied to all MTH tests over H-ZSM-5, H-SSZ-24 and H-SAPO-5. **Figure 4.8** exemplifies the application of the model to tests over H-SSZ-24 at 450 °C, wherein DME and methanol were fed over the zeolite catalyst in the absence and in the presence of AlPO-5. **Table 4.2** summarizes the simulated rate constants derived from the application of the deactivation model to each of the three catalysts tested. The reader is directed to Paper II for plots similar to **Figure 4.8** over H-ZSM-5 and H-SAPO-5.

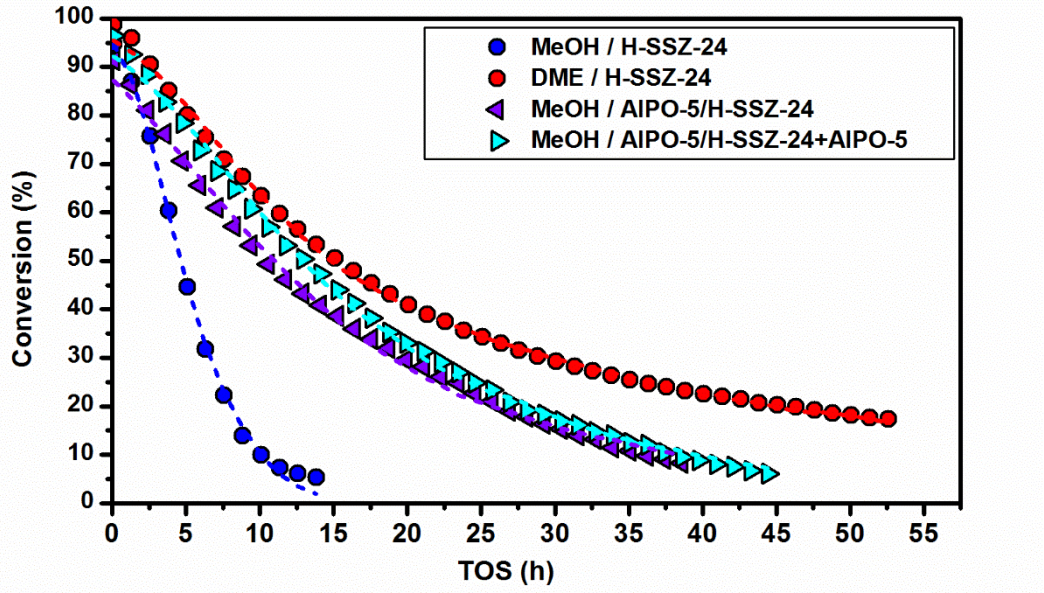

Figure 4.8. Deactivation profiles based on oxygenate conversion versus time-on-stream over H-SSZ-24 and AlPO-5/H-SSZ-24 at 450 °C. Symbols represent experimental data, while the simulated model conversion curves are represented by dashed lines.

Analyzing first the results over H-SSZ-24, the model predicted a product-governed deactivation profile with all feeds ($k_3 > k_2$), as also observed over other large-pore zeolites, H-Beta* and H-mordenite, during the MTH reaction [161]. Nevertheless, the contribution of reactants to deactivation is more important when the methanol feed is used compared to the DME feed. Interestingly, the reduction in methanol concentrations throughout the reactor when using AlPO-5 concurrently shifted the main deactivation route, leading to an intermediate situation compared to pure feeds of methanol and DME. Furthermore, the ratio $k_1/(k_2+k_3)$, that relates effluent product formation to coke formation, was in agreement with previously reported conversion capacities of this catalyst (**Table 4.1**).

Table 4.2. Simulated rate constants from deactivation model fit on MTH tests over H-ZSM-5 (350 °C), H-SSZ-24 and H-SAPO-5 (450 °C).

Catalyst	Feed	Simulated rate constants			Reaction/ Deactivation	Deactivation by reactants/products
		k_1	k_2	k_3	$k_1/(k_2+k_3)$	k_2/k_3
H-SSZ-24	**MeOH**	3.5	0.14	0.23	9.5	0.6
	DME	3.5	0.01	0.11	30.9	0.1
AlPO-5/H-SSZ-24	**MeOH**	2.6	0.04	0.10	19.2	0.3
AlPO-5/H-SSZ-24 +AlPO-5	**MeOH**	3.3	0.03	0.09	27.5	0.4
H-SAPO-5	**MeOH**	0.6	0.23	0.13	1.6	1.7
	DME	0.9	0.19	0.10	3.1	1.9
H-ZSM-5	**MeOH**	4.1	0.010	0	353.1	-
	DME/W	5.0	0.002	0.003	923.1	0.8
	DME	7.4	0.001	0	6695.5	-

The application of the model to H-SAPO-5 gave slightly higher deactivation rate constants from reactants and products with methanol feed, while DME feed gave slightly higher reaction rate constant. Together, these results agree with the small differences in carbon conversion capacities with methanol and DME feeds over this catalyst, what we attribute to the much faster rates of methanol dehydration reaction compared to hydrocarbon methylation rates.

At last, the deactivation model was applied to H-ZSM-5. This catalyst is known for its stability against deactivation in the MTH reaction, and consequently, it showed the lowest selectivity towards coke formation (large $k_1/(k_2+k_3)$). Besides, the ratios of the rate constants for reaction/deactivation for the 3 feeds were in agreement with the order in carbon conversion capacities (MeOH < DME/water < DME). The model also revealed the more important contribution of reactants to deactivation compared to products, oppositely to the large-pore materials H-SSZ-24 and H-SAPO-5. While methanol feed showed the highest rate constant for deactivation by reactants (k_2), DME feed gave an order of magnitude lower values. Furthermore, the model corroborates that introduction of water to the DME feed increases the coke formation rate due to the shift in Reaction (4.1) towards increasing methanol concentrations. Interestingly, the model further suggested that deactivation by products with DME/Water feed is of the same magnitude as deactivation by reactants. We are not in position to fully explain this result.

Nonetheless, the large water concentrations for this particular feed, which increase over time due to lesser extent of Reaction (4.1), might result in a strong competition of water with methanol, DME and hydrocarbons for the acid sites, as reported by De Wispelaere *et al.* over H-SAPO-34 [183]. Numerous articles in the literature have reported a positive effect of water addition to methanol feeds over different zeolitic materials, showing primarily slower deactivation rates in the presence of water [179-182]. Therefore, high water concentrations could be the reason for the relatively high values of k_3 with DME/W feed.

4.2.3. Product distribution

The startling differences observed in catalyst deactivation by methanol and DME reflect that the chemistry of the two oxygenates might not be completely equivalent in the MTH reaction. That disparity was also displayed in the product spectrum obtained. **Figure 4.9** illustrates the product yields sorted by product type: methane (C_1), ethylene and ethane traces (C_2), light alkenes (C_3-C_5 =), short alkanes (C_3-C_5 -), larger aliphatics (C_{6+}) and aromatics. Interestingly, DME feed produced an enriched alkene and aliphatics product distribution, while a methanol feed led to higher yields of ethylene, alkanes and aromatics. Considering the dual cycle mechanism (**Scheme 2.11**), alkanes are formed via hydrogen transfer reactions where monounsaturated alkenes give saturated alkanes and polyunsaturated hydrocarbons *i.e.* aromatics. Consequently, the higher yields of alkanes and aromatics reported for the methanol feed, together with the higher yields of alkenes and aliphatics for the DME feed are indicative of a shift towards a certain predominance of the arene-dominated cycle with methanol. In line with this hypothesis, methanol also gives higher yields of ethylene, which is mostly generated from aromatics dealkylation over H-ZSM-5 [137]. Importantly, methanol has been identified as a hydrogen transfer promoter during the MTH reaction as co-feeding methanol with olefins markedly induced larger hydrogen transfer-derived products compared to the feed of only olefins [164, 169]. Based on our results, methanol and DME induce hydrogen transfer reactions to a different extent, and a detail study on this specific topic will be described in **Sections 4.3** and **4.4**.

Notably, a DME/water feed resulted in an intermediate effluent product distribution, which is consistent with the intermediate DME/MeOH effluent concentrations observed with this feed in **Figure 4.5**. The yields of methane were very small in all cases and followed intriguingly different trends. Several routes for methane formation are proposed in the literature, *i.e.* methoxy groups reacting with methanol and DME [168], direct formation from methanol [80, 97] or even from alkenes, arenes and coke [83, 171, 252]. However, the data obtained in this study do not enable the discrimination among these possible routes.

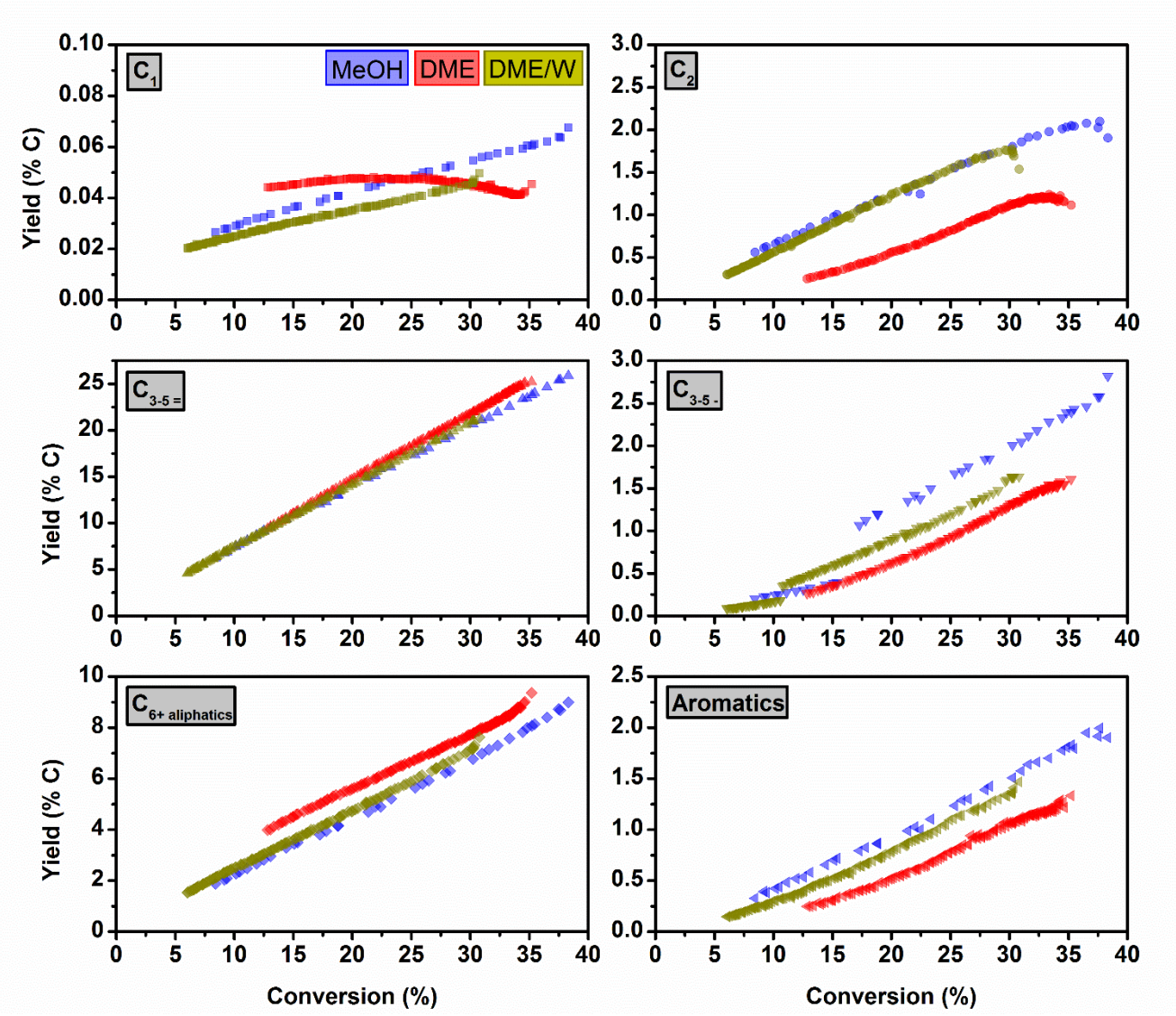

Figure 4.9. Yields of hydrocarbon fractions versus conversion during MTH over H-ZSM-5 at 350 °C by feeding DME (red), MeOH (blue) and DME/W (green). *Small deviations in C_{3-5} alkanes at low conversions are due to overlapping isobutane/MeOH signals under high MeOH concentrations.

The product distribution of MTH tests shown in **Figure 4.6** for H-SSZ-24, AlPO-5/H-SSZ-24 and H-SAPO-5 catalysts was also carefully analyzed to evaluate whether the trends over H-ZSM-5 could be extended to these materials. **Figure 4.10** and **Figure 4.11** display the product yields during the conversion of methanol and DME over the aforementioned catalysts at 450 °C. As it was the case for H-ZSM-5, H-SSZ-24 gave higher yields of ethylene, alkanes and aromatics with a methanol feed. Therefore, the hypothesis of methanol shifting the reaction mechanism towards the arene cycle also holds for this catalyst. However, when methanol was fed over AlPO-5 combined with H-SSZ-24, the product yields resembled to those of a DME feed (**Figure 4.10**). This result is fully consistent with the higher DME concentration throughout the reactor generated by the methanol dehydration activity of AlPO-5

(**Figure 4.6**). For the H-SAPO-5 catalyst, a nearly identical product distribution was achieved for methanol and DME feeds, showing that the methanol dehydration activity of this catalyst not only attenuated the effect on deactivation, but also on product distribution. The same trends for both catalysts were found at 350 °C, and the reader is referred to Paper II for more details.

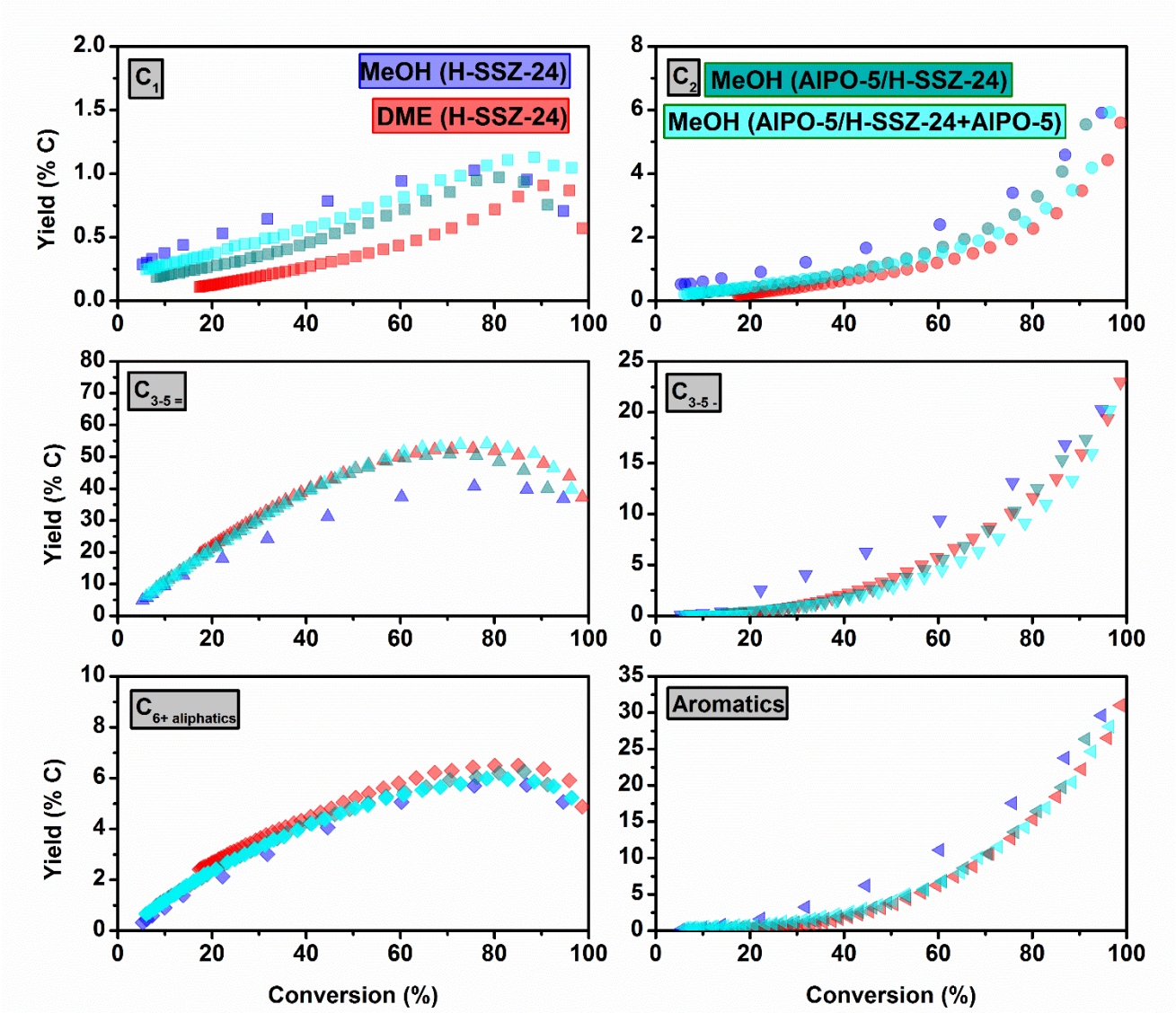

Figure 4.10. Yields of hydrocarbon fractions versus conversion during MTH over H-SSZ-24/H-SSZ-24+AlPO-5 mixes at 450 °C by feeding DME (red) and MeOH (blue).

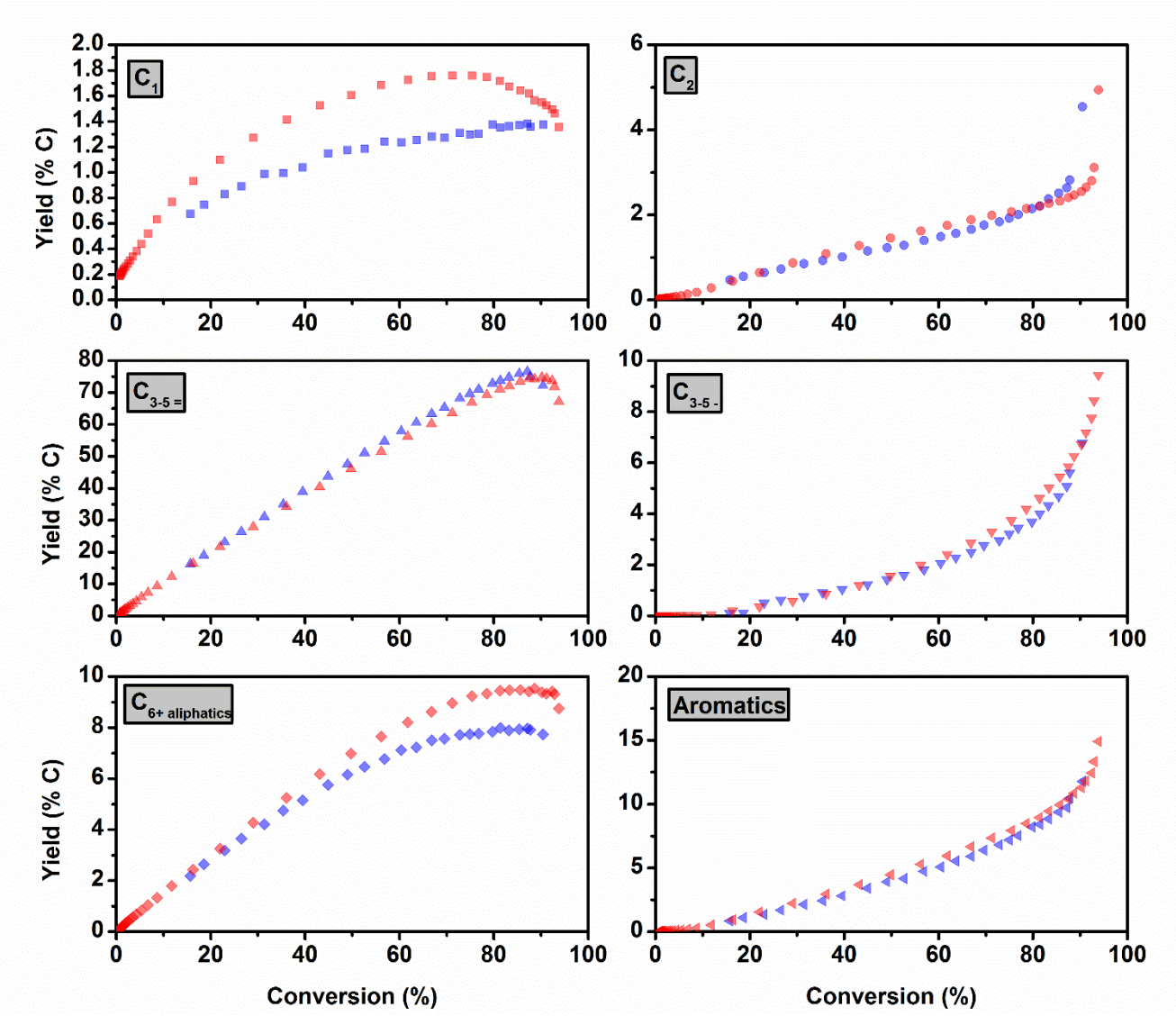

Figure 4.11. Yields of hydrocarbon fractions versus conversion during MTH over H-SAPO-5 at 450 °C by feeding DME (red) and MeOH (blue).

The significant promotion of hydrogen transfer reactions via methanol may have a kinetic origin due to the higher methylation rate of DME versus methanol, which has been reported in literature [218, 253]. Methylation and hydrogen transfer reactions are expected to have a common reactant of olefinic nature. Therefore, these reactions occur in a competitive manner during MTH as highlighted in **Scheme 4.1**, and the relative ratio of methylation/hydrogen transfer rates, which is likely different for DME and methanol, affects the relative concentration of active alkene and arene hydrocarbon pool species, and consequently, also the product distribution.

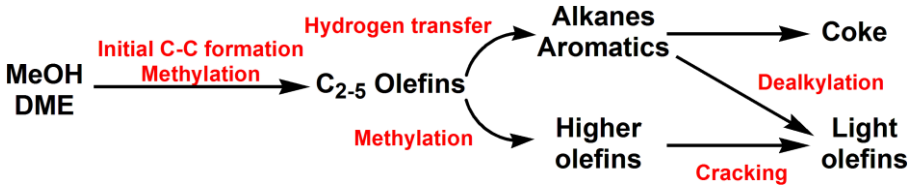

Scheme 4.1. Simplified MTH reaction pathway. Adapted from [163].

In summary, this section reveals novel insights concerning the reactivity of methanol and DME in the MTH reaction, but also raises new questions. It has been shown that the overall activity towards the MTH reaction is higher with DME compared to methanol over H-ZSM-5, suggesting faster kinetics of reactions involving the two oxygenates *i.e.* methylation of alkenes and arenes. Furthermore, it has also been proven that the rate of methanol-DME interconversion reaction is in the same order of magnitude as the MTH chemistry over zeolites. As a consequence, non-equilibrium concentrations of methanol and DME are found throughout the reactor. Importantly, zeotype materials with weakly acidic sites show much faster methanol-DME interconversion that leads to thermodynamic equilibrium concentrations of the two oxygenates under MTH operation.

Methanol has been identified as a promoter of deactivation to a substantially higher extent than DME, and a deactivation model was therefore derived to rationalize these findings. In addition to deactivation, a consistent difference in the product distribution of the MTH reaction when methanol and DME are used as feeds has been elucidated. Methanol leads to higher yields of ethylene, alkanes and aromatics, whereas DME gives higher yields of alkenes and aliphatics in general. These results point towards a shift in the reaction mechanism dominating hydrocarbon conversion, wherein methanol shows a higher propagation of the arene cycle than DME (**Scheme 2.11**). Importantly, the catalyst deactivation and product distribution effects to methanol are extensively observed over zeolites, but attenuated over the zeotype employed in this study. Therefore, if methanol-DME interconversion is sufficiently fast, deactivation and product distribution become less dependent on the oxygenate feed.

This section also raises some questions such as *"why is methanol leading to a faster deactivation than DME?", "which kind of deactivation route is attributed only to methanol?", "why is the product distribution of the MTH reaction different with methanol and DME?", "are there kinetics and/or mechanistic differences between methanol and DME affecting the product distribution?"*. To elucidate the answers to these questions, we surmised that analyzing the interaction of methanol and DME with some hydrocarbons involved in the MTH reaction would be a highly valuable tool. The following sections therefore report on thorough studies of the reactivity of methanol and DME with benzene and isobutene. These two hydrocarbon molecules were selected because they can act as representative molecules for the two competing cycles dominating the MTH reaction, the arene and alkene cycles,

respectively. Emphasis is given to discerning kinetic and mechanistic differences as well as setting those differences into the context of the MTH reaction.

4.3. Benzene co-reactions with methanol and DME: parallel reaction paths to toluene and diphenylmethane

In this section, the interaction of methanol and DME with benzene, as a representative molecule of the arene cycle in the MTH reaction, is described. Experiments were conducted at low reactant conversion levels to minimize the extent of secondary reactions, thereby avoiding a complex hydrocarbon pool composition and enabling the extraction of kinetic and mechanistic information. The primary reaction to be observed was benzene methylation to toluene, with methanol and DME forming water and methanol, respectively. Despite of the low conversion levels, by-products might be formed via secondary reactions as depicted in **Scheme 4.2**. Successive methylation reactions yield polymethylbenzenes (polyMBs), that may dealkylate before exiting the microporous structure of the catalysts to give light olefins.

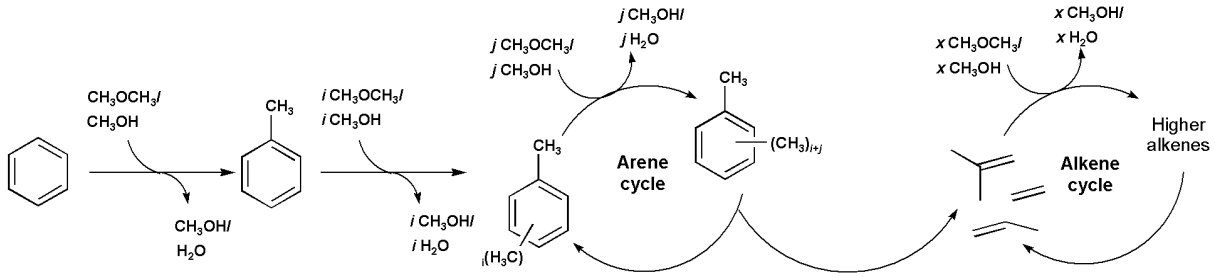

Scheme 4.2. Expected reactions during co-feed of benzene and MeOH/DME according to the dual-cycle mechanism. Adapted from [43, 64].

4.3.1. Comparative assessment of the reactivity of methanol and DME with benzene

The reactivity of methanol and DME with benzene was experimentally evaluated over the materials studied in the previous section: H-ZSM-5, H-SSZ-24 and H-SAPO-5. Our collaborators at the University of Ghent complemented the study by using theoretical methods that will be briefly commented upon. Focusing first on the experimental evaluation, benzene was co-reacted with equimolar amounts of methanol or DME. The net product formation rates over the three aforementioned materials at 250 and 300 °C are shown in **Figure 4.12**. Additional experiments over H-ZSM-5 at 350 °C are also reported. As the goal of these experiments was to elucidate differences in the behavior of methanol and DME, the right panels in **Figure 4.12** show the composition of the fraction of oxygenates in the effluent in terms of unconverted amounts of methanol and DME in order to assure the low extent of methanol-DME interconversion reaction during the tests.

These results reveal significant differences in both selectivities and overall activities among the three materials. However, these differences have been the focus of previous contributions and will not be covered here (see [43, 141, 254] for comparisons between the isostructural H-SSZ-24 and H-SAPO-5, and [200, 215] for comparison between zeolites with different topology, H-ZSM-5, H-Beta*, H-ZSM-58, H-ZSM-22). Instead, focusing on the differences observed between the methylating agents firstly at 250 °C, the use of DME led to approximately 5, 3 and 6 times faster net formation rate of toluene compared to methanol under the same contact time conditions over H-SAPO-5, H-SSZ-24 and H-ZSM-5, respectively. These results are in line with previous studies over H-ZSM-5 at 350 °C, where faster methylation rates of alkenes and methylbenzenes were reported with DME compared to methanol [218], and the results presented in **Section 4.2**, which displayed higher overall MTH activity for DME compared to methanol. Furthermore, only three main product groups were observed when using DME as co-feed: toluene, polyMBs and alkenes, in accordance with the methylation-dealkylation reaction path described in **Scheme 4.2**. However, when using methanol as co-feed, a fourth abundant product group appeared: Diphenylmethane and its methylated analogue, methyldiphenylmethane (DPMs). DPMs accounted for up to 31 mol% selectivity over the large pores zeolite H-SSZ-24. In contrast, these bulky hydrocarbons were hardly observed in the effluent when DME was used as the methylating agent (maximum 2 mol% selectivity over H-SSZ-24). Recent work from our group also reported the formation of DPM during benzene co-reactions reactions with methanol over H-SSZ-24 and H-SAPO-5, although its origin was not identified [43].

Experiments performed at 300 °C (**Figure 4.12**, middle panel) mostly reproduced the trends observed at 250 °C. The net rates of toluene formation were ~2, ~4 and ~1.5 times higher over H-ZSM-5, H-SSZ-24 and H-SAPO-5 with DME as the methylating agent compared to methanol. Total product formation rates were also faster over the zeolites H-SSZ-24 and H-ZSM-5 when using DME, but a similar total product formation rate with methanol and DME over H-SAPO-5 was observed at 300 °C. In this case, the high conversion of methanol into DME when co-feeding methanol and benzene over H-SAPO-5 (almost 50 mol% methanol converted to DME) complicates the separate assessment of methanol and DME as methylating agents, in contrast to the two zeolites (**Figure 4.12**, middle right panel). Therefore, these results conveniently agree with the high activity for methanol dehydration to DME over this catalyst reported in **Sections 4.1** and **4.2**. As observed at 250 °C, significant amounts of DPMs were observed when methanol was employed, but very small amounts were observed with DME. For all three catalysts, the net formation rate of DPM during methylation with methanol increased with increasing temperature, however relatively less than the increase in methylation rates, leading to an overall decrease in DPM selectivity at higher temperatures.

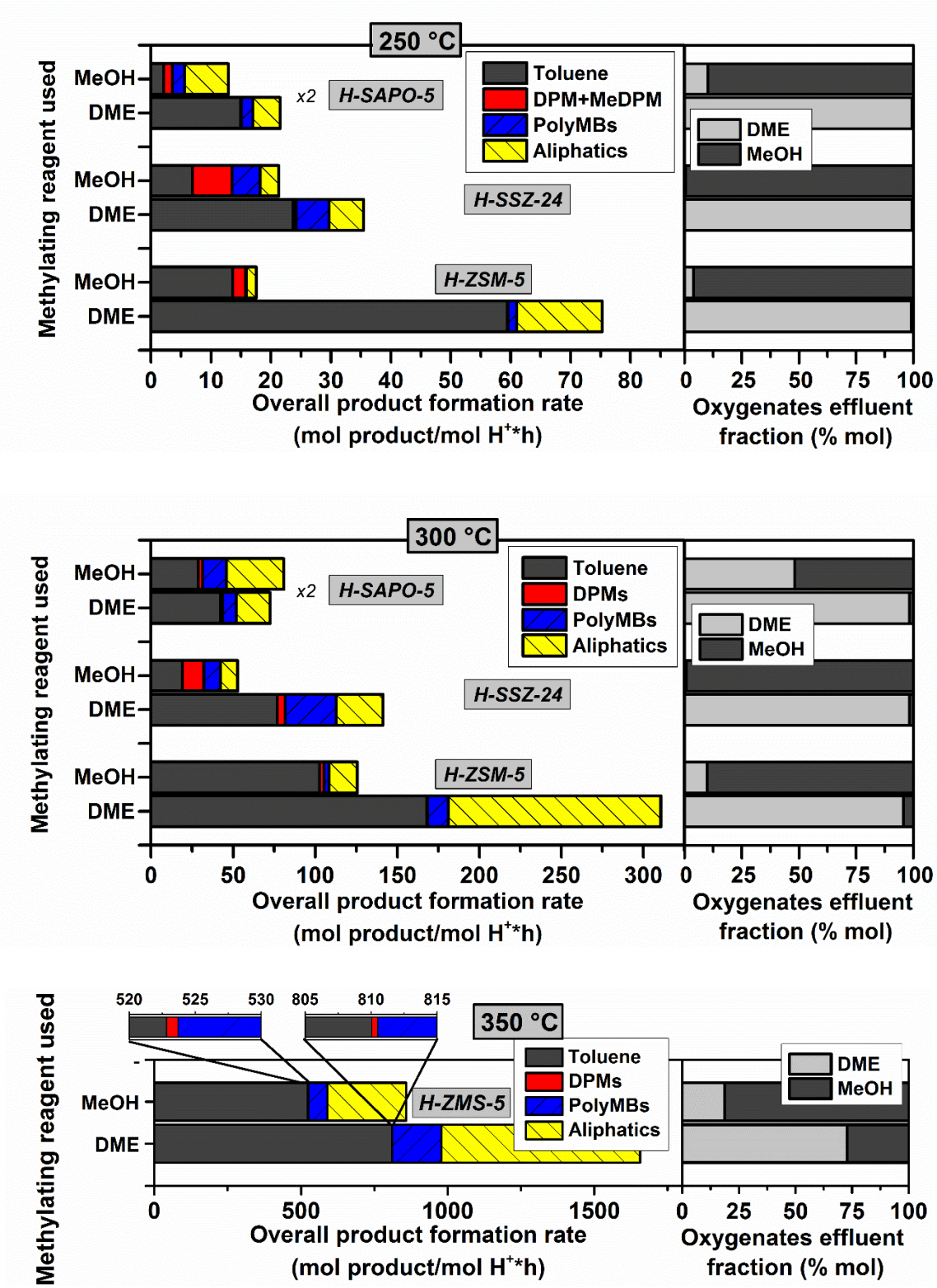

Figure 4.12. Net product formation rate (left) and oxygenates effluent fraction (right) during benzene co-reaction with oxygenates (60:60 mbar) over H-SAPO-5, H-SSZ-24 and H-ZSM-5 at 250 °C (top), 300 °C (middle) and 350 °C (only H-ZSM-5, bottom). Total flows = 54.5 mL/min (H-SAPO-5, H-SSZ-24), 100 mL/min (H-ZSM-5), benzene conversion < 1% (250 °C), <3% (300 °C), <9% (350 °C). Product formation rates for H-SAPO-5 were multiplied by a factor of 2 for better visualization of the results.

Despite the higher conversion levels and the increased prominence of the methanol – DME interconversion reaction at 350 °C, significant differences were still observed with respect to primary methylation and competing reactions over H-ZSM-5 (**Figure 4.12**, lower panel). DME remained the more active methylating agent, while methanol led to 10-times higher net formation rate of DPMs compared to DME. Together, the data presented here already establish a link between methanol (not DME) and DPM formation.

Concerning the theoretical assessment, it was calculated the probability for methanol or DME protonation, and the probability to form a pre-reactive complex for concerted methylation, based on molecular dynamics simulations of methanol or DME with benzene at 250 and 350 °C over H-SAPO-5, H-SSZ-24 and H-ZSM-5. This methodology was earlier successfully applied to explain the differences in reactivity between H-SAPO-5 and H-SSZ-24 for benzene methylation [141]. We opted to study the concerted mechanism because this reaction step was earlier found to be the dominant methylation mechanism under the applied experimental conditions [43, 44]. The results at both temperatures look very similar, and those for 250 °C are displayed in **Figure 4.13** (results at 350 °C are shown in Paper I). A clear clustering of the results per material can be observed. The most striking difference between methanol and DME is observed in the probability for it to form favorable pre-reactive complexes for benzene methylation. This probability differs by more than a factor of 2, indicating a higher intrinsic reactivity of DME than methanol towards methylation. Therefore, the analysis of the theoretical results is in line with the experimental observations.

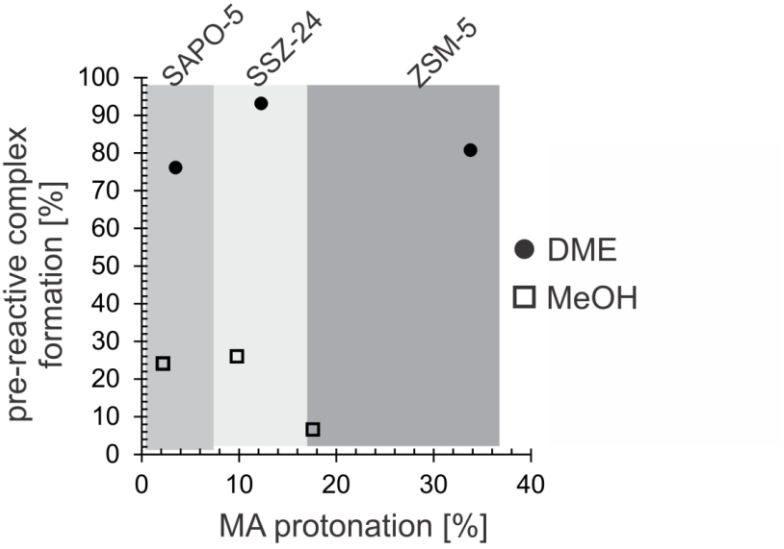

Figure 4.13. Probability for methanol or DME protonation (horizontal axis) and probability that a pre-reactive complex is formed (vertical axis) for benzene methylation during 50 ps MD runs of the co-adsorbed complexes in H-SAPO-5, H-SSZ-24 and H-ZSM-5 at 250 °C.

4.3.2. Mechanistic insights into the reactivity of methanol with benzene

The intriguing formation of DPMs in the presence of methanol directed our attention to its formation mechanism because these bulky compounds have been previously categorized as coke precursors during hydrocarbon transformations reactions over zeolites [255, 256]. It is possible that methanol is directly involved as a reactant, or that either methanol and/or water, which is not present during reactions with DME (or at least to a very low extent), could have an assisting role. For instance, water and methanol have been recently assigned assisting roles during polyMB side-chain methylation in SAPO-34 [128]. To distinguish between these possibilities, co-feed studies of benzene and toluene with and without the addition of water, methanol and DME, were carried out over H-ZSM-5 at 250 and 300 °C. Under these reaction conditions, we could emulate the conditions where DPM was formed in the previous section, with a significant excess of benzene over toluene (60:1.5 mbar). As shown in **Figure 4.14**, no reaction occurred between only benzene and toluene. Importantly, only addition of methanol yielded significant amounts of DPMs. Thus, the possibility for water-assisted reactions between toluene and benzene was excluded and the presence of methanol can be regarded as essential to the formation of DPMs.

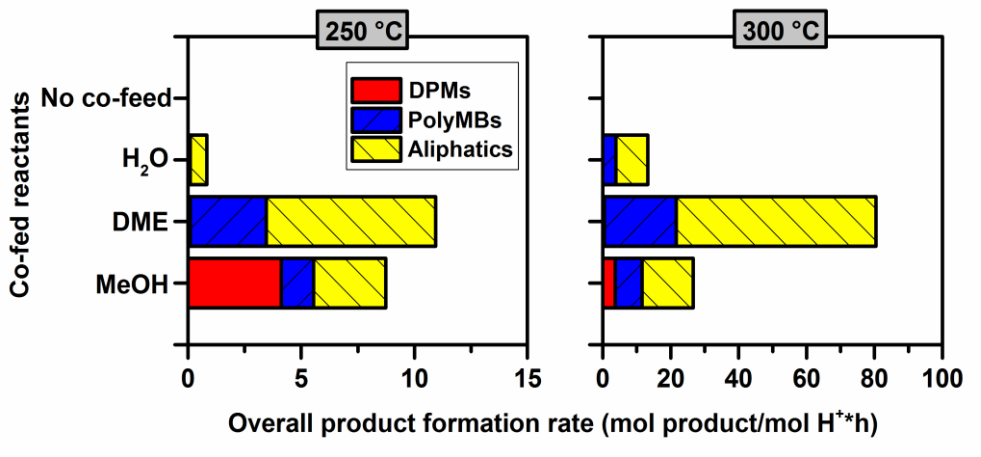

Figure 4.14. Net formation of products during toluene phenylation when co-feeding benzene: toluene:MeOH/DME/H_2O (60:1.5:10 mbar) on H-ZSM-5 at 250 °C (left) and 300 °C (right). Total flow = 100 mL/min, benzene conversion < 1, 3% at 250 and 300 °C.

At this point, we further evaluated the seemingly determinant role of methanol by co-reacting benzene, toluene and ^{13}C-MeOH under similar conditions to those used in the aforementioned experiment. **Figure 4.15** illustrates the isotopic distributions observed in DPM and *o*-xylene, that is considered as representative toluene methylation product. Clearly, both products presented a dominating isotope distribution containing one labelled carbon coming from methanol. This confirms the direct participation of methanol in DPM formation, ruling out the possibility for an assisting role. These

experimental findings clearly indicate that benzene may undergo two parallel reactions when fed together with methanol: a methylation reaction leading to toluene (and to subsequent methylation/dealkylation products), and another reaction in which methanol reacts with two benzene molecules to form DPM. Since no significant reactivity was observed between toluene and benzene, toluene cannot be an intermediate in this latter reaction leading to DPM.

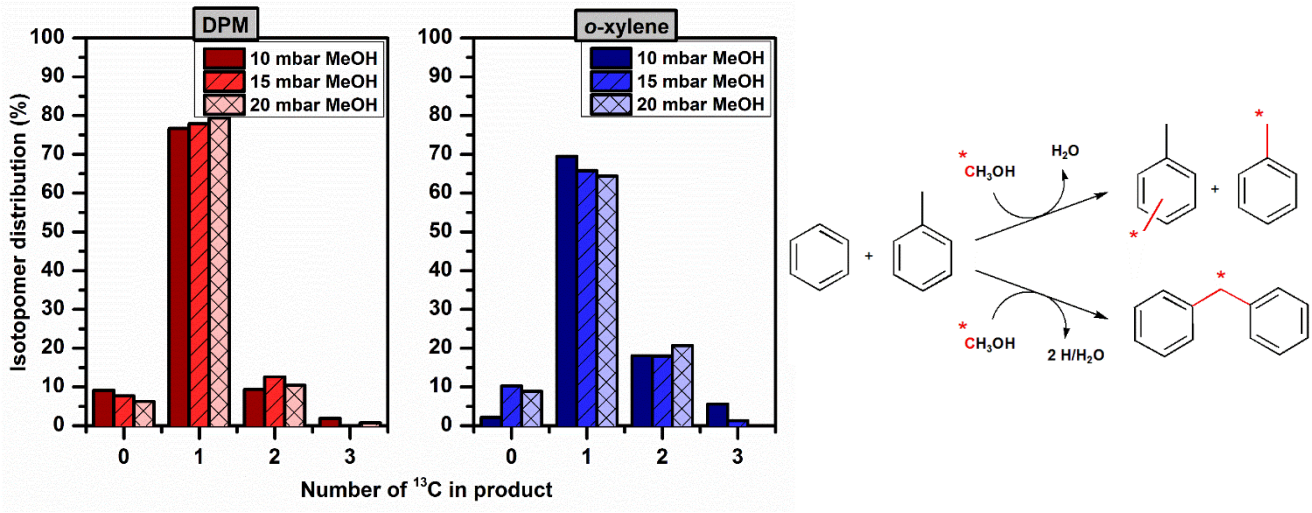

Figure 4.15. Isotopomer distribution of DPM (left) and *o*-xylene (middle) during co-feed of benzene:toluene:^{13}MeOH (60:1.5:10-20 mbar) over H-ZSM-5 at 250 °C. Total flow = 100 mL/min, benzene conversion < 1%. Competitive reaction pathways during co-feed of benzene, toluene and methanol (right).

Aiming to gain additional mechanistic information on the apparent competitive formation of DPM and toluene in the presence of methanol, a series of experiments that systematically varied benzene and methanol partial pressures were performed at 250 °C over H-ZSM-5. The results are collected in **Figure 4.16** as a logarithmic plot of net formation rates. The rate of toluene formation showed a positive reaction order in benzene partial pressure, with zeroth order in methanol at the lowest pressures, in agreement with previously reported benzene methylation studies [200, 210]. These results indicate that Brønsted acid sites are saturated in methanol under the tested conditions. However, high methanol partial pressures showed a slight decay in toluene formation. In contrast to toluene, DPM showed a positive reaction order in methanol and a negative reaction order in benzene. These results together with the negative order in methanol for toluene formation suggest that the reactions leading to toluene and DPM compete for the same active site.

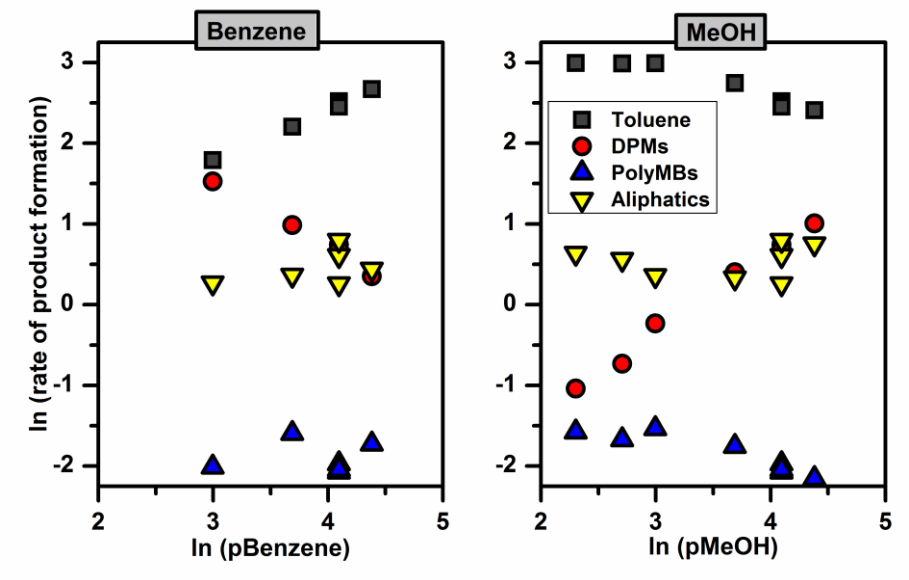

Figure 4.16. Net product formation rates variation with benzene (left) and MeOH (right) partial pressures during benzene co-reaction over H-ZSM-5 at 250 °C. Benzene partial pressures were varied in the range 20-80 mbar while keeping MeOH at 60 mbar, while MeOH partial pressures were varied in the range 10-80 mbar, while maintaining benzene at 60 mbar. Total flows = 100 mL/min, benzene conversion < 1%.

Once the positive reaction order for methanol in DPM formation was determined, the two competitive paths were evaluated by co-reaction of benzene with either CH_3OH and CD_3OH over H-ZSM-5 at 250-350 °C. The results are shown in **Figure 4.17**. The rate of toluene formation (left-hand panel) was independent of the methanol isotope used (k_H/k_D ~1), as expected for a reaction in which C-C bond formation between benzene and a methyl group is the rate-determining step. Nevertheless, the formation rate of DPM (left-hand panel) was consistently reduced along the broad temperature range measured when CD_3OH was used, revealing a primary kinetic isotope effect with k_H/k_D ~ 2. Therefore, the rate-determining step in DPM formation involves C-H (D) bond breaking in methanol. The isotopomer distribution of DPM at 250 °C is shown in the right-hand panel, and clearly reveals a shift corresponding to 2 mass units when CD_3OH was used as a co-reactant. This result is fully consistent with C-H (D) bond rupture in methanol during the rate determining step towards DPM formation, which leads to the incorporation of a $-CH_2-$ entity from methanol in DPM, and point towards methanol dehydrogenation on top a methanol sorbate at the Brønsted site.

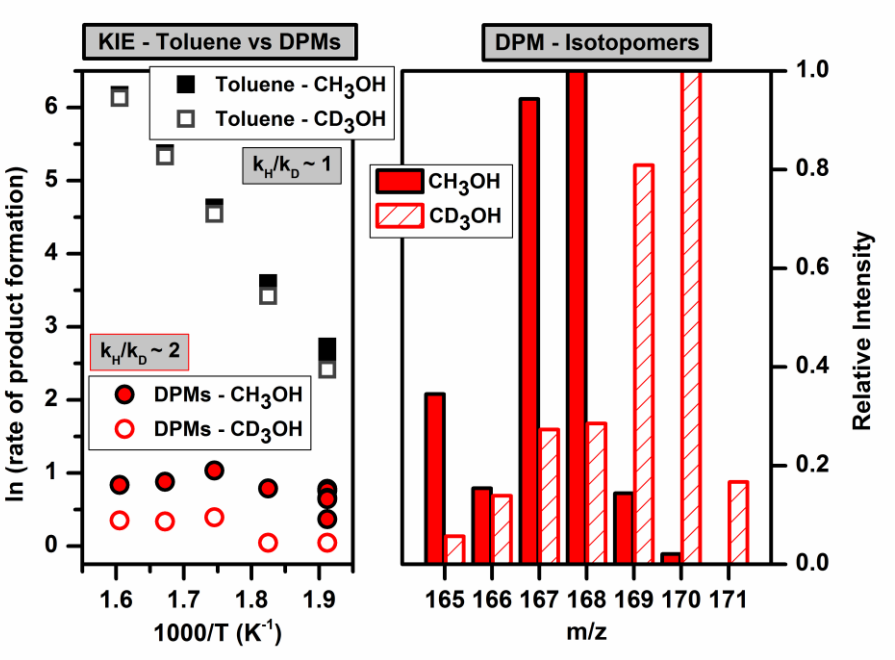

Figure 4.17. Temperature correlation for the rate formation of toluene and DPMs (left) and DPM isotopomer distribution observed at 250 °C (right) during the co-feed of 60:60 mbar benzene:MeOH (filled symbols) and benzene:MeOH-D3 (empty symbols) on H-ZSM-5 at 250-350 °C. Total flows = 100 mL/min, benzene conversion < 9%.

Under the assumption that methanol dehydrogenates, it is reasonable to propose that formaldehyde (CH_2O), which presents the -CH_2– entity observed in DPM, may be formed. Indeed, the synthesis of DPM has been reported from benzene and formaldehyde over zeolitic materials [257, 258], matching well with our hypothesis. Importantly, a theoretical reaction pathway from formaldehyde and benzene to DPM was found by our collaborators at the University of Ghent and it is presented in Paper I. It is important to mention that numerous experimental and theoretical studies have reported the formation of formaldehyde during the initial stages of the MTH reaction in the so-called methane-formaldehyde mechanism **Scheme 2.5** [85, 87, 90, 91, 95-101, 167] or in methanol-induced hydrogen transfer reaction with alkenes **Scheme 2.15** [164]. Importantly, Fan and co-workers recently assessed this initial stage of the MTH reaction with methanol and DME using theoretical methods. They concluded that formaldehyde was the most stable species derived from methanol prior to the first C-C bond formation, while DME showed $CH_3OCH_2^+$ cations as the most stable species involved in the initial C-C bonds [96]. This role for $CH_3OCH_2^+$ cations was also pointed out by Peng *et al.* [259]. The work presented in this section is not fully related to C-C couplings that lead to the first hydrocarbons of the MTH reaction. However, it seems to share some key points with the methane-formaldehyde mechanism, since formation of formaldehyde in this process is not very energetically demanding, but rather the subsequent C-C formation requires prohibitively high energies [90, 96]. Therefore, it is likely that

methanol-methanol reactions are not entirely outcompeted by methylation reactions under our reaction conditions. The highest selectivities towards DPM (though not yields) were observed at the lowest temperatures studied, as low as 250 °C. However, when the temperature was increased, methylation kinetics became considerably faster, and DPM formation became less relevant, but still occurred in the presence of methanol. More details regarding the formation of formaldehyde in the MTH reaction will be presented in **Section 4.5**. It is important to note that it is not clear what precise role the $CH_3OCH_2^+$ cations play during DPM formation, though a minor role is expected for them according to our benzene-DME co-reactions.

Finally, in order to strengthen our hypothesis suggesting formaldehyde formation from methanol as a key step towards DPM, benzene was co-reacted with a methanol stream containing formaldehyde, and the results were compared with benzene-methanol co-reaction under the same contact time conditions. **Figure 4.18** compares the products derived from the competitive pathways elucidated so far, leading to toluene and DPMs as an Arrhenius-type plot in the temperature range 250-350 °C. The addition of formaldehyde clearly led to a decrease of toluene in the effluent, while maintaining the same apparent activation energy, suggesting that formaldehyde competes with methanol for adsorption at the Brønsted sites and thereby slows down the methylation pathway. In contrast, the net DPM formation rate followed an exponential trend with temperature in the presence of formaldehyde as well as a clear promotion effect at 300 and 350 °C, strongly supporting the key role of formaldehyde in the reaction pathway towards DPM.

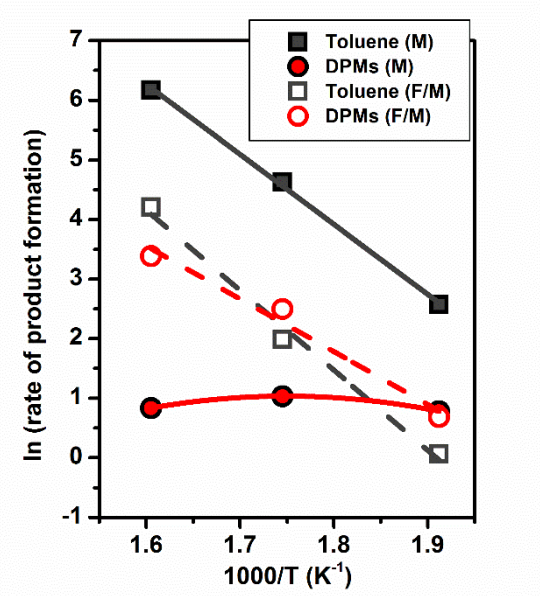

Figure 4.18. Arrhenius-type plot for toluene and diphenylmethane formation when feeding 60 mbar benzene with 60 mbar MeOH and 58:1:1 mbar MeOH:methane:formaldehyde (F/MeOH) in temperature range 250-350 °C. Total flows = 100 mL/min, benzene conversion < 1, 3, 9% at 250, 300 and 350 °C, respectively. Benzene co-reaction with MeOH and F/MeOH are plotted with filled and empty symbols, respectively.

4.3.3. Implications in the MTH reaction

Throughout **Section 4.3**, the reader has been conducted through a systematic study reflecting the distinct behavior of methanol and DME with benzene. Benzene was considered as a representative active hydrocarbon molecule belonging to the arene cycle in the context of the MTH reaction. Therefore, some conclusions of this detailed study may be extrapolated to broader MTH chemistry.

First, DME showed faster benzene methylation rates and activity towards consecutive methylation and dealkylation in relation to methanol, matching well with its higher overall MTH activity reported in **Section 4.2** (**Figure 4.4**).

Second, a different product selectivity was observed with the two oxygenates interacting with benzene, independently of catalyst topology and acidity. Whereas DME dominantly promoted (successive) methylation of arenes and dealkylation leading to toluene, polyMBs and alkenes, the use of methanol formed considerable amounts of DPMs in addition to the aforementioned products. These differences were augmented at the lowest temperature studied (250 °C), and decreased at relevant MTH temperatures (350 °C). The formation of DPMs was rationalized based on a hydrogen transfer reaction from methanol (that barely occurred with DME) and yielded formaldehyde as an intermediate. Therefore, these results indicate a different activity of methanol and DME towards methylation and a

specific hydrogen transfer reaction yielding formaldehyde, and those differences may impact the product distribution of the MTH reaction as it was reported in **Section 4.2** (Figure 4.9 and **Figure 4.10**).

Third, formaldehyde has been classified as a coke promoter during the MTH reaction [166, 260]. We rationalize that its formation derives exclusively from methanol and it is proposed as an intermediate to give DPM when reacting with benzene. Furthermore, DPM-like compounds have been found to act as coke precursors during hydrocarbon transformations in zeolitic materials [255, 261]. Consequently, the results presented in this section identify a plausible route from methanol to coke precursors via formaldehyde, which is not observed for DME. Again, these findings are fully consistent with the considerably faster deactivation rates observed with a methanol feed under MTH operation over zeolite catalysts compared to a DME feed (Figure 4.5 and **Figure 4.6**) and the output drawn by our semi-empirical deactivation model (**Table 4.2**), that clearly attributed a stronger deactivation character to methanol compared to DME.

4.4. Isobutene co-reactions with methanol and DME: methylation versus hydrogen transfer

Analogously to the previous section, where the reactivity of methanol and DME towards benzene was studied as a representative molecule of the arene cycle, this section reflects the reactivity of methanol and DME towards isobutene, as a representative molecule of the alkene cycle in the MTH reaction. It is worth mentioning that this hydrocarbon is the most thermodynamically favored C_4 alkene isomer under the typical MTH conditions, and it is therefore an abundant effluent product during the conversion of methanol and DME to hydrocarbons over different zeolites [125, 141, 262-264]. Furthermore, it has been earlier found that branched hydrocarbons are more effective in hydrogen transfer reactions than linear hydrocarbons because they can adsorb as stable tertiary carbocations under MTH operating conditions [230-232, 234, 265, 266]. Accordingly, the co-reaction of methanol and DME with isobutene is presented as an ideal reaction to represent not only alkene cycle reactivity, but also to reflect how the two oxygenates affect the relative propagation of the two catalytic cycles in MTH because the alkene and arene cycles are connected via hydrogen transfer reactions, as shown in **Scheme 4.3**. Importantly, H-ZSM-5 nanosheets were selected as the catalyst for this study for two reasons: 1) H-ZSM-5 is the most industrially relevant MTG and MTP catalyst, wherein the alkene and the arene cycle are clearly observed [49, 137], 2) the nanosheet morphology shortens the diffusion path of reactants and products [229, 242], thereby setting the focus of the study on the kinetic origin of the propagation of the alkene and the arene cycle via competitive methylation and hydrogen transfer.

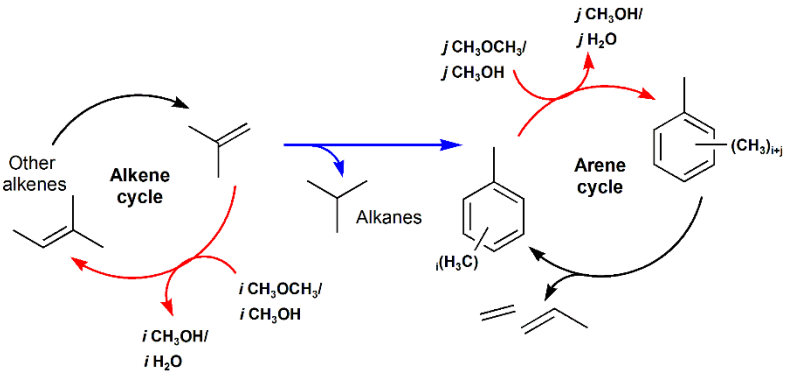

Scheme 4.3. Schematic simplified reactivity of isobutene within the context of the dual cycle mechanism.

4.4.1. Comparative assessment of the reactivity of isobutene alone and reacted with methanol/DME

In contrast to the relatively low reactivity of benzene alone shown in the previous section, isobutene is a fairly active hydrocarbon itself when reacted over zeolitic materials. For instance, isomerization, dimerization, oligomerization, cracking and hydrogen transfer reactions are expected to occur [267, 268]. Therefore, it becomes important to discern the products that pure isobutene reactions over our tested zeolite may lead to, and compare the products to those formed when methanol and DME are added to the feed.

Figure 4.19 illustrates the formation rate of products grouped in families during the reaction of 40 mbar isobutene alone, 40:40 mbar methanol:isobutene and 40:40 mbar DME:isobutene feeds over H-ZSM-5 at similar contact times and at 350 °C. The colored **Scheme 4.4** aims to guide the reader to a description of the dominant reaction pathways that are proposed to rationalize the formation of the effluent products observed in reactions involving only isobutene and isobutene with methanol and DME.

A methanol/isobutene feed promoted the formation of alkanes (predominantly isobutane in this case) and a series of polyunsaturated hydrocarbons (dienes, cycloalkenes and aromatics), as compared to a pure isobutene feed. These results support the important role of methanol as promoter in methanol-induced hydrogen transfer reactions, which seem much faster than olefin-induced hydrogen transfer reactions [164]. In spite of the higher total conversion rate of the DME/isobutene feed, a lower net formation rate of alkanes and polyunsaturated hydrocarbons was observed relative to the methanol/isobutene feed. However, these results also reveal that DME promotes hydrogen transfer reactions with respect to the pure isobutene feed, but to a lesser degree than methanol. Interestingly, a reduction in the formation rate of C_4 isomers in the presence of methanol and DME is observed, relative to the pure isobutene feed. Under the low conversion levels achieved (< 18%), it is expected that isomerization is the main reaction involved in the formation of C_4 isomers from isobutene. As earlier reported by Svelle *et al.*, the presence of oxygenates with alkenes suppresses alkene isomerization rates, in favor of competing reactions [203]. The formation of the remaining of products, C_3, C_5 and C_{6+} is rationalized in the following subsection.

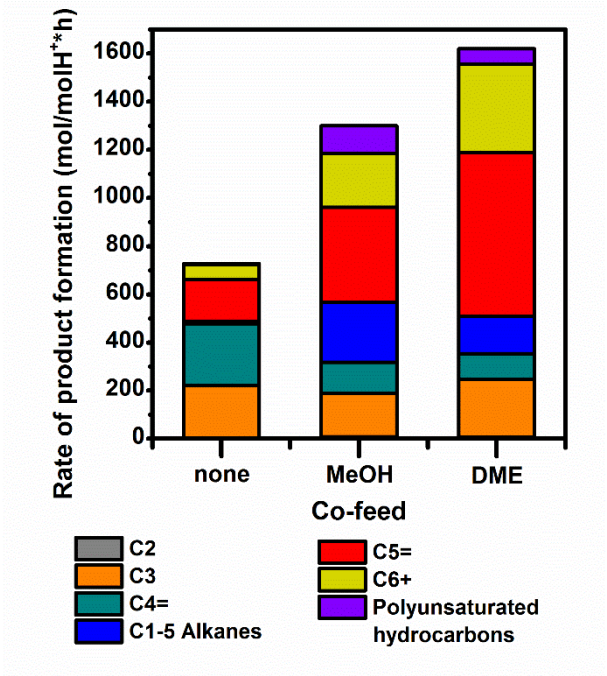

Figure 4.19. Net product formation rates of reaction of isobutene (40 mbar) alone and co-reacted with MeOH (40 mbar) and DME (40 mbar) over H-ZSM-5 at 350 °C. Total flow = 100 mL/min. Total conversion = 9.5-17.4 %.

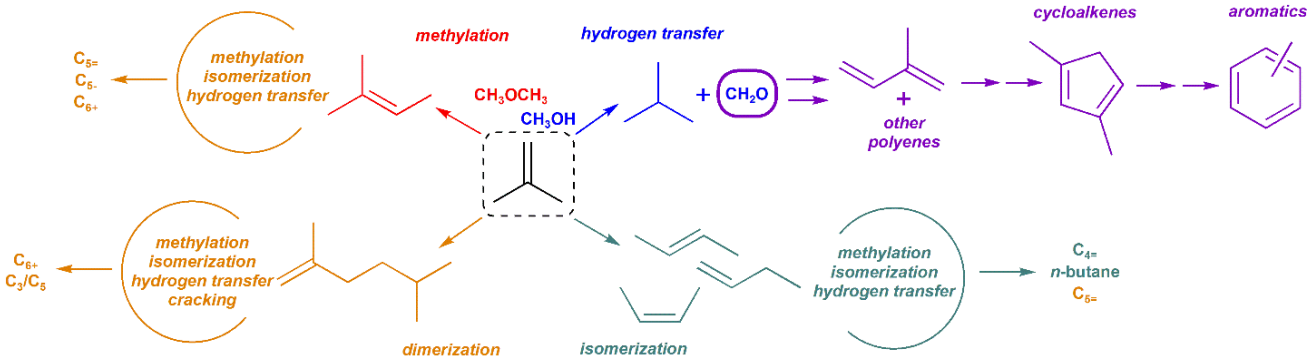

Scheme 4.4. Proposed predominant reaction pathways of the co-reactions of isobutene with MeOH/DME. The colored scheme aims to serve as guide to describe the origin of all products.

4.4.2. Comparative assessment of the reactivity of isobutene with methanol and DME

In this subsection, emphasis is set on further exploring the differences observed in the previous section in the co-reaction of isobutene with methanol and DME. For this purpose, equimolar isobutene and MeOH/DME mixtures were co-reacted over H-ZSM-5 nanosheets at 350 °C and all effluent products were carefully analyzed. It was found that the net formation rates of primary and secondary products gradually changed (**Figure 4.20**). Care was taken that the interconversion between methanol and DME did not affect the desired MeOH/DME concentrations during the catalytic tests, and it is corroborated in **Figure 4.21**, which reflects the molar fractions of unconverted methanol and DME normalized to 100.

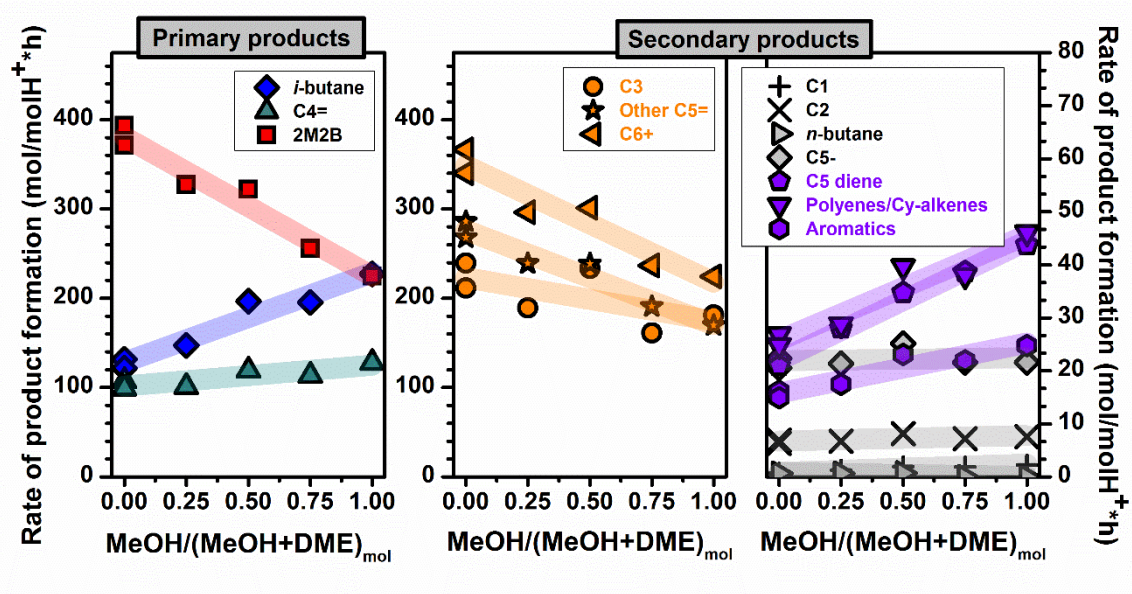

Figure 4.20. Net product formation rates during co-reactions of isobutene (40 mbar) with different MeOH/DME mixtures (40 mbar) over H-ZSM-5 at 350 °C. Total flow = 100 mL/min. Total conversion = 12.7-17.8 %.

Focusing first on the primary products observed (**Figure 4.20** – left panel), it is shown that larger fractions of DME in the feed promotes the formation of 2-methyl-2-butene (2M2B), which is the direct methylation product expected from isobutene [209]. In contrast, increasing the fraction of methanol in the oxygenate co-feed, and despite the lower overall activity, leads to a steadily promotion in the formation of isobutane, which is the direct hydrogen transfer product from isobutene. These results, combined with the nearly null isobutane formation from only isobutene feed, corroborates that methanol presents a stronger ability than DME to carry out hydrogen transfer reactions. The last product family in **Figure 4.20** – left panel shows that the formation rate of linear C_4 isomers from isobutene is suppressed to a similar extent by methanol and DME.

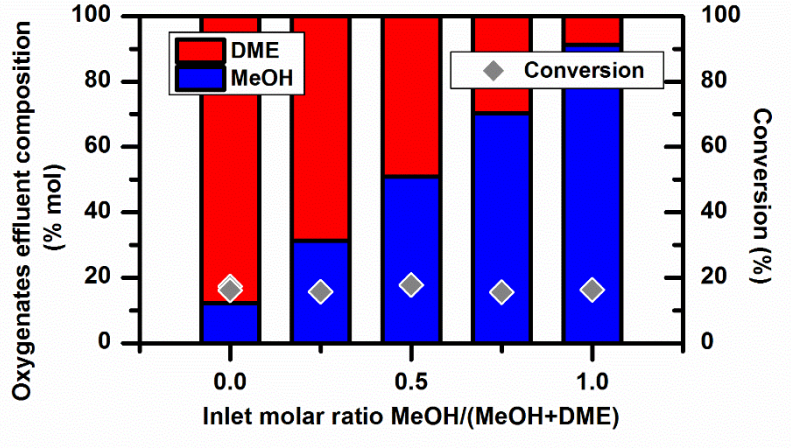

Figure 4.21. Unconverted oxygenates in the effluent expressed as molar fraction normalized to 100 % and conversion of reactants during co-reactions of isobutene (40 mbar) with different MeOH/DME mixtures (40 mbar) over H-ZSM-5 at 350 °C. Total flow = 100 mL/min. Total conversion = 12.7-17.8 %.

Secondary products of the co-reaction between isobutene and the oxygenates are plotted in **Figure 4.20** – middle and right panels. They are grouped according to their formation rate trend with increasing methanol fractions in the feed. The products in the middle panel are promoted by DME, while most of the products in the right panel are promoted by methanol. The reader is remitted to **Scheme 4.4** to visualize the reaction pathways proposed for the formation of the products.

The C_{6+} monoalkene hydrocarbons are grouped together in **Figure 4.20** (middle panel). These products may result from different reaction pathways, *i.e.* C_5 sequential methylation or dimerization/(cracking). The extent of the dimerization/(cracking) route can be estimated from experiments with pure isobutene feed (**Figure 4.19**) because DME and methanol are not involved in this reaction pathway. Clearly, the formation rates of C_{6+} monoalkenes is much faster in the presence of methanol and DME. Therefore, these results suggest that the majority of these products are formed via sequential methylation reactions. As this product family is promoted by DME compared to methanol, the results are consistent with faster methylation kinetics for DME. The same trend is observed in the formation rates of C_5 alkene isomers, which do not include 2M2B, the primary isobutene methylation product [209]. These products may derive from methylation/isomerization and/or dimerization/cracking reactions. As also observed for C_{6+} monoalkene hydrocarbons, C_5 alkene isomers are promoted by DME compared to methanol, and substantially suppressed in the absence of the oxygenates (**Figure 4.19**). Hence, it is concluded that methylation/isomerization is the dominant reaction pathway, and the faster methylation kinetics of DME is responsible for their increase rates compared to methanol. The last product group that is promoted by DME corresponds to C_3, nearly exclusively propene. This short hydrocarbon might be formed either directly from DME, via cracking of higher alkenes or via aromatics dealkylation over H-

ZSM-5 [48, 137, 269-271]. The low conversion levels, small amount of aromatics produced and numerous reaction steps needed suggest a negligible contribution of dealkylation reactions to the C_3 fraction. Thus, its formation from hydrogen transfer-derived products (aromatics) can be ruled out. The most probable routes are then alkene cracking or direct DME conversion.

Methanol, in addition to the hydrogen-rich product (isobutane), promotes a series of hydrogen-deficient products to satisfy stoichiometric demands (**Figure 4.20** – right panel): C_5 diene (isoprene), polyenes-cycloalkenes and aromatics. These products are shown in the blue pathway in **Scheme 4.4**. A mass balance of hydrogen transfer products is shown in **Figure 4.22** by reflecting an estimation for the ratio of number of saturated/unsaturated bonds created during the hydrogen transfer reactions in the effluent products. This ratio should ideally be equal to 1 in the absence of hydrocarbons retention. However, the ratio is slightly over 1, implying an excess of saturated hydrocarbons. The reason for this deviation might be due to: 1) the precision to determine alkanes in the C_1-C_5 fractions is considerably higher than the precision to measure the extent of unsaturation in C_{6+} hydrocarbons, 2) unsaturated hydrocarbons, such as aromatics, are likely accumulated within the zeolite structure, leading to coke deposits and preventing us from accounting for the unsaturated bonds created in their formation. Indeed, regeneration of the catalyst was necessary after every kinetic test due to the loss of activity reflected in our reference experiment, which was repeated in between measurements to assure that the tests were not affected by catalyst deactivation.

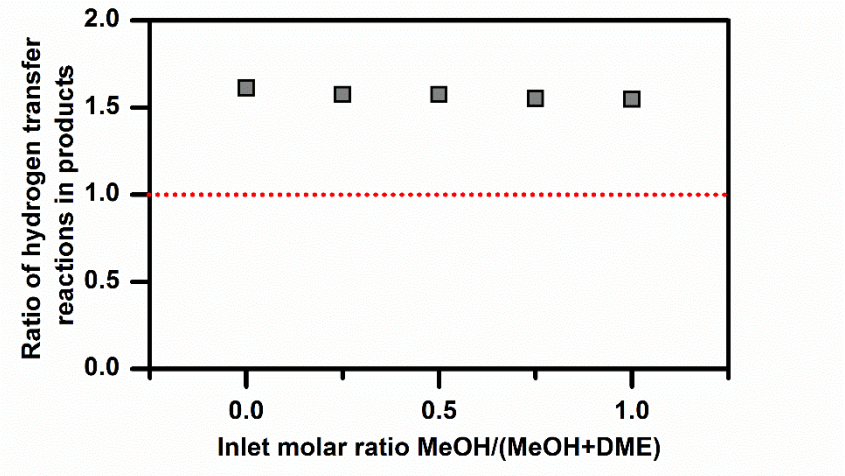

Figure 4.22. Estimated ratio of hydrogen transfer reactions leading to the observed amounts of alkanes over polyunsaturated and cyclic hydrocarbons, respectively, during isobutene co-reactions with methanol and DME over H-ZSM-5 at 350 °C. Total flow = 100 mL/min. Total conversion = 12.7-17.8 %.

At this point, it becomes relevant to discuss the origin of isoprene, the most abundant hydrogen-deficient product observed in the effluent. It is notable that butadiene was not observed, and this observation suggests that diene formation is preceded by an addition reaction instead of alkene dehydrogenation. Furthermore, the opposite trends observed in the formation rates of 2M2B and isoprene with increasing methanol fractions (**Figure 4.20**) suggest that 2M2B is not an intermediate in isoprene formation. It is conceivable to think that an already oxidized molecule from methanol, such as formaldehyde, may explain the observed trends in isoprene formation, as it was also proposed to explain the formation of DPM in the co-reactions of methanol and benzene (**Section 4.3**). Indeed, the synthesis of isoprene and other polyenes from alkenes and aldehydes via Prins reactions over zeolites is well documented [272-275], and recent studies have supported the presence of formaldehyde in the course of the MTH reaction [96, 164, 260]. It is therefore proposed that methanol induces hydrogen transfer reactions leading to alkanes and formaldehyde as reduced and oxidized molecules, respectively. A similar pathway was earlier suggested by Langner in the 1980s in order to explain the formation of alkanes in the course of the MTH reaction, although this proposal received little attention [106]. Once formed, formaldehyde can react with isobutene and other alkenes in the hydrocarbon pool to first form unsaturated alcohols, that rapidly dehydrate in the strongly acidic zeolite environment, to give isoprene and polyene hydrocarbons, respectively. These polyenes then cyclize to cycloalkenes that in turn act as intermediates in the formation of aromatic molecules during MTH as indicated previously by the groups of Haw and Hunger, and reflected in **Scheme 4.4** [114, 224]. The observation that all these hydrogen deficient products were promoted by increasing the methanol fraction in the feed is consistent with the selective formaldehyde formation from methanol, and its role in promoting the blue pathway in **Scheme 4.4**. In summary, a distinctive kinetic and mechanistic role of methanol and DME in their interaction with isobutene is observed. While DME presents much faster methylation rates than hydrogen transfer rates, methanol shows very similar rates for methylation and hydrogen transfer reactions. Furthermore, it is proposed the formation of formaldehyde from methanol via hydrogen transfer, and as a result, formaldehyde can affect the formation of secondary products.

To further investigate the formation mechanism of the most relevant products, ^{13}C-MeOH and non-labelled isobutene were co-reacted. The isotopomer distribution of isobutene, isobutane, 2M2B and isoprene are reflected in **Figure 4.23**. Isobutene in the effluent does not contain labelled carbon, meaning that the conversion level is sufficiently low not to produce substantial amounts of isobutene via secondary reactions, facilitating the mechanistic interpretation of the data. With regards to the main hydrogen transfer product, non-labelled isobutane dominates the isotopomer distribution, and thus corroborates its direct formation from isobutene. As expected, the main methylation product, 2M2B,

shows the incorporation of one labelled carbon from methanol. This confirms that direct methylation of isobutene is the main pathway involved in its formation, and other pathways *i.e.* dimerization/cracking are not significant under the tested conditions. In the same way, mono-labelled isoprene dominates the isotopomer distribution, proving the direct incorporation of the methanol carbon into the diene product. These results are also consistent with the hypothesis involving an already-oxidized derivative from methanol (formaldehyde) and isobutene in the formation of isoprene.

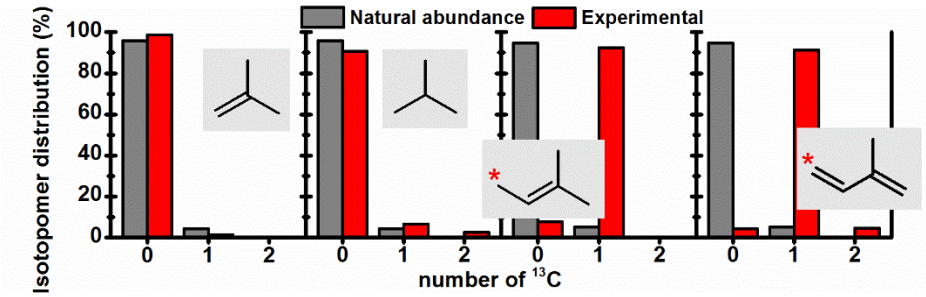

Figure 4.23. Isotopomer distribution of isobutene, isobutane, 2-methyl-2-butene and isoprene during co-reactions of isobutene (40 mbar) with ^{13}C-MeOH (40 mbar) over H-ZSM-5 at 350 °C. Flow = 100 mL/min. Total conversion = 17.8%.

Finally, our collaborators at the University of Ghent carried out a series of theoretical calculations by means of DFT and molecular dynamics simulations to complement the experimental observations. **Figure 4.24** displays the free energy profiles for isobutene methylation to 2M2B and hydrogen transfer to isobutane with methanol and DME over H-ZSM-5 at 350 °C, computed via static DFT calculations. Plausible methylation and hydrogen transfer mechanisms were found, and are shown in **Figure 4.24**. The hydrogen transfer mechanisms identified that formation of isobutane is plausibly accompanied by formaldehyde in the case of methanol (P_{HT}) or a methoxymethyl cation, $CH_3OCH_2^+$, in the case of DME (P_{HT}'), in line with the previously hypothesized formaldehyde formation from methanol. Importantly, the differences between the overall free energy barriers for the methylation and hydrogen transfer reactions were found to be 10 kJ/mol for methanol and 33 kJ/mol for DME. Therefore, these results supported the experimental observations because they reflect the highly competitive methylation-hydrogen transfer activity observed in methanol-isobutene co-reactions, and the weaker competition observed in DME-isobutene tests. The reader is remitted to Paper III for more details on the theoretical calculations.

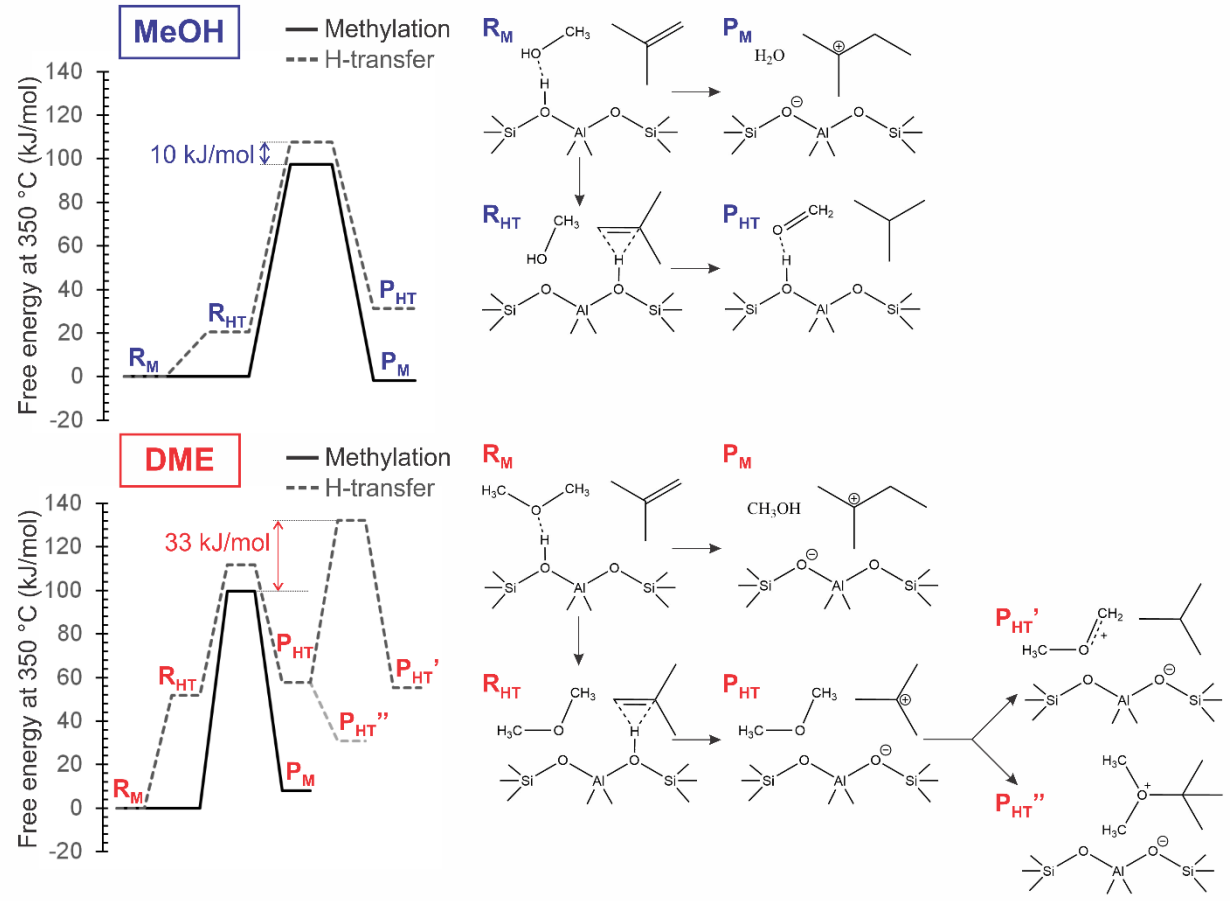

Figure 4.24. Free energy profile of isobutene methylation and hydrogen transfer reactions with MeOH (top) and DME (bottom). The right panels show the mechanism and stable states as indicated in the free energy profiles. Figure courtesy of Dr Kristof De Wispelaere.

4.4.3. Implications in the MTH reaction

In order to extrapolate the important differences observed between methanol and DME in terms of methylation versus hydrogen transfer reactions, and also the series of secondary reactions observed to the overall MTH reaction, we carried out a co-feed isobutene/oxygenates study increasing the total conversion levels from ~15 % ("kinetic conditions") to ~45 %. In this way, a larger pool of hydrocarbons is formed and will reflect more similarities to the real MTH hydrocarbon pool. For simplicity, the products were split in just four groups: alkenes, alkanes, aromatics and isoprene. **Figure 4.25** illustrates the product yields evolution with contact time. All yields increase with contact time applied, except for isoprene yields, supporting its intermediate role in the formation of more stable hydrocarbons, being the aromatics the end-products (**Scheme 4.4**). Furthermore, the yields of alkenes, alkanes and polyunsaturated hydrocarbons remain markedly different for methanol and DME co-feeds under these broad conversion levels. As also observed at lower conversions, alkanes and aromatics (hydrogen transfer products) are produced in a substantially larger extent in the presence of methanol. Therefore,

the reactivity of the hydrocarbon pool is clearly influenced by the proportions of methanol and DME in the reaction media.

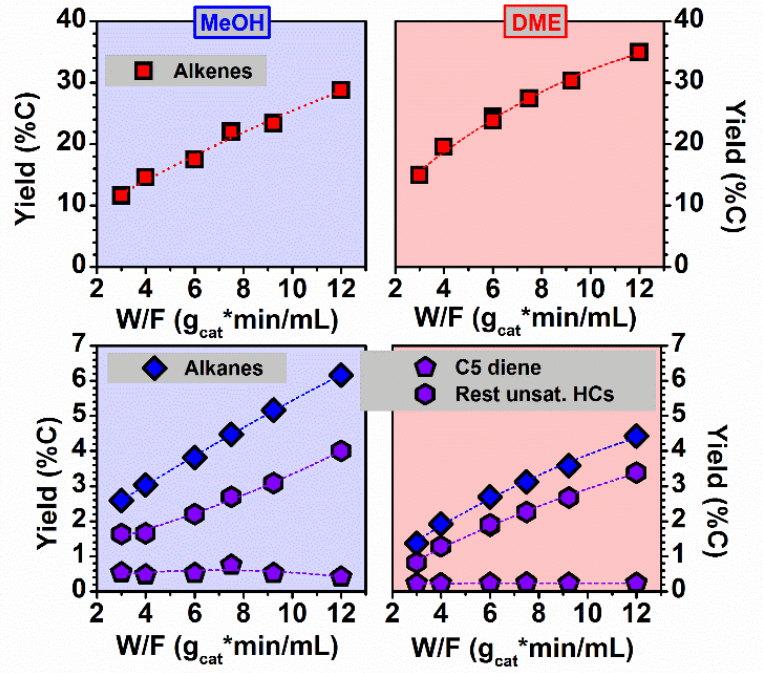

Figure 4.25. Yield of products (%C) during co-reactions of isobutene (40 mbar) with MeOH (40 mbar) and DME (40 mbar) over H-ZSM-5 at 350 °C. Total conversion = 16.4-43.0 %.

These results imply that the product distribution during the MTH reaction is affected by the ratio of MeOH/DME throughout the reactor. As a result, it is stated that methanol propagates the extension of the arene cycle compared to DME due to: 1) the promotion of hydrogen transfer reactions and 2) the role of formaldehyde (derived from methanol) on promoting dienes as important intermediates in aromatics formation. These results fully agree with the data presented in **Section 4.2**, where methanol feeds over zeolites, H-ZSM-5 and H-SSZ-24, clearly showed a consistently larger proportion of alkanes and arenes in their product distribution, relative to similar experiments with DME feeds.

As also mentioned in **Section 4.3**, formaldehyde is again postulated to be formed from methanol during the co-reaction with isobutene (but not from DME), and its role as coke-promoter [166, 260] may be highly relevant to explain the apparent methanol-induced deactivation presented in **Section 4.2**, and it will be discussed in the following subsection.

4.5. Perspectives on formaldehyde presence during the MTH reaction

Even though many similarities between the reactivity of methanol and DME have been found through the course of this study, the results presented in **Sections 4.2**, **4.3** and **4.4** reflected some important differences in the behavior of the two oxygenates as MTH reactants. Primarily, these differences are attributed to the higher capacity of methanol to participate in hydrogen transfer reactions in relation to DME. As a consequence, methanol is able to facilitate the transfer of 2H atoms to get oxidized into formaldehyde. In this section, we examine all possible routes through which formaldehyde formation may occur from methanol and it is investigated its effect on the MTH chemistry.

4.5.1. On the formation of formaldehyde

Different routes towards formaldehyde from methanol in the course of the MTH reaction are presented in **Scheme 4.5** with the concurrent formation of a reduced product. Some of the routes have been demonstrated plausible in the literature, while others are more speculative. It is likely that multiple routes can occur simultaneously depending on the precise reaction conditions. The first pathway refers to the disproportionation reaction between two methanol molecules leading to methane and formaldehyde. This reaction might be relevant under high methanol concentration conditions *i.e.* the initial stages of the MTH reaction, or after the methanol breakthrough because methanol concentrations in the reactor increase due to catalyst deactivation [90, 91, 96-98, 168, 276]. Alternatively, an alkene may act as methanol oxidizing agent leading to the formation of a C_{2+} alkane and formaldehyde [106, 164]. We also hypothesize that aromatics and/or cyclic alkenes may act as hydrogen donor acceptors [106]. These two routes might become relevant during the autocatalytic stage of the MTH reaction, where methanol, olefins and aromatics co-exist. Finally, if no reducing agent is acting, methanol dehydrogenation can lead to H_2 and formaldehyde [101]. This reaction might occur whenever methanol is present through the reactor, but likely to be outcompeted in the presence of olefins and aromatics. Thermodynamic considerations are assessed by calculating the Gibbs free energies for the reactions illustrated in **Scheme 4.5** at relevant tested temperatures: 250, 350 and 450 °C. Isobutene and benzene were chosen as representative oxidizing molecules in the second and fourth pathways, while isobutane and 1,3-cyclohexadiene were selected as plausible reduced products. Clearly, methanol dehydrogenation to hydrogen and formaldehyde, and isobutene hydrogen transfer to isobutane and formaldehyde showed the lowest energy demands, suggesting that these routes are more thermodynamically favored compared to benzene reduction to 1,3-cyclohexadiene and methanol disproportionation to formaldehyde and methane.

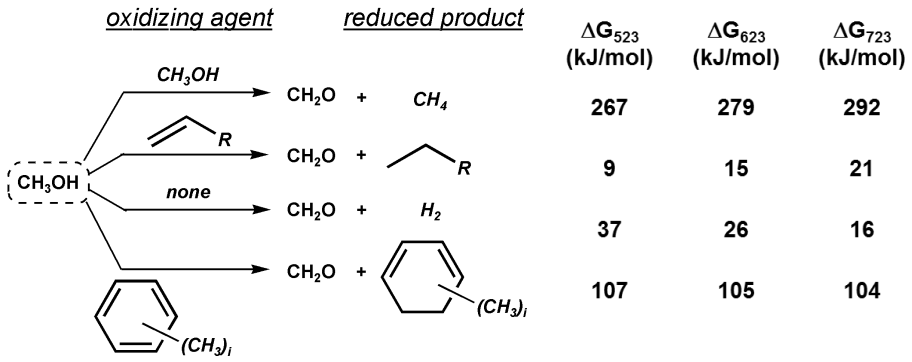

ΔG_{523} (kJ/mol)	ΔG_{623} (kJ/mol)	ΔG_{723} (kJ/mol)
267	279	292
9	15	21
37	26	16
107	105	104

Scheme 4.5. Plausible reaction routes from methanol to formaldehyde in MTH. R refers to hydrocarbon chain part of an alkene. Thermodynamic data were calculated based on [277, 278]. Isobutene and isobutane were selected as possible oxidizing agent and reduced product for the second pathway, while benzene and 1,3-cyclohexadiene were chosen as plausible oxidizing agent and reduced product for the fourth pathway. Gibbs free energies were computed at relevant tested conditions: 250, 350 and 450 °C, and atmospheric pressure.

Recapitulating the results observed in the interaction of benzene and methanol, the formation of DPM promoted by methanol requires that 2H atoms are transferred into another molecule to fulfill stoichiometric demands as shown in **Scheme 4.6**. Therefore, we followed methane, alkanes, H_2 and cyclohexenes formation to track all possibilities involving the formation of formaldehyde and a reduced molecule during the co-reaction of methanol-benzene over H-ZSM-5 in the experiments shown in **Figure 4.12**. Methane and alkane yields were too low to fully account for DPM yields. H_2 was not detected in quantifiable amounts using a mass spectrometer and GC with mol sieve column and TC detector. However, it should be noted that the sensitivity to hydrogen was lower than to hydrocarbons. Finally, cyclohexenes were not detected, but the large excess of benzene together with similar elution times of benzene and cyclohexenes in our 150m-long GC column do not allow us to discard their formation. The reason for the discrepancy in oxidation and reduction products in the effluent is thus yet to be revealed, and it was not possible to clearly identify the mechanism through which formaldehyde was formed in this case.

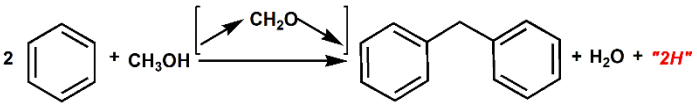

Scheme 4.6. Stoichiometric co-reaction of benzene and methanol to DPM.

Regarding the case where isobutene and methanol were co-reacted, hydrogen transfer reaction products were identified: isobutane and other alkanes were the main reduced hydrocarbons, while a series of dienes, polyunsaturated aliphatic hydrocarbons and aromatics were the dominant oxidized products detected. It was also found the essential role of methanol in the promotion of these products and its direct incorporation into the oxidized products, *i.e.* isoprene, via formaldehyde. Therefore, the preferred

pathway through which formaldehyde is formed under these conditions is possibly the route where a methanol molecule and an alkene (isobutene) molecule react to produce formaldehyde and an alkane (isobutane). The relatively low energy barrier for this reaction, computed by the theoretical calculations presented in **Section 4.4**, and the earlier presented thermodynamic considerations support this route as feasible under MTH conditions.

4.5.2. On the reactivity of formaldehyde in the MTH reaction

Before analyzing the potential reactivity of formaldehyde in the MTH reaction, **Scheme 4.7** aims at rationalizing formaldehyde reactivity when interacting with benzene and isobutene based on the results presented in **Sections 4.3** and **4.4**. Once formaldehyde is formed, it can rapidly react with olefins (isobutene), if present, to give dienes (isoprene), that in turn propagate the formation of aromatics. If formaldehyde interacts with aromatics (benzene), it is able to promote the condensation of aromatics, such as diphenylmethanes, which are likely to induce the formation of coke. Indeed, **Section 4.2** correspondingly reflected a clear correlation between high methanol concentrations and fast deactivation in the MTH reaction. Importantly, the comparison of the deactivation of H-SSZ-24 with and without the use of AlPO-5 shown in **Figure 4.6**, suggested a deactivation process that is based on methanol only. We attribute that pathway to the formation of formaldehyde from methanol because (1) formaldehyde can be formed from methanol, but not from DME, and (2) formaldehyde is known to enhance coke formation, *i.e.* via condensation of aromatics such as DPM, and thus accelerate deactivation [90, 96, 166]. Very recently, the group of Bhan corroborated the negative impact of formaldehyde on catalyst deactivation and attempted to improve the lifetime of H-SAPO-34 and H-SSZ-13 catalysts in the MTH reaction by selectively decomposing formaldehyde formed [260, 279]. For that purpose, they combined the zeolitic catalysts with basic Y_2O_3, that converted formaldehyde into CO and H_2, and observed up to 5-fold increase in conversion capacities of the catalysts.

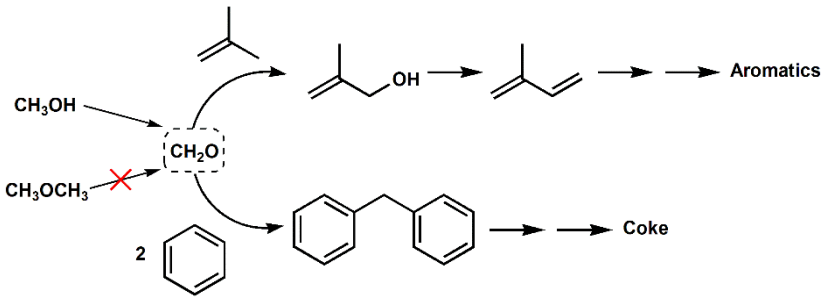

Scheme 4.7. Proposed reaction pathways of formaldehyde, formed from methanol, with isobutene and benzene, and consecutive promotion of aromatics and coke, respectively.

With the aim of strengthening our hypothesis on the formation of formaldehyde from methanol and its negative impact on catalyst stability, we compared the deactivation behaviour (**Figure 4.26**) and product distribution (**Figure 4.27**) of a methanol feed containing formaldehyde to those of a pure methanol feed over the same H-ZSM-5 catalyst used in **Section 4.2** at 350 °C. Clearly, the presence of formaldehyde reduced the conversion capacity of the catalyst, corroborating the coke-promoter claims attributed to this aldehyde in the MTH reaction [166, 260]. Concerning the product distribution, the co-feed of formaldehyde propagated the extension of the arene cycle, as larger yields of aromatics and ethylene, but lower yields of light olefins and aliphatics were obtained compared to the pure methanol feed. Interestingly, alkane yields were also reduced. At first instance, it could compromise the idea of higher prevalence of the arene cycle. However, the introduction of formaldehyde results in the formation of polyenes that in turn enhance the formation of aromatics without the need to form saturated alkane hydrocarbons in the process.

Therefore, co-feeding formaldehyde with methanol seemingly augmented the differences already observed between methanol and DME by accelerating deactivation and propagating the arene cycle (**Section 4.2**). These results agree well with the idea that formaldehyde is formed selectively from methanol and rationalize the mechanistic differences found on the interaction of benzene and isobutene with methanol and DME (**Sections 4.3** and **4.4**).

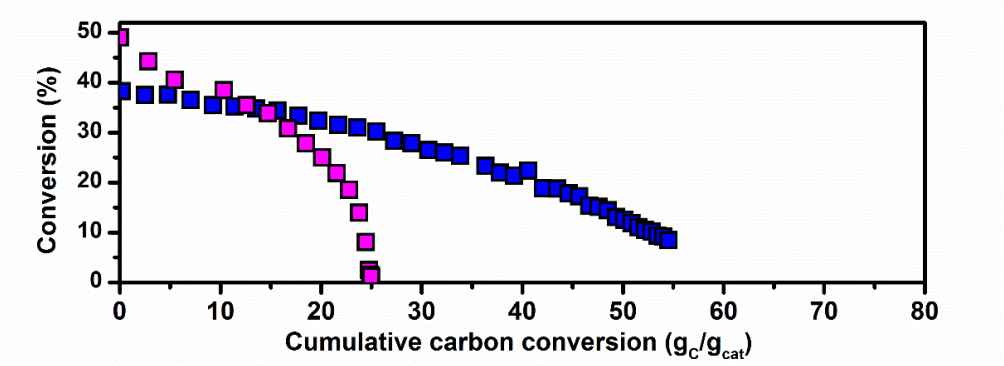

Figure 4.26. Cumulative carbon conversion during MTH reaction over H-ZSM-5 at 350 °C with MeOH and MeOH/CH_2O (approximately 1-2% CH_2O) feeds.

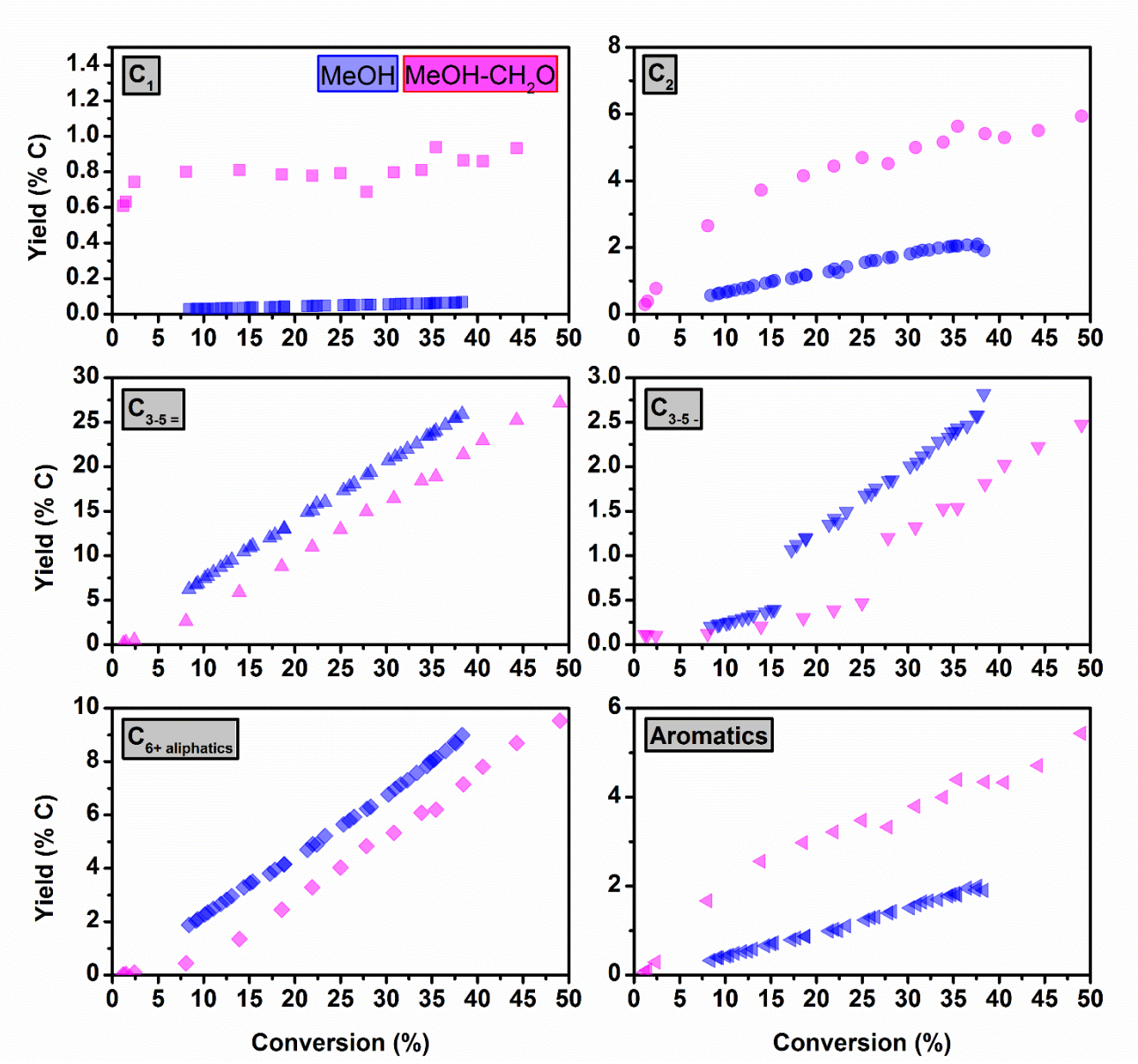

Figure 4.27. Yields of hydrocarbon fractions versus conversion during MTH over H-ZSM-5 at 350 °C during MTH reaction over H-ZSM-5 at 350 °C with MeOH and MeOH/CH_2O (approximately 1-2% CH_2O) feeds.

4.6. Main conclusions

- The rate of benzene methylation is significantly faster if DME acts as methylating agent compared to methanol regardless catalyst topology and acidity. Since DME methylates faster, products derived from sequential methylation and dealkylation, such as polyMBs and light olefins, are also formed faster. Methanol, in addition to the methylation and dealkylation products, promotes the formation of DPMs. This is explained by a parallel reaction pathway of methylation versus hydrogen transfer reactions. It is hypothesized that the hydrogen transfer pathway leads to formaldehyde from only methanol, and the aldehyde acts as intermediate in DPM formation.

- The rate of isobutene methylation is also affected by the choice of methylating reagent. DME methylates ostensibly faster than methanol over H-ZSM-5. Furthermore, the hydrogen transfer reaction of isobutene to isobutane is presented as a highly competitive reaction to methylation, and methanol promotes again the hydrogen transfer pathway to a larger extent than DME. The explanation is found by relatively similar energy barriers assigned to methylation and hydrogen transfer reactions for methanol-isobutene co-reaction. Furthermore, plausible isobutene hydrogen transfer mechanisms are proposed, where methanol and DME act as hydrogen donors. When methanol participates in hydrogen transfer reactions with isobutene, isobutane and formaldehyde are formed, while DME leads to isobutane and methoxymethyl cation. As a result, formaldehyde, derived from methanol, shapes the product spectrum of the secondary reactions by promoting formation of polyunsaturated alkenes, cyclic alkenes and arenes at last.

- The generally accepted concept of methanol-DME equilibration prior hydrocarbon products formation has been found not to be always applicable. The interconversion reaction between methanol and DME competes with the MTH chemistry over the same acid sites in zeolites. The rates of the reactions are in the same order of magnitude. In contrast, zeotype materials possess weakly acidic P-OH groups that drive methanol and DME to thermodynamic equilibrium concentrations. As a result, methanol concentrations are always higher during the course of the MTH reaction over zeolites compared to zeotypes.

- As consequence of the fast methylation kinetics attributed to DME, this oxygenate presents higher overall MTH activity than methanol. Apart from the disparity in activity associated to the two oxygenates, a distinctive deactivation pattern is obtained by usage of methanol and DME feedstocks. In spite of catalyst topology, methanol possesses a stronger deactivating role than DME, which is associated to its participation in hydrogen transfer reactions leading formaldehyde, a known coke-promoter in MTH, which facilitates condensation of aromatics (*i.e.* DPMs). Since high methanol concentrations are obtained over zeolites, the deactivating role of methanol is augmented. Zeotypes instead, leading to higher DME concentrations due additional weakly acidic P-OH groups involved in methanol-DME interconversion, mitigate the deactivation differences observed between methanol and DME as MTH feed reactants. A deactivation model has been found to correlate well with the experimental observations.

- The different activity towards methylation and hydrogen transfer reactions attributed to methanol and DME is also reflected in the product distribution of the MTH reaction, as a shift in the propagation of the catalytic cycles dominating the hydrocarbon transformations is observed. Since methanol promotes hydrogen transfer reactions, the product spectrum of the MTH reaction is richer in alkanes, aromatics and ethylene. Contrary, DME yields a richer product distribution in olefins larger than ethylene and aliphatic hydrocarbons in general. This is consistent with methanol promoting the propagation of the arene cycle. It is hypothesized that the propagation of the arene cycle by methanol is due to kinetic effects (highly competitive methylation and hydrogen transfer) and mechanistic effects (formaldehyde from methanol promoting aromatics formation). Again, these differences between methanol and DME are stressed over zeolites, but reduced over zeotypes due to their higher activity in the methanol-DME interconversion reaction.

- Concerning the impact of the thesis, it is highlighted that the methodology developed along this work, combining the parallel use of methanol and DME as oxygenates in different fractions. This strategy has been proved to help deconvoluting the origin of a wide range of effluent products during kinetic and mechanistic investigations.

- Even though the use of DME as feedstock or combined with methanol/(recycled hydrocarbons) is already industrially applied, the insights gained throughout the course of this work are still relevant. The influence of additional methanol dehydration sites on the reaction mechanism and on the rate of deactivation adds another parameter to ongoing research studies, aimed at improving the conversion capacity of MTH catalysts.

4.7. Suggestions for further work

- Even though the co-reactions of benzene and isobutene with methanol and DME provided important kinetic and mechanistic information, by-product formation needs to be minimized in order to extract more precise kinetic data, *i.e.* activation energies, pre-exponential factors, reaction orders. The use of nanolayered or nanosized catalysts is envisioned as a good approach for this goal because nanosized catalysts reduce the diffusion paths of reactant and product hydrocarbons, thereby also reducing the residence time of these molecules within the reactive zeolitic environments. As a consequence, lesser number of secondary reactions will occur. Nevertheless, extraction of precise hydrogen transfer kinetic data is still difficult due the fact that common carbocationic intermediates are shared with other competitive reactions (methylation, cracking, isomerization).

- Investigate the feasibility of methanol dehydrogenation to formaldehyde and hydrogen with more sensitive equipment than the one used in the benzene-methanol co-reaction study, such as more sensitive TCD detectors or gas-phase infrared spectroscopy, mainly aiming at detecting and quantifying hydrogen.

- Spectroscopic *operando* infrared studies are suggested on co-reactions of methanol and DME with hydrocarbons in order to elucidate possible different intermediates from both oxygenates *i.e.* formaldehyde from methanol or methoxymethyl cation from DME.

- Explore the effect of Lewis acidity on elementary reactions occurring in MTH. Even though, isolated Lewis sites did not produce almost any products in isobutene-oxygenates co-reactions (Paper III), a close proximity between Lewis and Brønsted sites has been suggested in literature to enhance the strength of acid sites. Therefore, extend the study of co-reactions of benzene and isobutene with methanol and DME over samples with similar Brønsted acidity and different degree of Lewis acidity, might be relevant to discern the role of Lewis acid sites in methylation and hydrogen transfer reactions, as it is known that the rate of both reactions depends on acid strength.

- Investigate the effect of Lewis acidity in zeolitic catalysts, alumina and other possible components of industrial catalysts on methanol-DME interconversion, and determine whether they are able to tune the concentration of methanol and DME in the course of the MTH reaction.

- Explore the incorporation of weakly acidic functions over zeolites aiming to achieve an acidity able to catalyze methanol dehydration, but unable to carry out MTH chemistry. Therefore, methanol concentrations in the reactor and inside the zeolite crystals will be reduced, possibly leading to more stable zeolite catalysts for MTH.

References

[1] J.J. Berzelius, Quelques Idées sur une Nouvelle Force Agissant Dans les Combinaisons des Corps Organiques, Ann. Chim., 61 (1836) 146-151.
[2] J.J. Berzelius, Sur un Force Jusqu'ici Peu Remarquée qui est Probablement Active Dans la Formation des Composés Organiques, Jahres-Bericht, 14 (1835) 237.
[3] I. Chorkendorff, J.W. Niemantsverdriet, Introduction to Catalysis, in: Concepts of Modern Catalysis and Kinetics, Wiley-VCH Verlag GmbH & Co. KGaA, 2005, pp. 1-21.
[4] J. Yu, Chapter 3 - Synthesis of Zeolites, in: H.v.B.A.C. Jiří Čejka, S. Ferdi (Eds.) Stud. Surf. Sci. Catal., Elsevier, 2007, pp. 39-103.
[5] Database of Zeolite Structures. http://www.iza-structure.org, in.
[6] A. Corma, Inorganic Solid Acids and Their Use in Acid-Catalyzed Hydrocarbon Reactions, Chem. Rev., 95 (1995) 559-614.
[7] J. Weitkamp, Zeolites and catalysis, Solid State Ionics, 131 (2000) 175-188.
[8] G. Gnana kumar, Zeolites and Composites, in: Nanomaterials and Nanocomposites, Wiley-VCH Verlag GmbH & Co. KGaA, 2016, pp. 187-222.
[9] A. Dyer, An Introduction To Zeolite Molecular Sieves, John Wiley & sons, Chichester, 1988.
[10] R.M. Barrer, D.A. Ibbitson, Occlusion of hydrocarbons by chabazite and analcite, Transactions of the Faraday Society, 40 (1944) 195-206.
[11] A. Züttel, Materials for hydrogen storage, Mater. Today, 6 (2003) 24-33.
[12] R.P. Townsend, E.N. Coker, Ion exchange in zeolites, in: Stud. Surf. Sci. Catal., 2001, pp. 467-524.
[13] R.P. Townsend, Ion exchange in zeolites: Some recent developments in theory and practice, Pure Appl. Chem., 58 (1986) 1359-1366.
[14] J.-L. Guth, H. Kessler, Synthesis of Aluminosilicate Zeolites and Related Silica-Based Materials, in: J. Weitkamp, L. Puppe (Eds.) Catalysis and Zeolites: Fundamentals and Applications, Springer Berlin Heidelberg, Berlin, Heidelberg, 1999, pp. 1-52.
[15] E.M. Flanigen, B.M. Lok, R.L. Patton, S.T. Wilson, Aluminophosphate molecular sieves and the Periodic Table, in: Stud. Surf. Sci. Catal., 1986, pp. 103-112.
[16] B.M. Lok, C.A. Messina, R.L. Patton, R.T. Gajek, T.R. Cannan, E.M. Flanigen, Silicoaluminophosphate Molecular Sieves: Another New Class of Microporous Crystalline Inorganic Solids, J. Am. Chem. Soc., 106 (1984) 6092-6093.
[17] M. Hartmann, L. Kevan, Transition-Metal Ions in Aluminophosphate and Silicoaluminophosphate Molecular Sieves: Location, Interaction with Adsorbates and Catalytic Properties, Chem. Rev., 99 (1999) 635-663.
[18] A. Corma, State of the art and future challenges of zeolites as catalysts, J. Catal., 216 (2003) 298-312.
[19] S.T. Wilson, B.M. Lok, C.A. Messina, T.R. Cannan, E.M. Flanigen, Aluminophosphate molecular sieves: A new class of microporous crystalline inorganic solids, J. Am. Chem. Soc., 104 (1982) 1146-1147.
[20] P.B. Weisz, Polyfunctional Heterogeneous Catalysis, in: Advances in Catalysis, 1962, pp. 137-190.
[21] P.B. Weisz, V.J. Frilette, Intracrystalline and molecular-shape-selective catalysis by zeolite salts [2], J. Phys. Chem., 64 (1960) 382.
[22] J.A. Rabo, P.E. Pickert, R.L. Mays, Pentane and hexane isomerization with Linde catalyst MB 5390, Preprints, 5 (1960).
[23] P.B. Venuto, L.A. Hamilton, P.S. Landis, J.J. Wise, Organic reactions catalyzed by crystalline aluminosilicates. I. Alkylation reactions, J. Catal., 5 (1966) 81-98.
[24] P.B. Venuto, L.A. Hamilton, P.S. Landis, Organic reactions catalyzed by crystalline aluminosilicates. II. Alkylation reactions: Mechanistic and aging considerations, J. Catal., 5 (1966) 484-493.

[25] P.B. Venuto, P.S. Landis, Organic reactions catalyzed by crystalline aluminosilicates. III. Condensation reactions of carbonyl compounds, J. Catal., 6 (1966) 237-244.
[26] P.S. Landis, P.B. Venuto, Organic reactions catalyzed by crystalline aluminosilicates. IV. Beckmann rearrangement of ketoximes to amides, J. Catal., 6 (1966) 245-252.
[27] P.B. Venuto, E.N. Givens, L.A. Hamilton, P.S. Landis, Organic reactions catalyzed by crystalline aluminosilicates. V. Dehydrohalogenation and related reactions, J. Catal., 6 (1966) 253-262.
[28] C.J. Plank, E.J. Rosinski, W.P. Hawthorne, Acidic crystalline aluminosilicates: New superactive, superselective cracking catalysts, Industrial & Engineering Chemistry Product Research and Development, 3 (1964) 165-169.
[29] V. Van Speybroeck, K. Hemelsoet, L. Joos, M. Waroquier, R.G. Bell, C.R.A. Catlow, Advances in theory and their application within the field of zeolite chemistry, Chem. Soc. Rev., 44 (2015) 7044-7111.
[30] S.M. Csicsery, Shape-selective catalysis in zeolites, Zeolites, 4 (1984) 202-213.
[31] R.J. Argauer, G.R. Landolt, Crystalline zeolite zsm-5 and method of preparing the same, in, Google Patents, 1972.
[32] L.B. Young, S.A. Butter, W.W. Kaeding, Shape selective reactions with zeolite catalysts. III. Selectivity in xylene isomerization, toluene-methanol alkylation, and toluene disproportionation over ZSM-5 zeolite catalysts, J. Catal., 76 (1982) 418-432.
[33] W.W. Kaeding, C. Chu, L.B. Young, S.A. Butter, Shape-selective reactions with zeolite catalysts. II. Selective disproportionation of toluene to produce benzene and p-Xylene, J. Catal., 69 (1981) 392-398.
[34] W.W. Kaeding, S.A. Butter, Production of chemicals from methanol. I. Low molecular weight olefins, J. Catal., 61 (1980) 155-164.
[35] C.D. Chang, Hydrocarbons from Methanol, Catalysis Reviews, 25 (1983) 1-118.
[36] D.H. Olson, W.O. Haag, R.M. Lago, Chemical and physical properties of the ZSM-5 substitutional series, J. Catal., 61 (1980) 390-396.
[37] M. Choi, K. Na, J. Kim, Y. Sakamoto, O. Terasaki, R. Ryoo, Stable single-unit-cell nanosheets of zeolite MFI as active and long-lived catalysts, Nature, 461 (2009) 246-249.
[38] C. Fernandez, I. Stan, J.P. Gilson, K. Thomas, A. Vicente, A. Bonilla, J. Pérez-Ramírez, Hierarchical ZSM-5 zeolites in shape-selective xylene isomerization: Role of mesoporosity and acid site speciation, Chemistry - A European Journal, 16 (2010) 6224-6233.
[39] K.A. Łukaszuk, P. del Campo Huertas, A. Molino, M. Nielsen, D. Rojo-Gama, J.S. Martinez-Espin, K.P. Lillerud, U. Olsbye, S. Bordiga, P. Beato, S. Svelle, Fossil Fuels: The Effect of Zeolite Catalyst Particle Morphology on Catalyst Performance in the Conversion of Methanol to Hydrocarbons, in: Nanotechnology for Energy Sustainability, Wiley-VCH Verlag GmbH & Co. KGaA, 2017, pp. 1-40.
[40] S. Van Donk, A.H. Janssen, J.H. Bitter, K.P. De Jong, Generation, characterization, and impact of mesopores in zeolite catalysts, Cat. Rev. - Sci. Eng., 45 (2003) 297-319.
[41] R.F. Lobo, M.E. Davis, Synthesis and characterization of pure-silica and boron-substituted SSZ-24 using N(16) methylsparteinium bromide as structure-directing agent, Microporous Mater., 3 (1994) 61-69.
[42] B.M. Weckhuysen, R.R. Rao, J.A. Martens, R.A. Schoonheydt, Transition metal ions in microporous crystalline aluminophosphates: Isomorphous substitution, Eur. J. Inorg. Chem., (1999) 565-577.
[43] M. Westgård Erichsen, K. De Wispelaere, K. Hemelsoet, S.L.C. Moors, T. Deconinck, M. Waroquier, S. Svelle, V. Van Speybroeck, U. Olsbye, How zeolitic acid strength and composition alter the reactivity of alkenes and aromatics towards methanol Dedicated to the memory of Haldor Topsøe, J. Catal., 328 (2015) 186-196.
[44] K. De Wispelaere, S. Bailleul, V. Van Speybroeck, Towards molecular control of elementary reactions in zeolite catalysis by advanced molecular simulations mimicking operating conditions, Catalysis Science and Technology, 6 (2016) 2686-2705.
[45] F.J. Keil, Methanol-to-hydrocarbons: Process technology, Microporous Mesoporous Mater., 29 (1999) 49-66.

[46] C.D. Chang, J.C.W. Kuo, W.H. Lang, S.M. Jacob, J.J. Wise, A.J. Silvestri, Process Studies on the Conversion of Methanol to Gasoline, Industrial & Engineering Chemistry Process Design and Development, 17 (1978) 255-260.
[47] C.D. Chang, A.J. Silvestri, The conversion of methanol and other O-compounds to hydrocarbons over zeolite catalysts, J. Catal., 47 (1977) 249-259.
[48] S. Ilias, A. Bhan, Mechanism of the catalytic conversion of methanol to hydrocarbons, ACS Catalysis, 3 (2013) 18-31.
[49] U. Olsbye, S. Svelle, M. Bjørgen, P. Beato, T.V.W. Janssens, F. Joensen, S. Bordiga, K.P. Lillerud, Conversion of methanol to hydrocarbons: How zeolite cavity and pore size controls product selectivity, Angew. Chem. Int. Ed., 51 (2012) 5810-5831.
[50] M. Stöcker, Microporous Mesoporous Mater., 2 (1999) 9-13.
[51] T. Mokrani, M. Scurrell, Gas Conversion to Liquid Fuels and Chemicals: The Methanol Route-Catalysis and Processes Development, Catalysis Reviews, 51 (2009) 1-145.
[52] S. Teketel, M.W. Erichsen, F.L. Bleken, S. Svelle, K.P. Lillerud, U. Olsbye, Chapter 6 Shape selectivity in zeolite catalysis. The Methanol to Hydrocarbons (MTH) reaction, in: Catalysis, RSC, 2014, pp. 179-217.
[53] N. Nesterenko, J. Aguilhon, P. Bodart, D. Minoux, J.P. Dath, Chapter 5 - Methanol to Olefins: An Insight Into Reaction Pathways and Products Formation A2 - Sels, Bert F, in: L.M. Kustov (Ed.) Zeolites and Zeolite-Like Materials, Elsevier, Amsterdam, 2016, pp. 189-263.
[54] P. Tian, Y. Wei, M. Ye, Z. Liu, Methanol to Olefins (MTO): From Fundamentals to Commercialization, ACS Catalysis, 5 (2015) 1922-1938.
[55] T.V.W. Janssens, A new approach to the modeling of deactivation in the conversion of methanol on zeolite catalysts, J. Catal., 264 (2009) 130-137.
[56] C.D. Chang, The New Zealand Gas-to-Gasoline plant: An engineering tour de force, Catal. Today, 13 (1992) 103-111.
[57] J. Cobb, New Zealand Synfuel: The Story of the World's First Natural Gas to Gasoline Plant, Cobb/Horwood Publications, Auckland, New Zealand, 1985.
[58] C.J. Maiden, The New Zealand Gas-to-Gasoline Project, Stud. Surf. Sci. Catal., 36 (1988) 1-16.
[59] D. Liederman, S.M. Jacob, S.E. Voltz, J.J. Wise, Process Variable Effects in the Conversion of Methanol to Gasoline in a Fluid Bed Reactor, Industrial & Engineering Chemistry Process Design and Development, 17 (1978) 340-346.
[60] R.F. Socha, C.D. Chang, R.M. Gould, S.E. Kane, A.A. Avidan, Fluid-Bed Studies of Olefin Production from Methanol, in: Industrial Chemicals via C₁ Processes, American Chemical Society, 1987, pp. 34-41.
[61] R.F. Socha, C.D. Chang, R.M. Gould, S.E. Kane, A.A. Avidan, Fluid-bed studies of olefin production from methanol, ; Mobil Research and Development Corp., Princeton, NJ, 1986.
[62] A.A. Avidan, Gasoline and Distillate Fuels From Methanol, in: C.D.C.R.F.H. D.M. Bibby, S. Yurchak (Eds.) Stud. Surf. Sci. Catal., Elsevier, 1988, pp. 307-323.
[63] J. Topp-Jørgensen, Topsøe Integrated Gasoline Synthesis – The Tigas Process, in: C.D.C.R.F.H. D.M. Bibby, S. Yurchak (Eds.) Stud. Surf. Sci. Catal., Elsevier, 1988, pp. 293-305.
[64] M. Westgård Erichsen, J.S. Martinez-Espin, F. Joensen, S. Teketel, P. del Campo Huertas, K.P. Lillerud, S. Svelle, P. Beato, U. Olsbye, Syngas to Liquids via Oxygenates, in: Small-Scale Gas to Liquid Fuel Synthesis, CRC Press, 2015, pp. 441-474.
[65] G. Bellussi, R. Millini, P. Pollesel, An industrial perspective on the impact of Haldor Topsøe on research and development in catalysis by zeolites, J. Catal., 328 (2015) 11-18.
[66] G. Ondrey, The commercial debut for a gas-to-gasoline process, Chemical Engineering, 121 (2014) 11.
[67] S.W. Kaiser, METHANOL CONVERSION TO LIGHT OLEFINS OVER SILICOALUMINOPHOSPHATE MOLECULAR-SIEVES, Arabian Journal for Science and Engineering, 10 (1985) 361-366.

[68] S. Wilson, P. Barger, The characteristics of SAPO-34 which influence the conversion of methanol to light olefins, Microporous Mesoporous Mater., 29 (1999) 117-126.
[69] T. Inui, E. Araki, T. Sezume, T. Ishihara, Y. Takegami, Selective synthesis of lower olefins by catalytic conversion of methanol, React. Kinet. Catal. Lett., 18 (1982) 1-5.
[70] B.V. Vora, T.L. Marker, P.T. Barger, H.R. Nilsen, S. Kvisle, T. Fuglerud, Economic route for natural gas conversion to ethylene and propylene, in: Stud. Surf. Sci. Catal., 1997, pp. 87-98.
[71] J. Grootjans, V. Vanrysselberghe, W. Vermeiren, Integration of the Total Petrochemicals-UOP olefins conversion process into a naphtha steam cracker facility, Catal. Today, 106 (2005) 57-61.
[72] J.J. Senetar, E. Romers, Scale-up of advanced MTO technology and integrated OCP technology, in: AIChE Annual Meeting, Conference Proceedings, 2011.
[73] M. Ye, H. Li, Y. Zhao, T. Zhang, Z. Liu, Chapter Five - MTO Processes Development: The Key of Mesoscale Studies, in: B.M. Guy, L. Jinghai (Eds.) Advances in Chemical Engineering, Academic Press, 2015, pp. 279-335.
[74] H. Koempel, W. Liebner, Lurgi's Methanol To Propylene (MTP®) Report on a successful commercialisation, Stud. Surf. Sci. Catal., 167 (2007) 261-267.
[75] S. Haag, M. Rothaemel, F. Lin Lin, F. Castillo-Welter, M. Gorny, Methanol to Propylene: A Proven Technology for on-purpose Propylene Production, in: Synthesis Gas Chemistry. DGMK Conference, Dresden, Germany, 2015.
[76] M. Conte, J.A. Lopez-Sanchez, Q. He, D.J. Morgan, Y. Ryabenkova, J.K. Bartley, A.F. Carley, S.H. Taylor, C.J. Kiely, K. Khalid, G.J. Hutchings, Modified zeolite ZSM-5 for the methanol to aromatics reaction, Catalysis Science and Technology, 2 (2012) 105-112.
[77] J. Zhang, W. Qian, C. Kong, F. Wei, Increasing para-Xylene Selectivity in Making Aromatics from Methanol with a Surface-Modified Zn/P/ZSM-5 Catalyst, ACS Catalysis, 5 (2015) 2982-2988.
[78] E.T.C. Vogt, G.T. Whiting, A. Dutta Chowdhury, B.M. Weckhuysen, Chapter Two - Zeolites and Zeotypes for Oil and Gas Conversion, in: C.J. Friederike (Ed.) Advances in Catalysis, Academic Press, 2015, pp. 143-314.
[79] M. Stöcker, Methanol-to-hydrocarbons: Catalytic materials and their behavior, Microporous Mesoporous Mater., 29 (1999) 3-48.
[80] G.J. Hutchings, R. Hunter, Hydrocarbon formation from methanol and dimethyl ether: a review of the experimental observations concerning the mechanism of formation of the primary products, Catal. Today, 6 (1990) 279-306.
[81] U. Olsbye, S. Svelle, K.P. Lillerud, Z.H. Wei, Y.Y. Chen, J.F. Li, J.G. Wang, W.B. Fan, The formation and degradation of active species during methanol conversion over protonated zeotype catalysts, Chem. Soc. Rev., 44 (2015) 7155-7176.
[82] J.F. Haw, W. Song, D.M. Marcus, J.B. Nicholas, The mechanism of methanol to hydrocarbon catalysis, Acc. Chem. Res., 36 (2003) 317-326.
[83] H. Schulz, "Coking" of zeolites during methanol conversion: Basic reactions of the MTO-, MTP- and MTG processes, Catal. Today, 154 (2010) 183-194.
[84] V. Van Speybroeck, K. De Wispelaere, J. Van Der Mynsbrugge, M. Vandichel, K. Hemelsoet, M. Waroquier, First principle chemical kinetics in zeolites: The methanol-to-olefin process as a case study, Chem. Soc. Rev., 43 (2014) 7326-7357.
[85] S.N. Khadzhiev, M.V. Magomedova, E.G. Peresypkina, Mechanism of olefin synthesis from methanol and dimethyl ether over zeolite catalysts: A review, Petroleum Chemistry, 54 (2014) 245-269.
[86] P.B. Venuto, P.S. Landis, Organic Catalysis over Crystalline Aluminosilicates, in: Advances in Catalysis, 1968, pp. 259-371.
[87] S.R. Blaszkowski, R.A. Van Santen, Theoretical study of C-C bond formation in the methanol-to-gasoline process, J. Am. Chem. Soc., 119 (1997) 5020-5027.
[88] G.A. Olah, H. Doggweiler, J.D. Felberg, S. Frohlich, M.J. Grdina, R. Karpeles, T. Keumi, S.I. Inaba, W.M. Ip, K. Lammertsma, G. Salem, D.C. Tabor, Onium ylide chemistry. 1. Bifunctional acid-base-

catalyzed conversion of heterosubstituted methanes into ethylene and derived hydrocarbons. The onium ylide mechanism of the C1 → C2 conversion, J. Am. Chem. Soc., 106 (1984) 2143-2149.
[89] J.H.C. van Hooff, J.P. van den Berg, J.P. Wolthuizen, A. Volmer, REACTION MECHANISM OF THE FIRST C-C BOND FORMATION IN THE METHANOL TO GASOLINE PROCESS, in, 1984, pp. 489-496.
[90] D. Lesthaeghe, V. Van Speybroeck, G.B. Marin, M. Waroquier, Understanding the failure of direct C-C coupling in the zeolite-catalyzed methanol-to-olefin process, Angew. Chem. Int. Ed., 45 (2006) 1714-1719.
[91] G.J. Hutchings, F. Gottschalk, M.V.M. Hall, R. Hunter, Hydrocarbon formation from methylating agents over the zeolite catalyst ZSM-5. Comments on the mechanism of carbon-carbon bond and methane formation, J. Chem. Soc. Faraday Trans., 83 (1987) 571-583.
[92] Y. Ono, T. Mori, Mechanism of methanol conversion into hydrocarbons over ZSM-5 zeolite, J. Chem. Soc. Faraday Trans., 77 (1981) 2209-2221.
[93] T.R. Forester, R.F. Howe, In situ FTIR studies of methanol and dimethyl ether in ZSM-5, J. Am. Chem. Soc., 109 (1987) 5076-5082.
[94] R.D. Smith, J.H. Futrell, Evidence for complex formation in the reactions of CH+<inf>3</inf> and CD+<inf>3</inf> with CH<inf>3</inf>OH, CD<inf>3</inf>OD, and C<inf>2</inf>H<inf>5</inf>OH, Chem. Phys. Lett., 41 (1976) 64-67.
[95] J. Nováková, L. Kubelková, K. Habersberger, Z. Dolejšek, Catalytic activity of dealuminated Y and HZSM-5 zeolites measured by the temperature-programmed desorption of small amounts of preadsorbed methanol and by the low-pressure flow reaction of methanol, J. Chem. Soc. Faraday Trans., 80 (1984) 1457-1465.
[96] Z. Wei, Y. Chen, J. Li, W. Guo, S. Wang, M. Dong, Z. Qin, J. Wang, H. Jiao, W. Fan, Stability and Reactivity of Intermediates of Methanol Related Reactions and C-C Bond Formation over H-ZSM-5 Acidic Catalyst: A Computational Analysis, J. Phys. Chem. C, 120 (2016) 6075-6087.
[97] L. Kubelková, J. Nováková, K. Nedomová, Reactivity of surface species on zeolites in methanol conversion, J. Catal., 124 (1990) 441-450.
[98] J. Nováková, L. Kubelková, Z. Dolejšek, Primary reaction steps in the methanol-to-olefin transformation on zeolites, J. Catal., 108 (1987) 208-213.
[99] O. Dewaele, V.L. Geers, G.F. Froment, G.B. Marin, The conversion of methanol to olefins: A transient kinetic study, Chem. Eng. Sci., 54 (1999) 4385-4395.
[100] W. Song, D.M. Marcus, H. Fu, J.O. Ehresmann, J.F. Haw, An oft-studied reaction that may never have been: Direct catalytic conversion of methanol or dimethyl ether to hydrocarbons on the solid acids HZSM-5 or HSAPO-34, J. Am. Chem. Soc., 124 (2002) 3844-3845.
[101] Y. Liu, S. Müller, D. Berger, J. Jelic, K. Reuter, M. Tonigold, M. Sanchez-Sanchez, J.A. Lercher, Formation Mechanism of the First Carbon-Carbon Bond and the First Olefin in the Methanol Conversion into Hydrocarbons, Angew. Chem. Int. Ed., 55 (2016) 5723-5726.
[102] A.D. Chowdhury, K. Houben, G.T. Whiting, M. Mokhtar, A.M. Asiri, S.A. Al-Thabaiti, S.N. Basahel, M. Baldus, B.M. Weckhuysen, Inside Back Cover: Initial Carbon–Carbon Bond Formation during the Early Stages of the Methanol-to-Olefin Process Proven by Zeolite-Trapped Acetate and Methyl Acetate (Angew. Chem. Int. Ed. 51/2016), Angew. Chem. Int. Ed., 55 (2016) 15929-15929.
[103] S. Kolboe, Methanol reactions on ZSM-5 and other zeolite catalysts: Autocatalysis and reaction mechanism, Acta Chem. Scand., 40A (1986) 711-713.
[104] W. Wang, A. Buchholz, M. Seiler, M. Hunger, Evidence for an Initiation of the Methanol-to-Olefin Process by Reactive Surface Methoxy Groups on Acidic Zeolite Catalysts, J. Am. Chem. Soc., 125 (2003) 15260-15267.
[105] N.Y. Chen, W.J. Reagan, Evidence of autocatalysis in methanol to hydrocarbon reactions over zeolite catalysts, J. Catal., 59 (1979) 123-129.
[106] B.E. Langner, Reactions of methanol on zeolites with different pore structures, Applied Catalysis, 2 (1982) 289-302.

[107] R.M. Dessau, R.B. LaPierre, On the mechanism of methanol conversion to hydrocarbons over HZSM-5, J. Catal., 78 (1982) 136-141.
[108] R.M. Dessau, On the H-ZSM-5 catalyzed formation of ethylene from methanol or higher olefins, J. Catal., 99 (1986) 111-116.
[109] T. Mole, G. Bett, D. Seddon, Conversion of methanol to hydrocarbons over ZSM-5 zeolite: An examination of the role of aromatic hydrocarbons using 13carbon- and deuterium-labeled feeds, J. Catal., 84 (1983) 435-445.
[110] T. Mole, J.A. Whiteside, D. Seddon, Aromatic co-catalysis of methanol conversion over zeolite catalysts, J. Catal., 82 (1983) 261-266.
[111] I.M. Dahl, S. Kolboe, On the reaction mechanism for propene formation in the MTO reaction over SAPO-34, Catal. Lett., 20 (1993) 329-336.
[112] I.M. Dahl, S. Kolboe, On the Reaction Mechanism for Hydrocarbon Formation from Methanol over SAPO-34. I. Isotopic Labeling Studies of the Co-Reaction of Ethene and Methanol, J. Catal., 149 (1994) 458-464.
[113] I.M. Dahl, S. Kolboe, On the reaction mechanism for hydrocarbon formation from methanol over SAPO-34: 2. Isotopic labeling studies of the Co-reaction of propene and methanol, J. Catal., 161 (1996) 304-309.
[114] J.F. Haw, J.B. Nicholas, W. Song, F. Deng, Z. Wang, T. Xu, C.S. Heneghan, Roles for cyclopentenyl cations in the synthesis of hydrocarbons from methanol on zeolite catalyst HZSM-5, J. Am. Chem. Soc., 122 (2000) 4763-4775.
[115] P.W. Goguen, T. Xu, D.H. Barich, T.W. Skloss, W. Song, Z. Wang, J.B. Nicholas, J.F. Haw, Pulse-quench catalytic reactor studies reveal a carbon-pool mechanism in methanol-to-gasoline chemistry on zeolite HZSM-5 [1], J. Am. Chem. Soc., 120 (1998) 2650-2651.
[116] W. Song, H. Fu, J.F. Haw, Supramolecular origins of product selectivity for methanol-to-olefin catalysis on HSAPO-34, J. Am. Chem. Soc., 123 (2001) 4749-4754.
[117] W. Song, J.F. Haw, J.B. Nicholas, C.S. Heneghan, Methylbenzenes are the organic reaction centers for methanol-to-olefin catalysis on HSAPO-34 [12], J. Am. Chem. Soc., 122 (2000) 10726-10727.
[118] B. Arstad, S. Kolboe, The reactivity of molecules trapped within the SAPO-34 cavities in the methanol-to-hydrocarbons reaction [11], J. Am. Chem. Soc., 123 (2001) 8137-8138.
[119] O. Mikkelsen, S. Kolboe, The conversion of methanol to hydrocarbons over zeolite H-beta, Microporous Mesoporous Mater., 29 (1999) 173-184.
[120] R.F. Sullivan, C.J. Egan, G.E. Langlios, R.P. Sieg, A new reaction that occurs in the hydrocracking of certain aromatic hydrocarbons, J. Am. Chem. Soc., 83 (1961) 1156-1160.
[121] M.W. Erichsen, M. Mortén, S. Svelle, O. Sekiguchi, E. Uggerud, U. Olsbye, Conclusive Evidence for Two Unimolecular Pathways to Zeolite-Catalyzed De-alkylation of the Heptamethylbenzenium Cation, ChemCatChem, 7 (2015) 4143-4147.
[122] M. Bjørgen, U. Olsbye, D. Petersen, S. Kolboe, The methanol-to-hydrocarbons reaction: Insight into the reaction mechanism from [12C]benzene and [13C]methanol coreactions over zeolite H-beta, J. Catal., 221 (2004) 1-10.
[123] B. Arstad, J.B. Nicholas, J.F. Haw, Theoretical Study of the Methylbenzene Side-Chain Hydrocarbon Pool Mechanism in Methanol to Olefin Catalysis, J. Am. Chem. Soc., 126 (2004) 2991-3001.
[124] B. Arstad, S. Kolboe, O. Swang, Theoretical study Of the heptamethylbenzenium ion. Intramolecular isomerizations and C<inf>2</inf>, C<inf>3</inf>, C<inf>4</inf> alkene elimination, J. Phys. Chem. A, 109 (2005) 8914-8922.
[125] D.M. McCann, D. Lesthaeghe, P.W. Kletnieks, D.R. Guenther, M.J. Hayman, V. Van Speybroeck, M. Waroquier, J.F. Haw, A Complete Catalytic Cycle for Supramolecular Methanol-to-Olefins Conversion by Linking Theory with Experiment, Angew. Chem., 120 (2008) 5257-5260.
[126] C.M. Wang, Y.D. Wang, Z.K. Xie, Z.P. Liu, Methanol to olefin conversion on hsapo-34 zeolite from periodic density functional theory calculations: A complete cycle of side chain hydrocarbon pool mechanism, J. Phys. Chem. C, 113 (2009) 4584-4591.

[127] D. Lesthaeghe, V. Van Speybroeck, M. Waroquier, Theoretical evaluation of zeolite confinement effects on the reactivity of bulky intermediates, PCCP, 11 (2009) 5222-5226.
[128] K. De Wispelaere, K. Hemelsoet, M. Waroquier, V. Van Speybroeck, Complete low-barrier side-chain route for olefin formation during methanol conversion in H-SAPO-34, J. Catal., 305 (2013) 76-80.
[129] S. Xu, A. Zheng, Y. Wei, J. Chen, J. Li, Y. Chu, M. Zhang, Q. Wang, Y. Zhou, J. Wang, F. Deng, Z. Liu, Direct observation of cyclic carbenium ions and their role in the catalytic cycle of the methanol-to-olefin reaction over chabazite zeolites, Angew. Chem. Int. Ed., 52 (2013) 11564-11568.
[130] C. Wang, Y. Chu, A. Zheng, J. Xu, Q. Wang, P. Gao, G. Qi, Y. Gong, F. Deng, New Insight into the Hydrocarbon-Pool Chemistry of the Methanol-to-Olefins Conversion over Zeolite H-ZSM-5 from GC-MS, Solid-State NMR Spectroscopy, and DFT Calculations, Chemistry - A European Journal, 20 (2014) 12432-12443.
[131] G. Sastre, Confinement effects in methanol to olefins catalysed by zeolites: A computational review, Frontiers of Chemical Science and Engineering, 10 (2016) 76-89.
[132] M. Westgård Erichsen, Mechanistic studies of acid-catalysed hydrocarbon reactions in zeolitic materials, in: Department of Chemistry, University of Oslo, 2014.
[133] W. Wang, Y. Jiang, M. Hunger, Mechanistic investigations of the methanol-to-olefin (MTO) process on acidic zeolite catalysts by in situ solid-state NMR spectroscopy, Catal. Today, 113 (2006) 102-114.
[134] Y. Jiang, J. Huang, V.R. Reddy Marthala, Y.S. Ooi, J. Weitkamp, M. Hunger, In situ MAS NMR–UV/Vis investigation of H-SAPO-34 catalysts partially coked in the methanol-to-olefin conversion under continuous-flow conditions and of their regeneration, Microporous Mesoporous Mater., 105 (2007) 132-139.
[135] M. Seiler, W. Wang, A. Buchholz, M. Hunger, Direct Evidence for a Catalytically Active Role of the Hydrocarbon Pool Formed on Zeolite H-ZSM-5 During the Methanol-to-Olefin Conversion, Catal. Lett., 88 (2003) 187-191.
[136] S. Svelle, F. Joensen, J. Nerlov, U. Olsbye, K.P. Lillerud, S. Kolboe, M. Bjørgen, Conversion of methanol into hydrocarbons over zeolite H-ZSM-5: Ethene formation is mechanistically separated from the formation of higher alkenes, J. Am. Chem. Soc., 128 (2006) 14770-14771.
[137] M. Bjørgen, S. Svelle, F. Joensen, J. Nerlov, S. Kolboe, F. Bonino, L. Palumbo, S. Bordiga, U. Olsbye, Conversion of methanol to hydrocarbons over zeolite H-ZSM-5: On the origin of the olefinic species, J. Catal., 249 (2007) 195-207.
[138] W. Skistad, S. Teketel, F.L. Bleken, P. Beato, S. Bordiga, M.H. Nilsen, U. Olsbye, S. Svelle, K.P. Lillerud, Methanol Conversion to Hydrocarbons (MTH) Over H-ITQ-13 (ITH) Zeolite, Top. Catal., 57 (2014) 143-158.
[139] F. Bleken, W. Skistad, K. Barbera, M. Kustova, S. Bordiga, P. Beato, K.P. Lillerud, S. Svelle, U. Olsbye, Conversion of methanol over 10-ring zeolites with differing volumes at channel intersections: Comparison of TNU-9, IM-5, ZSM-11 and ZSM-5, PCCP, 13 (2011) 2539-2549.
[140] S. Teketel, W. Skistad, S. Benard, U. Olsbye, K.P. Lillerud, P. Beato, S. Svelle, Shape selectivity in the conversion of methanol to hydrocarbons: The catalytic performance of one-dimensional 10-ring zeolites: ZSM-22, ZSM-23, ZSM-48, and EU-1, ACS Catalysis, 2 (2012) 26-37.
[141] M. Westgård Erichsen, S. Svelle, U. Olsbye, The influence of catalyst acid strength on the methanol to hydrocarbons (MTH) reaction, Catal. Today, 215 (2013) 216-223.
[142] S. Ilias, R. Khare, A. Malek, A. Bhan, A descriptor for the relative propagation of the aromatic- and olefin-based cycles in methanol-to-hydrocarbons conversion on H-ZSM-5, J. Catal., 303 (2013) 135-140.
[143] A. Hwang, D. Prieto-Centurion, A. Bhan, Isotopic tracer studies of methanol-to-olefins conversion over HSAPO-34: The role of the olefins-based catalytic cycle, J. Catal., 337 (2016) 52-56.
[144] M. Zhang, S. Xu, Y. Wei, J. Li, J. Chen, J. Wang, W. Zhang, S. Gao, X. Li, C. Wang, Z. Liu, Methanol conversion on ZSM-22, ZSM-35 and ZSM-5 zeolites: Effects of 10-membered ring zeolite structures on methylcyclopentenyl cations and dual cycle mechanism, RSC Advances, 6 (2016) 95855-95864.

[145] C.M. Wang, Y.D. Wang, Y.J. Du, G. Yang, Z.K. Xie, Similarities and differences between aromatic-based and olefin-based cycles in H-SAPO-34 and H-SSZ-13 for methanol-to-olefins conversion: Insights from energetic span model, Catalysis Science and Technology, 5 (2015) 4354-4364.
[146] L. Qi, J. Li, L. Xu, Z. Liu, Evolution of the reaction mechanism during the MTH induction period over the 2-dimensional FER zeolite, RSC Advances, 6 (2016) 56698-56704.
[147] Z. Liu, X. Dong, Y. Zhu, A.H. Emwas, D. Zhang, Q. Tian, Y. Han, Investigating the Influence of Mesoporosity in Zeolite Beta on Its Catalytic Performance for the Conversion of Methanol to Hydrocarbons, ACS Catalysis, 5 (2015) 5837-5845.
[148] N.H. Ahn, S. Seo, S.B. Hong, Small-pore molecular sieves SAPO-57 and SAPO-59: synthesis, characterization, and catalytic properties in methanol-to-olefins conversion, Catalysis Science & Technology, 6 (2016) 2725-2734.
[149] M. Dyballa, P. Becker, D. Trefz, E. Klemm, A. Fischer, H. Jakob, M. Hunger, Parameters influencing the selectivity to propene in the MTO conversion on 10-ring zeolites: Directly synthesized zeolites ZSM-5, ZSM-11, and ZSM-22, Applied Catalysis A: General, 510 (2016) 233-243.
[150] D. Rojo-Gama, S. Etemadi, E. Kirby, K.P. Lillerud, P. Beato, S. Svelle, U. Olsbye, Time- and space-resolved study of the methanol to hydrocarbons (MTH) reaction - influence of zeolite topology on axial deactivation patterns, Faraday Discuss., (2017).
[151] J.S. Martinez-Espin, M. Morten, T.V.W. Janssens, S. Svelle, P. Beato, U. Olsbye, New insights in catalyst deactivation and product distribution of zeolites in the Methanol-To-Hydrocarbons (MTH) reaction with methanol and dimethyl ether feeds, Catalysis Science & Technology, (2017).
[152] B.P.C. Hereijgers, F. Bleken, M.H. Nilsen, S. Svelle, K.P. Lillerud, M. Bjørgen, B.M. Weckhuysen, U. Olsbye, Product shape selectivity dominates the Methanol-to-Olefins (MTO) reaction over H-SAPO-34 catalysts, J. Catal., 264 (2009) 77-87.
[153] F. Bleken, M. Bjørgen, L. Palumbo, S. Bordiga, S. Svelle, K.-P. Lillerud, U. Olsbye, The Effect of Acid Strength on the Conversion of Methanol to Olefins Over Acidic Microporous Catalysts with the CHA Topology, Top. Catal., 52 (2009) 218-228.
[154] S. Teketel, S. Svelle, K.-P. Lillerud, U. Olsbye, Shape-Selective Conversion of Methanol to Hydrocarbons Over 10-Ring Unidirectional-Channel Acidic H-ZSM-22, ChemCatChem, 1 (2009) 78-81.
[155] S. Teketel, U. Olsbye, K.-P. Lillerud, P. Beato, S. Svelle, Selectivity control through fundamental mechanistic insight in the conversion of methanol to hydrocarbons over zeolites, Microporous Mesoporous Mater., 136 (2010) 33-41.
[156] P. del Campo, U. Olsbye, K.P. Lillerud, S. Svelle, P. Beato, Impact of post-synthetic treatments on unidirectional H-ZSM-22 zeolite catalyst: Towards improved clean MTG catalytic process, Catal. Today.
[157] A. Molino, K.A. Lukaszuk, D. Rojo-Gama, K.P. Lillerud, U. Olsbye, S. Bordiga, S. Svelle, P. Beato, Conversion of methanol to hydrocarbons over zeolite ZSM-23 (MTT): Exceptional effects of particle size on catalyst lifetime, Chem. Commun., (2017).
[158] R. Khare, Z. Liu, Y. Han, A. Bhan, A mechanistic basis for the effect of aluminum content on ethene selectivity in methanol-to-hydrocarbons conversion on HZSM-5, J. Catal., 348 (2017) 300-305.
[159] T. Liang, J. Chen, Z. Qin, J. Li, P. Wang, S. Wang, G. Wang, M. Dong, W. Fan, J. Wang, Conversion of Methanol to Olefins over H-ZSM-5 Zeolite: Reaction Pathway Is Related to the Framework Aluminum Siting, ACS Catalysis, 6 (2016) 7311-7325.
[160] X. Sun, S. Mueller, H. Shi, G.L. Haller, M. Sanchez-Sanchez, A.C. Van Veen, J.A. Lercher, On the impact of co-feeding aromatics and olefins for the methanol-to-olefins reaction on HZSM-5, J. Catal., 314 (2014) 21-31.
[161] D. Rojo-Gama, S. Etemadi, E. Kirby, K.P. Lillerud, P. Beato, S. Svelle, U. Olsbye, Time- and space-resolved study of the methanol to hydrocarbons (MTH) reaction - influence of zeolite topology on axial deactivation patterns, Faraday Discuss., (2017. DOI: 10.1039/C6FD00187D).
[162] T.V.W. Janssens, S. Svelle, U. Olsbye, Kinetic modeling of deactivation profiles in the methanol-to-hydrocarbons (MTH) reaction: A combined autocatalytic-hydrocarbon pool approach, J. Catal., 308 (2013) 122-130.

[163] S. Müller, Y. Liu, M. Vishnuvarthan, X. Sun, A.C. Van Veen, G.L. Haller, M. Sanchez-Sanchez, J.A. Lercher, Coke formation and deactivation pathways on H-ZSM-5 in the conversion of methanol to olefins, J. Catal., 325 (2015) 48-59.
[164] S. Müller, Y. Liu, F.M. Kirchberger, M. Tonigold, M. Sanchez-Sanchez, J.A. Lercher, Hydrogen transfer pathways during zeolite catalyzed methanol conversion to hydrocarbons, J. Am. Chem. Soc., (2016).
[165] T.E. Daubert, R.P. Danner, DIPPR tables. Physical and Thermodynamic Properties of Pure Chemicals. Data Compilation., in.
[166] R. Hunter, G.J. Hutchings, Hydrocarbon formation from methanol using WO3/Al2O3 and zeolite H-ZSM-5 catalysts: further evidence on the reaction mechanism, J. Chem. Soc., Chem. Commun., (1987) 377-379.
[167] P. Nachtigall, J. Sauer, Chapter 20 Applications of quantum chemical methods in zeolite science, in: J. Čejka, H. van Bekkum, A. Corma, F. Schüth (Eds.) Stud. Surf. Sci. Catal., Elsevier, 2007, pp. 701-XXI.
[168] Z. Wei, Y.-Y. Chen, J. Li, P. Wang, B. Jing, Y. He, M. Dong, H. Jiao, Z. Qin, J. Wang, W. Fan, Methane formation mechanism in the initial methanol-to-olefins process catalyzed by SAPO-34, Catalysis Science & Technology, 6 (2016) 5526-5533.
[169] X. Sun, S. Müller, Y. Liu, H. Shi, G.L. Haller, M. Sanchez-Sanchez, A.C. Van Veen, J.A. Lercher, On reaction pathways in the conversion of methanol to hydrocarbons on HZSM-5, J. Catal., 317 (2014) 185-197.
[170] M. Bjørgen, U. Olsbye, S. Svelle, S. Kolboe, Conversion of Methanol to Hydrocarbons: The Reactions of the Heptamethylbenzenium Cation over Zeolite H-Beta, Catal. Lett., 93 (2004) 37-40.
[171] H. Schulz, M. Wei, Pools and Constraints in Methanol Conversion to Olefins and Fuels on Zeolite HZSM5, Top. Catal., 57 (2014) 683-692.
[172] J.F. Haw, D.M. Marcus, Well-defined (supra)molecular structures in zeolite methanol-to-olefin catalysis, Top. Catal., 34 (2005) 41-48.
[173] F.L. Bleken, K. Barbera, F. Bonino, U. Olsbye, K.P. Lillerud, S. Bordiga, P. Beato, T.V.W. Janssens, S. Svelle, Catalyst deactivation by coke formation in microporous and desilicated zeolite H-ZSM-5 during the conversion of methanol to hydrocarbons, J. Catal., 307 (2013) 62-73.
[174] D. Chen, K. Moljord, T. Fuglerud, A. Holmen, The effect of crystal size of SAPO-34 on the selectivity and deactivation of the MTO reaction, Microporous Mesoporous Mater., 29 (1999) 191-203.
[175] Y. Li, M. Zhang, D. Wang, F. Wei, Y. Wang, Differences in the methanol-to-olefins reaction catalyzed by SAPO-34 with dimethyl ether as reactant, J. Catal., 311 (2014) 281-287.
[176] M. Ghavipour, R.M. Behbahani, R.B. Rostami, A.S. Lemraski, Methanol/dimethyl ether to light olefins over SAPO-34: Comprehensive comparison of the products distribution and catalyst performance, Journal of Natural Gas Science and Engineering, 21 (2014) 532-539.
[177] P. Pérez-Uriarte, A. Ateka, A.T. Aguayo, A.G. Gayubo, J. Bilbao, Kinetic model for the reaction of DME to olefins over a HZSM-5 zeolite catalyst, Chem. Eng. J., 302 (2016) 801-810.
[178] P. Pérez-Uriarte, A. Ateka, M. Gamero, A.T. Aguayo, J. Bilbao, Effect of the Operating Conditions in the Transformation of DME to olefins over a HZSM-5 Zeolite Catalyst, Ind. Eng. Chem. Res., 55 (2016) 6569-6578.
[179] A.J. Marchi, G.F. Froment, Catalytic conversion of methanol into light alkenes on mordenite-like zeolites, Applied Catalysis A, General, 94 (1993) 91-106.
[180] A.J. Marchi, G.F. Froment, Catalytic conversion of methanol to light alkenes on SAPO molecular sieves, Applied Catalysis, 71 (1991) 139-152.
[181] X. Wu, R.G. Anthony, Effect of feed composition on methanol conversion to light olefins over SAPO-34, Applied Catalysis A: General, 218 (2001) 241-250.
[182] Y. Kumita, J. Gascon, E. Stavitski, J.A. Moulijn, F. Kapteijn, Shape selective methanol to olefins over highly thermostable DDR catalysts, Applied Catalysis A: General, 391 (2011) 234-243.

[183] K. De Wispelaere, C.S. Wondergem, B. Ensing, K. Hemelsoet, E.J. Meijer, B.M. Weckhuysen, V. Van Speybroeck, J. Ruiz-Martínez, Insight into the Effect of Water on the Methanol-to-Olefins Conversion in H-SAPO-34 from Molecular Simulations and in Situ Microspectroscopy, ACS Catalysis, (2016) 1991-2002.
[184] P. Pérez-Uriarte, M. Gamero, A. Ateka, M. Díaz, A.T. Aguayo, J. Bilbao, Effect of the Acidity of HZSM-5 Zeolite and the Binder in the DME Transformation to Olefins, Industrial & Engineering Chemistry Research, 55 (2016) 1513-1521.
[185] P.S. Sai Prasad, J.W. Bae, S.-H. Kang, Y.-J. Lee, K.-W. Jun, Single-step synthesis of DME from syngas on Cu–ZnO–Al2O3/zeolite bifunctional catalysts: The superiority of ferrierite over the other zeolites, Fuel Process. Technol., 89 (2008) 1281-1286.
[186] S. Hassanpour, F. Yaripour, M. Taghizadeh, Performance of modified H-ZSM-5 zeolite for dehydration of methanol to dimethyl ether, Fuel Process. Technol., 91 (2010) 1212-1221.
[187] G.R. Moradi, F. Yaripour, P. Vale-Sheyda, Catalytic dehydration of methanol to dimethyl ether over mordenite catalysts, Fuel Process. Technol., 91 (2010) 461-468.
[188] F. Yaripour, M. Mollavali, S.M. Jam, H. Atashi, Catalytic dehydration of methanol to dimethyl ether catalyzed by aluminum phosphate catalysts, Energy Fuels, 23 (2009) 1896-1900.
[189] G.R. Moradi, S. Nosrati, F. Yaripor, Effect of the hybrid catalysts preparation method upon direct synthesis of dimethyl ether from synthesis gas, Catal. Commun., 8 (2007) 598-606.
[190] F. Yaripour, F. Baghaei, I. Schmidt, J. Perregaarad, Synthesis of dimethyl ether from methanol over aluminium phosphate and silica-titania catalysts, Catal. Commun., 6 (2005) 542-549.
[191] J. Sun, G. Yang, Y. Yoneyama, N. Tsubaki, Catalysis chemistry of dimethyl ether synthesis, ACS Catalysis, 4 (2014) 3346-3356.
[192] A.J. Jones, E. Iglesia, Kinetic, Spectroscopic, and Theoretical Assessment of Associative and Dissociative Methanol Dehydration Routes in Zeolites, Angew. Chem. Int. Ed., 53 (2014) 12177-12181.
[193] W. Dai, W. Kong, G. Wu, N. Li, L. Li, N. Guan, Catalytic dehydration of methanol to dimethyl ether over aluminophosphate and silico-aluminophosphate molecular sieves, Catal. Commun., 12 (2011) 535-538.
[194] S.P. Naik, H. Du, H. Wan, V. Bui, J.D. Miller, W.W. Zmierczak, A comparative study of ZnO-CuO-Al2O3/SiO 2-Al2O3 composite and hybrid catalysts for direct synthesis of dimethyl ether from syngas, Ind. Eng. Chem. Res., 47 (2008) 9791-9794.
[195] G. Bercic, J. Levec, Intrinsic and global reaction rate of methanol dehydration over γ-Al2O3 pellets, Ind. Eng. Chem. Res., 31 (1992) 1035-1040.
[196] S.D. Kim, S.C. Baek, Y.-J. Lee, K.-W. Jun, M.J. Kim, I.S. Yoo, Effect of γ-alumina content on catalytic performance of modified ZSM-5 for dehydration of crude methanol to dimethyl ether, Applied Catalysis A: General, 309 (2006) 139-143.
[197] M. Xu, J.H. Lunsford, D.W. Goodman, A. Bhattacharyya, Synthesis of dimethyl ether (DME) from methanol over solid-acid catalysts, Applied Catalysis A: General, 149 (1997) 289-301.
[198] S. Jiang, J.S. Hwang, T. Jin, T. Cai, W. Cho, Y.S. Baek, S.E. Park, Dehydration of Methanol to Dimethyl Ether over ZSM-5 Zeolite, Bull. Korean Chem. Soc., 25 (2004) 185-189.
[199] A.M. Vos, K.H.L. Nulens, F. De Proft, R.A. Schoonheydt, P. Geerlings, Reactivity descriptors and rate constants for electrophilic aromatic substitution: Acid zeolite catalyzed methylation of benzene and toluene, J. Phys. Chem. B, 106 (2002) 2026-2034.
[200] J. Van Der Mynsbrugge, M. Visur, U. Olsbye, P. Beato, M. Bjorgen, V. Van Speybroeck, S. Svelle, Methylation of benzene by methanol: Single-site kinetics over H-ZSM-5 and H-beta zeolite catalysts, J. Catal., 292 (2012) 201-212.
[201] S.R. Blaszkowski, R.A. Van Santen, Alkylation and transalkylation reactions of aromatics, in: ACS Symp. Ser., 1999, pp. 307-320.
[202] S. Svelle, M. Visur, U. Olsbye, Saepurahman, M. Bjørgen, Mechanistic aspects of the zeolite catalyzed methylation of alkenes and aromatics with methanol: A review, Top. Catal., 54 (2011) 897-906.

[203] S. Svelle, P.O. Rønning, U. Olsbye, S. Kolboe, Kinetic studies of zeolite-catalyzed methylation reactions. Part 2. Co-reaction of [12C]propene or [12C]n-butene and [13C]methanol, J. Catal., 234 (2005) 385-400.
[204] S. Svelle, P.O. Rønning, S. Kolboe, Kinetic studies of zeolite-catalyzed methylation reactions: 1. Coreaction of [12C]ethene and [13C]methanol, J. Catal., 224 (2004) 115-123.
[205] S. Svelle, B. Arstad, S. Kolboe, O. Swang, A theoretical investigation of the methylation of alkenes with methanol over acidic zeolites, J. Phys. Chem. B, 107 (2003) 9281-9289.
[206] V. Van Speybroeck, J. Van der Mynsbrugge, M. Vandichel, K. Hemelsoet, D. Lesthaeghe, A. Ghysels, G.B. Marin, M. Waroquier, First Principle Kinetic Studies of Zeolite-Catalyzed Methylation Reactions, J. Am. Chem. Soc., 133 (2011) 888-899.
[207] S. Svelle, C. Tuma, X. Rozanska, T. Kerber, J. Sauer, Quantum chemical modeling of zeolite-catalyzed methylation reactions: Toward chemical accuracy for barriers, J. Am. Chem. Soc., 131 (2009) 816-825.
[208] I.M. Hill, S.A. Hashimi, A. Bhan, Kinetics and mechanism of olefin methylation reactions on zeolites, J. Catal., 285 (2012) 115-123.
[209] I.M. Hill, Y.S. Ng, A. Bhan, Kinetics of butene isomer methylation with dimethyl ether over zeolite catalysts, ACS Catalysis, 2 (2012) 1742-1748.
[210] I. Hill, A. Malek, A. Bhan, Kinetics and mechanism of benzene, toluene, and xylene methylation over H-MFI, ACS Catalysis, 3 (2013) 1992-2001.
[211] S. Svelle, M. Bjørgen, Mechanistic proposal for the zeolite catalyzed methylation of aromatic compounds, J. Phys. Chem. A, 114 (2010) 12548-12554.
[212] V. Van Speybroeck, K. Hemelsoet, K. De Wispelaere, Q. Qian, J. Van der Mynsbrugge, B. De Sterck, B.M. Weckhuysen, M. Waroquier, Mechanistic Studies on Chabazite-Type Methanol-to-Olefin Catalysts: Insights from Time-Resolved UV/Vis Microspectroscopy Combined with Theoretical Simulations, ChemCatChem, 5 (2013) 173-184.
[213] J.H. Ahn, R. Kolvenbach, S.S. Al-Khattaf, A. Jentys, J.A. Lercher, Methanol usage in toluene methylation with medium and large pore zeolites, ACS Catalysis, 3 (2013) 817-825.
[214] D. Lesthaeghe, B. De Sterck, V. Van Speybroeck, G.B. Marin, M. Waroquier, Zeolite Shape-Selectivity in the gem-Methylation of Aromatic Hydrocarbons, Angew. Chem. Int. Ed., 46 (2007) 1311-1314.
[215] J. Van der Mynsbrugge, J. De Ridder, K. Hemelsoet, M. Waroquier, V. Van Speybroeck, Enthalpy and Entropy Barriers Explain the Effects of Topology on the Kinetics of Zeolite-Catalyzed Reactions, Chemistry – A European Journal, 19 (2013) 11568-11576.
[216] J.H. Ahn, R. Kolvenbach, C. Neudeck, S.S. Al-Khattaf, A. Jentys, J.A. Lercher, Tailoring mesoscopically structured H-ZSM5 zeolites for toluene methylation, J. Catal., 311 (2014) 271-280.
[217] T. Maihom, B. Boekfa, J. Sirijaraensre, T. Nanok, M. Probst, J. Limtrakul, Reaction mechanisms of the methylation of ethene with methanol and dimethyl ether over h-zsm-5: An ONIOM study, J. Phys. Chem. C, 113 (2009) 6654-6662.
[218] S. Svelle, S. Kolboe, O. Swang, U. Olsbye, Methylation of alkenes and methylbenzenes by dimethyl ether or methanol on acidic zeolites, J. Phys. Chem. B, 109 (2005) 12874-12878.
[219] R.Y. Brogaard, R. Henry, Y. Schuurman, A.J. Medford, P.G. Moses, P. Beato, S. Svelle, J.K. Nørskov, U. Olsbye, Methanol-to-hydrocarbons conversion: The alkene methylation pathway, J. Catal., 314 (2014) 159-169.
[220] I.I. Ivanova, A. Corma, Surface Species Formed and Their Reactivity during the Alkylation of Toluene by Methanol and Dimethyl Ether on Zeolites As Determined by in Situ 13C MAS NMR, The Journal of Physical Chemistry B, 101 (1997) 547-551.
[221] J. Van Der Mynsbrugge, S.L.C. Moors, K. De Wispelaere, V. Van Speybroeck, Insight into the formation and reactivity of framework-bound methoxide species in h-zsm-5 from static and dynamic molecular simulations, ChemCatChem, 6 (2014) 1906-1918.

[222] A. Corma, M. Faraldos, A. Mifsud, Influence of the level of dealumination on the selective adsorption of olefins and paraffins and its implication on hydrogen transfer reactions during catalytic cracking on USY zeolites, Applied Catalysis, 47 (1989) 125-133.
[223] W. Dai, G. Cao, L. Yang, G. Wu, M. Dyballa, M. Hunger, N. Guan, L. Li, Insights into the catalytic cycle and activity of methanol-to-olefin conversion over low-silica AlPO-34 zeolites with controllable Brønsted acid density, Catalysis Science and Technology, 7 (2017) 607-618.
[224] W. Dai, C. Wang, M. Dyballa, G. Wu, N. Guan, L. Li, Z. Xie, M. Hunger, Understanding the Early Stages of the Methanol-to-Olefin Conversion on H-SAPO-34, ACS Catalysis, 5 (2015) 317-326.
[225] W. Dai, M. Dyballa, G. Wu, L. Li, N. Guan, M. Hunger, Intermediates and dominating reaction mechanism during the early period of the methanol-to-olefin conversion on SAPO-41, J. Phys. Chem. C, 119 (2015) 2637-2645.
[226] R. Batchu, V.V. Galvita, K. Alexopoulos, K. Van der Borght, H. Poelman, M.F. Reyniers, G.B. Marin, Role of intermediates in reaction pathways from ethene to hydrocarbons over H-ZSM-5, Applied Catalysis A: General, 538 (2017) 207-220.
[227] R. Khare, S.S. Arora, A. Bhan, Implications of Cofeeding Acetaldehyde on Ethene Selectivity in Methanol-to-Hydrocarbons Conversion on MFI and Its Mechanistic Interpretation, ACS Catalysis, 6 (2016) 2314-2331.
[228] I.A. Bakare, O. Muraza, M. Yoshioka, Z.H. Yamani, T. Yokoi, Conversion of methanol to olefins over Al-rich ZSM-5 modified with alkaline earth metal oxides, Catalysis Science & Technology, 6 (2016) 7852-7859.
[229] R. Khare, D. Millar, A. Bhan, A mechanistic basis for the effects of crystallite size on light olefin selectivity in methanol-to-hydrocarbons conversion on MFI, J. Catal., 321 (2015) 23-31.
[230] D.A. Simonetti, R.T. Carr, E. Iglesia, Acid strength and solvation effects on methylation, hydride transfer, and isomerization rates during catalytic homologation of C 1 species, J. Catal., 285 (2012) 19-30.
[231] D.A. Simonetti, J.H. Ahn, E. Iglesia, Catalytic Co-Homologation of Alkanes and Dimethyl Ether and Promotion by Adamantane as a Hydride Transfer Co-Catalyst, ChemCatChem, 3 (2011) 704-718.
[232] D.A. Simonetti, J.H. Ahn, E. Iglesia, Mechanistic details of acid-catalyzed reactions and their role in the selective synthesis of triptane and isobutane from dimethyl ether, J. Catal., 277 (2011) 173-195.
[233] V.B. Kazansky, M.V. Frash, R.A. Van Santen, A quantum-chemical study of hydride transfer in catalytic transformations of paraffins on zeolites. Pathways through adsorbed nonclassical carbonium ions, Catal. Lett., 48 (1997) 61-67.
[234] M. Boronat, P. Viruela, A. Corma, Theoretical Study of Bimolecular Reactions between Carbenium Ions and Paraffins: The Proposal of a Common Intermediate for Hydride Transfer, Disproportionation, Dehydrogenation, and Alkylation, The Journal of Physical Chemistry B, 103 (1999) 7809-7821.
[235] P. Cnudde, K. De Wispelaere, J. Van der Mynsbrugge, M. Waroquier, V. Van Speybroeck, Effect of temperature and branching on the nature and stability of alkene cracking intermediates in H-ZSM-5, J. Catal., 345 (2017) 53-69.
[236] C. Tuma, J. Sauer, Protonated Isobutene in Zeolites: tert-Butyl Cation or Alkoxide?, Angew. Chem. Int. Ed., 44 (2005) 4769-4771.
[237] N. Hazari, E. Iglesia, J.A. Labinger, D.A. Simonetti, Selective homogeneous and heterogeneous catalytic conversion of methanol/dimethyl ether to triptane, Acc. Chem. Res., 45 (2012) 653-662.
[238] J.E. Bercaw, N. Hazari, J.A. Labinger, V.J. Scott, G.J. Sunley, Selective Methylative Homologation: An Alternate Route to Alkane Upgrading, J. Am. Chem. Soc., 130 (2008) 11988-11995.
[239] P. Sazama, B. Wichterlova, J. Dedecek, Z. Tvaruzkova, Z. Musilova, L. Palumbo, S. Sklenak, O. Gonsiorova, FTIR and 27Al MAS NMR analysis of the effect of framework Al- and Si-defects in micro- and micro-mesoporous H-ZSM-5 on conversion of methanol to hydrocarbons, Microporous Mesoporous Mater., 143 (2011) 87-96.

[240] B. Wichterlová, N. Žilkova, E. Uvarova, J. Čejka, P. Sarv, C. Paganini, J.A. Lercher, Effect of Broensted and Lewis sites in ferrierites on skeletal isomerization of n-butenes, Applied Catalysis A: General, 182 (1999) 297-308.
[241] B.T. Lønstad Bleken, L. Mino, F. Giordanino, P. Beato, S. Svelle, K.P. Lillerud, S. Bordiga, Probing the surface of nanosheet H-ZSM-5 with FTIR spectroscopy, PCCP, 15 (2013) 13363-13370.
[242] B.T.L. Bleken, D.S. Wragg, B. Arstad, A.E. Gunnæs, J. Mouzon, S. Helveg, L.F. Lundegaard, P. Beato, S. Bordiga, U. Olsbye, S. Svelle, K.P. Lillerud, Unit cell thick nanosheets of zeolite H-ZSM-5: Structure and activity, Top. Catal., 56 (2013) 558-566.
[243] R.J. Gorte, What do we know about the acidity of solid acids ?, Catal. Lett., 62 (1999) 1-13.
[244] C. Pereira, R.J. Gorte, Method for distinguishing Brønsted-acid sites in mixtures of H-ZSM-5, H-Y and silica-alumina, Applied Catalysis A, General, 90 (1992) 145-157.
[245] C. Sprung, Ph.D. Thesis, Kinetic investigation in methane steam reforming over a nickel catalyst in: Department of Chemistry, University of Oslo, 2012.
[246] M.J. Hayman, Ph.D. Thesis. Modification of Methanol-To-Olefins hydrocarbon pool species by oxygenates on acidic zeolites, in, University of Southern California, 2011.
[247] P.O. Rønning, Use of Isotopic Labelling in the Study of Methanol Conversion to Hydrocarbons over Zeolite H-ZSM-5, in: Department of Chemistry, University of Oslo, 1998.
[248] D. Rojo-Gama, S. Etemadi, E. Kirby, K.P. Lillerud, P. Beato, S. Svelle, U. Olsbye, Time- and space-resolved study of the Methanol to Hydrocarbons (MTH) reaction - influence of zeolite topology on deactivation patterns, Faraday Discuss., (2016).
[249] E. Gianotti, E.C. Oliveira, S. Coluccia, H.O. Pastore, L. Marchese, The surface acidity of mesoporous silicoaluminophosphates: A FTIR study, Stud. Surf. Sci. Catal., 154 (2004) 1498-1504.
[250] F.L. Bleken, T.V.W. Janssens, S. Svelle, U. Olsbye, Product yield in methanol conversion over ZSM-5 is predominantly independent of coke content, Microporous Mesoporous Mater., 164 (2012) 190-198.
[251] Y. Hirota, K. Murata, M. Miyamoto, Y. Egashira, N. Nishiyama, Light olefins synthesis from methanol and dimethylether over SAPO-34 nanocrystals, Catal. Lett., 140 (2010) 22-26.
[252] Z. Wen, T. Xia, M. Liu, K. Zhu, X. Zhu, Methane formation mechanism in methanol to hydrocarbon process: A periodic density functional theory study, Catal. Commun., 75 (2016) 45-49.
[253] J.S. Martinez-Espin, K. De Wispelaere, M. Westgard Erichsen, S. Svelle, T.V.W. Janssens, V. Van Speybroeck, P. Beato, U. Olsbye, Benzene co-reaction with methanol and dimethyl ether over zeolite and zeotype catalysts: Evidence of parallel reaction paths to toluene and diphenylmethane, J. Catal., (2017. http:/dx.doi.org/10.1016/DOI: j.jcat.2017.03.007) accepted.
[254] M. Westgård Erichsen, S. Svelle, U. Olsbye, H-SAPO-5 as methanol-to-olefins (MTO) model catalyst: Towards elucidating the effects of acid strength, J. Catal., 298 (2013) 94-101.
[255] M. Guisnet, P. Magnoux, Organic chemistry of coke formation, Applied Catalysis A: General, 212 (2001) 83-96.
[256] S. Morin, N.S. Gnep, M. Guisnet, Influence of coke deposits on the selectivity of m-xylene transformation and on the isomerization mechanism, Applied Catalysis A: General, 168 (1998) 63-68.
[257] M.J. Climent, A. Corma, H. García, J. Primo, Zeolites in organic reactions. Condensation of formaldehyde with benzene in the presence of HY zeolites, Applied Catalysis, 51 (1989) 113-125.
[258] Z. Hou, T. Okuhara, Catalytic synthesis of diphenylmethane from benzene and formalin with water-tolerant solid acids, Applied Catalysis A: General, 216 (2001) 147-155.
[259] C. Peng, H. Wang, P. Hu, Theoretical insights into how the first C-C bond forms in the methanol-to-olefin process catalysed by HSAPO-34, PCCP, 18 (2016) 14495-14502.
[260] A. Hwang, M. Kumar, J.D. Rimer, A. Bhan, Implications of methanol disproportionation on catalyst lifetime for methanol-to-olefins conversion by HSSZ-13, J. Catal., 346 (2017) 154-160.
[261] S. Morin, P. Ayrault, N.S. Gnep, M. Guisnet, Influence of the framework composition of commercial HFAU zeolites on their activity and selectivity in m-xylene transformation, Applied Catalysis A: General, 166 (1998) 281-292.

[262] V.n. Macho, M. Králik, E. Jurecekova, J. Hudec, L. Jurecek, Dehydration of C4 alkanols conjugated with a positional and skeletal isomerisation of the formed C4 alkenes, Applied Catalysis A: General, 214 (2001) 251-257.
[263] M. Zhang, S. Xu, J. Li, Y. Wei, Y. Gong, Y. Chu, A. Zheng, J. Wang, W. Zhang, X. Wu, F. Deng, Z. Liu, Methanol to hydrocarbons reaction over Hβ zeolites studied by high resolution solid-state NMR spectroscopy: Carbenium ions formation and reaction mechanism, J. Catal., 335 (2016) 47-57.
[264] M.B. Sayed, Comments on the mechanism of MTG/HZSM-5 conversion, J. Chem. Soc. Faraday Trans., 83 (1987) 1771-1778.
[265] J.H. Ahn, B. Temel, E. Iglesia, Selective Homologation Routes to 2,2,3-Trimethylbutane on Solid Acids, Angew. Chem. Int. Ed., 48 (2009) 3814-3816.
[266] M. Boronat, P. Viruela, A. Corma, Ab initio and density-functional theory study of zeolite-catalyzed hydrocarbon reactions: hydride transfer, alkylation and disproportionation, PCCP, 2 (2000) 3327-3333.
[267] M.A. Asensi, A. Corma, A. Martínez, Skeletal Isomerization of 1-Butene on MCM-22 Zeolite Catalyst, J. Catal., 158 (1996) 561-569.
[268] M. Guisnet, P. Andy, N.S. Gnep, E. Benazzi, C. Travers, Skeletal Isomerization ofn-Butenes, J. Catal., 158 (1996) 551-560.
[269] H. Yamazaki, H. Shima, H. Imai, T. Yokoi, T. Tatsumi, J.N. Kondo, Direct production of propene from methoxy species and dimethyl ether over H-ZSM-5, J. Phys. Chem. C, 116 (2012) 24091-24097.
[270] S. Svelle, M. Bjørgen, S. Kolboe, D. Kuck, M. Letzel, U. Olsbye, O. Sekiguchi, E. Uggerud, Intermediates in the methanol-to-hydrocarbons (MTH) reaction: A gas phase study of the unimolecular reactivity of multiply methylated benzenium cations, Catal. Lett., 109 (2006) 25-35.
[271] J.S. Buchanan, J.G. Santiesteban, W.O. Haag, Mechanistic considerations in acid-catalyzed cracking of olefins, J. Catal., 158 (1996) 279-287.
[272] C. Chang, W. Lang, W. Bell, W. Moser, Catalysis of Organic Reactions, by Moser, WR, Dekker, (1981) 73.
[273] M. Ai, The formation of isoprene by means of a vapor-phase prins reaction between formaldehyde and isobutene, J. Catal., 106 (1987) 280-286.
[274] I. Ivanova, V.L. Sushkevich, Y.G. Kolyagin, V.V. Ordomsky, Catalysis by coke deposits: Synthesis of isoprene over solid catalysts, Angew. Chem. Int. Ed., 52 (2013) 12961-12964.
[275] E. Dumitriu, V. Hulea, I. Fechete, C. Catrinescu, A. Auroux, J.F. Lacaze, C. Guimon, Prins condensation of isobutylene and formaldehyde over Fe-silicates of MFI structure, Applied Catalysis A: General, 181 (1999) 15-28.
[276] E.J. Munson, A.A. Kheir, N.D. Lazo, J.F. Haw, In situ solid-state NMR study of methanol-to-gasoline chemistry in zeolite HZSM-5, J. Phys. Chem., 96 (1992) 7740-7746.
[277] NIST Standard Reference Database 85, NIST/TRC Table Database, WinTable, Version 1.5, in.
[278] O.V. Dorofeeva, L.V. Gurvich, V.S. Jorish, Thermodynamic Properties of Twenty-One Monocyclic Hydrocarbons, J. Phys. Chem. Ref. Data, 15 (1986) 437-464.
[279] A. Hwang, A. Bhan, Bifunctional Strategy Coupling Y2O3-Catalyzed Alkanal Decomposition with Methanol-to-Olefins Catalysis for Enhanced Lifetime, ACS Catalysis, (2017) 4417-4422.

Chapter 5

Appendix